GEOLOGY OF THE UPPER GRANDE RONDE RIVER BASIN, UNION COUNTY, OREGON

DOGAMI Bulletin 107

Mark L. Ferns
Vicki S. McConnell
Ian P. Madin
Jenda A. Johnson

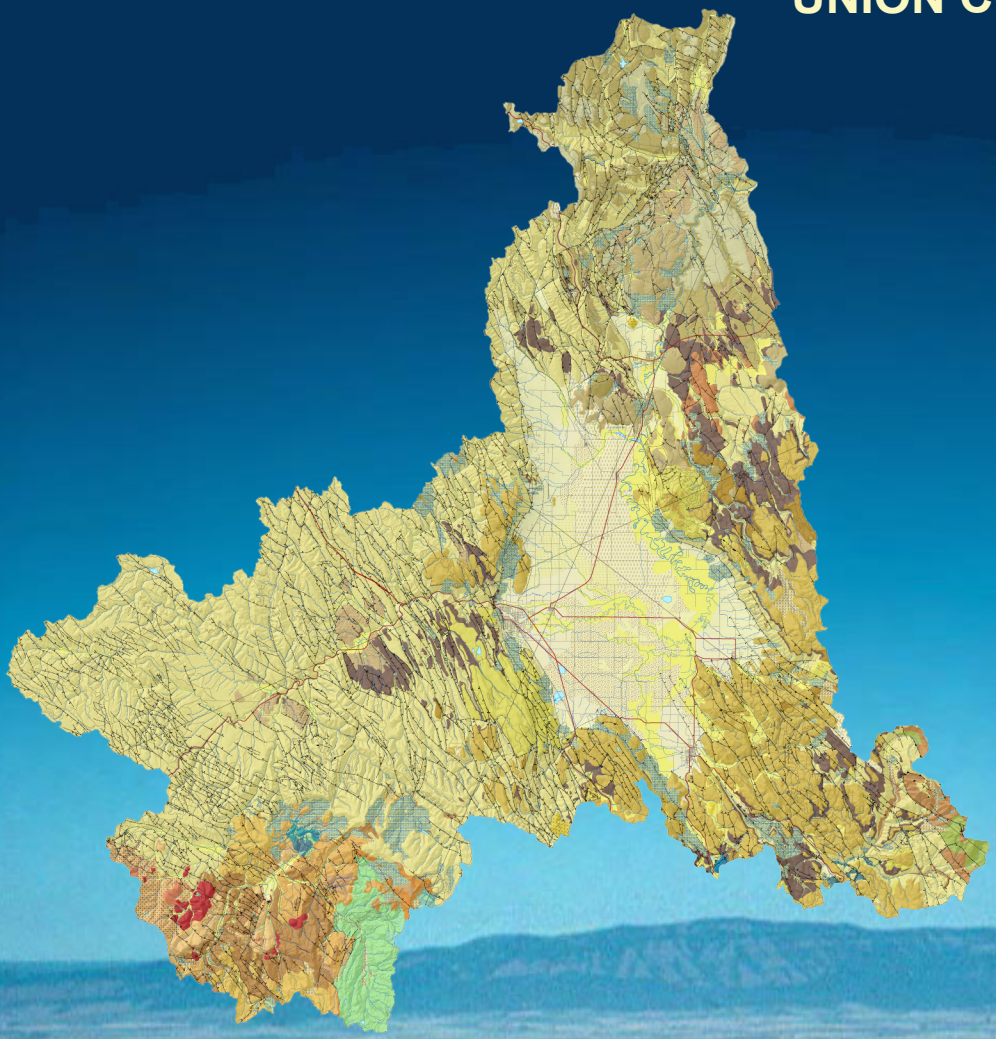

STATE OF OREGON
DEPARTMENT OF GEOLOGY AND MINERAL INDUSTRIES
VICKI S. McCONNELL, STATE GEOLOGIST

NOTICE

This map cannot serve as a substitute for site-specific investigations by qualified practitioners. Site-specific data may give results that differ from those shown on the maps. The views and conclusions contained in this document are those of the authors and should not be interpreted as necessarily representing the official policies, either expressed or implied, of the United States government.

NAVIGATING THIS PDF FILE AND THE CD

To navigate through this PDF document, touch the "**Bookmarks**" tab at the upper left of this document to open the section list. Touching any topic will take you immediately that section. A small triangle to the left of the bookmark indicates subheadings.

The Appendix in this document describes the data files on this CD.

Cover page photograph: View looking east across Grande Ronde Valley to Mount Emily.

Oregon Department of Geology and Mineral Industries Bulletin
Published in conformance with ORS 516.030

For copies of this publication or other information about Oregon geology and natural resources, contact:

Nature of the Northwest Information Center
800 NE Oregon Street #28, Suite 965
Portland, Oregon 97232
(971) 673-2331
http://www.NatureNW.org

Suggested citation: Ferns, M. L., McConnell, V. S., Madin, I. P., and Johnson, J. A., 2010, Geology of the upper Grande Ronde River basin, Union County, Oregon; Oregon Department of Geology and Mineral Industries Bulletin 107, scale 1:100,000, 65 p.

TABLE OF CONTENTS

LIST OF FIGURES

(continued)

(List of Figures, continued)

PLATE

Geology of the Upper Grande Ronde River Basin, Union County, Oregon

by Mark L. Ferns[1], Vicki S. McConnell[1], Ian P. Madin[1], and Jenda A. Johnson[2]

INTRODUCTION

The upper Grande Ronde River hydrologic basin encompasses an area of more than 4,200 km^2 in the north central part of the Blue Mountains Province of northeastern Oregon (Figure 1). The watershed includes the Grande Ronde River and all tributaries upstream from the confluence with the Wallowa River. The Grande Ronde River and its main tributary, Catherine Creek, begin in the south, flowing from glaciated uplands through forested canyon lands to meet in the nearly flat, fault-bounded plain of Grande Ronde Valley. Grande Ronde Valley is a nearly flat, alluvial plain fringed by gently sloping alluvial fans and forms a 570-km^2 fertile basin. After meandering northward, the combined streams leave the basin, merge with the Wallowa River, and continue north through deeply eroded canyon lands of the lower Grande Ronde River. Watershed elevations range from 2,060 m at Granite Peak, in the Wallowa Mountains, to 705 m at the confluence of the Grande Ronde and Wallowa rivers. The elevation of the valley floor varies from 835 to 915 m.

The main headwaters to the basin lie in the glaciated Wallowa Mountains to the east and in the Elkhorn Mountains to the south. Both mountainous regions are structural highlands cored with pre-Miocene basement rocks. Northwest-trending, fault-bounded ridges and valleys separate the Wallowa and Elkhorn mountains. The oldest rocks include exotic Paleozoic and Mesozoic oceanic and island arc fragments, Late Jurassic and Cretaceous intrusions, Paleocene and Eocene continental sedimentary rocks, and late Oligocene to early Miocene bimodal volcanic rocks. Early- to mid-Miocene tholeiitic flood basalt (Imnaha Basalt and Grande Ronde Basalt) laps onto highly eroded older basement rocks (Figure 2).

Two fault-bounded basins form the central part of the upper Grande Ronde basin: Grande Ronde Valley and the smaller Indian Valley in the north. Grande Ronde Valley is bordered both east and west by steep, northwest-trending, fault-bounded escarpments that expose Miocene Grande Ronde Basalt at the base and are capped by lava of the Powder River Volcanic Field.

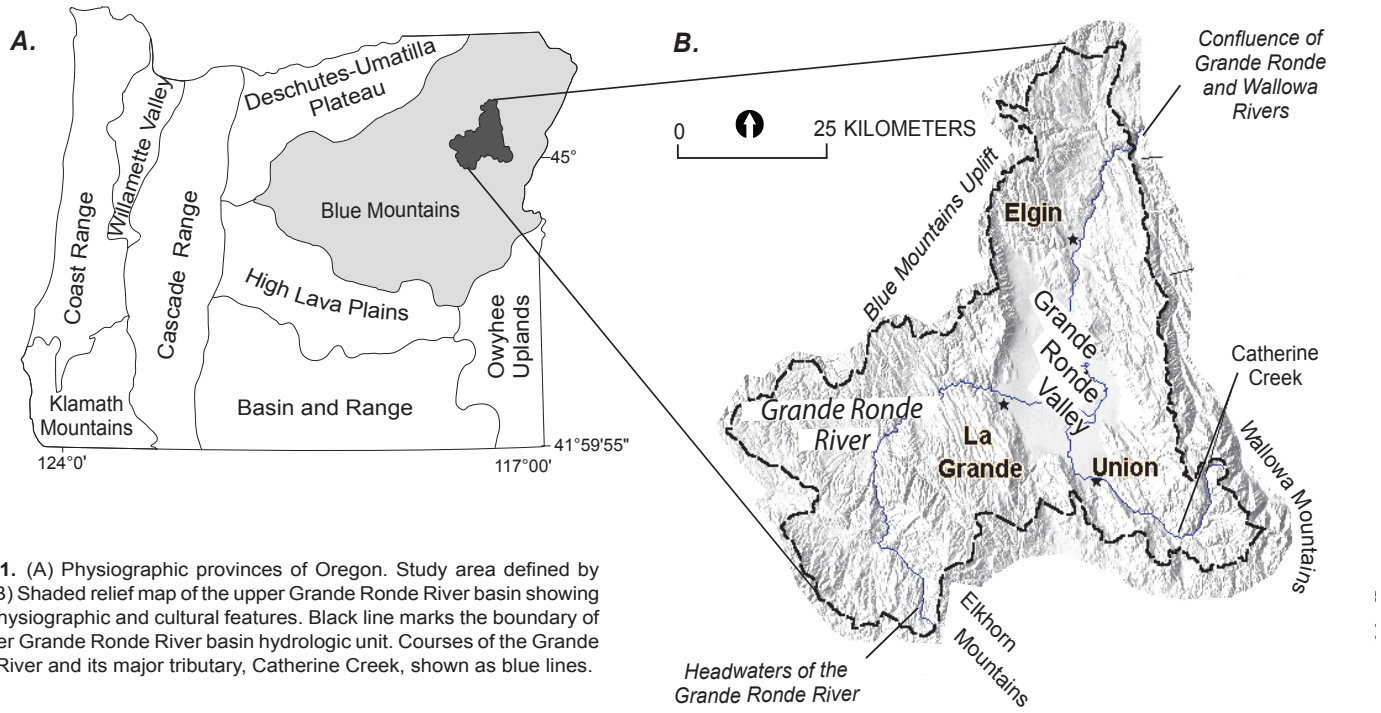

Figure 1. (A) Physiographic provinces of Oregon. Study area defined by black. (B) Shaded relief map of the upper Grande Ronde River basin showing major physiographic and cultural features. Black line marks the boundary of the upper Grande Ronde River basin hydrologic unit. Courses of the Grande Ronde River and its major tributary, Catherine Creek, shown as blue lines.

[1]Oregon Department of Geology and Mineral Industries
[2]1924 NE 47th Avenue, Portland OR 97213

The escarpments that flank the valley have cumulative vertical displacement in excess of 1,000 m and exhibit evidence for Quaternary movement. The valley is filled with as much as 600 m of late-Miocene, Pliocene, and Pleistocene sediment. Indian Valley is bounded on the southwest by a faulted escarpment and is filled with as much as 100 m of sediment and terrace gravel. The northern Grande Ronde Valley is separated from Indian Valley by late-Miocene to Pliocene alkaline and calc-alkaline shield volcanoes of the Elgin Volcanic Field.

The headwaters to Grande Ronde Valley lie in the heavily forested lands of parts of the Umatilla and Wallowa Whitman National Forests and are administered by the U.S. Forest Service. Part of the headwaters is under the jurisdiction of the Confederated Tribes of the Umatilla, which maintains treaty rights over much of the area. Private land holdings include large timber and grazing lands owned by the Boise Corporation and by various cattle ranchers.

More than half of the population (>24,000 people) in the basin lives in city of La Grande. Principal industries are agriculture, light manufacturing, and lumbering. Grain, grass seed, mint, potatoes, fruit, dairy products, and livestock are the main agricultural commodities produced in the valley.

Methodology and Previous Work

The geologic map of upper Grande Ronde River basin (see Appendix for GIS files) is compiled from maps of the La Grande 30′ × 60′ quadrangle (Ferns and others, 2001), quadrangles in Grande Ronde Valley (Ferns and Madin, 1999; Ferns and others, 2002a,b; McConnell and others, 2003), and unpublished mapping by M.L. Ferns in the northeast, V.S. McConnell in the southeast, and K.R. Pogue and others (1999) in the southwest. The compilation is a National Cooperative Geologic Mapping Program project partly funded by U.S. Geological Survey (USGS) assistance award 02HQAG2037. All geologic data were collected using air photos

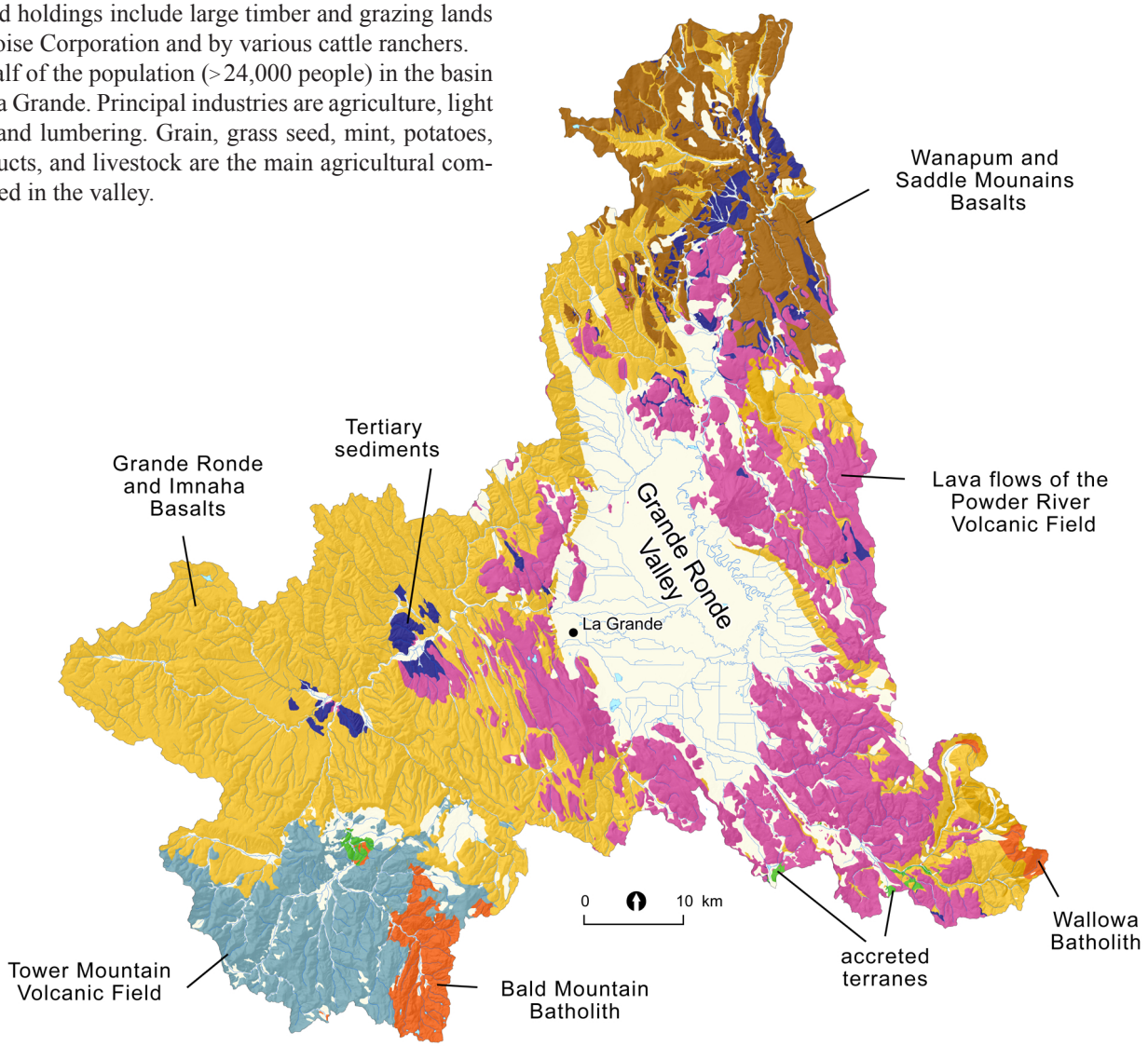

Figure 2. Shaded relief map showing the major lithologic features in the upper Grande Ronde River basin. Pre-Tertiary accreted terranes shown in green; Jurassic-Cretaceous intrusions shown in red; Oligocene Tower Mountain volcanic field shown in gray; Grande Ronde Basalt and Imnaha Basalt shown in orange; Miocene sediments shown in dark blue; Powder River Volcanic Field shown as pink; Wanapum Basalt and Saddle Mountains Basalt shown as brown; late Tertiary and Quaternary sediments shown as pale yellow. Note: Detailed geologic map is available in page size on page 65.

and standard USGS 1:24,000-scale topographic maps. Field data were converted into digital format with MapInfo™ Professional GIS software by heads-up digitizing using georeferenced 1:24,000 scale USGS digital raster images (DRGs) as base maps. These data were then converted to Esri ArcGIS™ shp files to create the map plate in Esri ArcMap™ 9.3.1. Geologic interpretations were aided by Geographic Information Systems (GIS) analyses based in part on georeferenced orthophoto quadrangles and shaded relief images derived from USGS 30-m DEM (digital elevation model) grids and, for the western part of the basin, a side-looking airborne radar image (EROS, 1990). Subsurface geological interpretations were guided by water well logs (Figure 3) obtained through the Oregon Department of Water Resources (OWRD) online GRID system (http://www.wrd.state.or.us/OWRD/GW/index.shtml) and well cuttings provided by local water well drillers. Mapping was supplemented with X-ray fluorescence (XRF) geochemical data (see Appendix) and $^{40}Ar/^{39}Ar$ radiometric age determinations of surface samples and water well cuttings (see Appendix).

Geologic units displayed on the 1:100,000 scale geologic map plot as part of this report include, for reasons of scale, composite units that combine several different units that could be displayed at the 1:24,000 scale. The geology database from which the 1:100,000-scale map was derived contains all of the original data collected at 1:24,000 scale resolution. Differences in resolution are shown in Figures 4 and 5.

Attributed geochemical, geochronological, structural, mineral resource, and water well lithology databases that contain point and line data are included with the map. All data sets contain geologic unit fields and location data that allow them to be plotted as separate overlays or incorporated into more detailed thematic maps. A geochemical database (see Appendix) includes all samples collected and analyzed during mapping (Figure 6), plus geochemical data from Bailey (1990), Wright and others (1979, 1980, 1982), Kuehn (1995), Shubat (1979), Ferns and McConnell (2003), M.H. Beeson (unpublished data), and S.P. Reidel (unpublished data).

Geothermal and mineral resource databases are modified extracts from statewide databases released by the Oregon Department of Geology and Mineral Industries (Gray, 1993; Black, 1994). Descriptive names for rock units are based in part on online British Geological Survey classification schemes (http://www.bgs.ac.uk/bgsrcs/: igneous rocks [Gillespie and Styles, 1999]; metamorphic rocks [Robertson, 1999]; sediments and sedimentary rocks [Hallsworth and Knox, 1999]). Volcanic rock names are assigned on the basis of geochemical data and were derived by plotting the data on total alkali versus silica (TAS) diagrams (after Le Maitre and others, 1989). Chemical analyses were recalculated to a 100 percent total without volatiles and with all iron calculated as Fe^{++}.

The first regional-scale geologic maps of the upper Grande Ronde River basin include a water resource investigation map by Hampton and Brown (1964) and 1:250,000-scale reconnaissance geologic maps of the Pendleton and Grangeville quadrangles (Walker, 1973, 1979). The western part of the basin is included on the La Grande 1:100,000-scale quadrangle (Ferns and others, 2001). Detailed studies in the basin include an engineering geology report for the La Grande area (Schlicker and Deacon, 1971) and a tectonic study of Grande Ronde Valley (Barrash and others, 1980), both of which contain 1:24,000 scale maps for the city of La Grande as well as a basin analysis of the southern Grande Ronde Valley (Ferns and others, 2002a). Other work includes structural studies by students from the University of Southern California (Gehrels, 1981; White, 1981) and more recent 1:24,000-scale geologic quadrangle maps such as the Limber Jim Creek quadrangle (Ferns and Taubeneck, 1994); Tucker Flat quadrangle (Madin, 1998), Fly Valley quadrangle (Ferns, 1999), Summerville quadrangle (Ferns and Madin, 1999); Imbler quadrangle (Ferns and others, 2002b); Mount Fanny and Little Catherine Creek quadrangles (V.S. McConnell and others, unpublished mapping); Gassett Bluff and Mount Moriah quadrangles (McConnell and others, 2004), and Union and Cove quadrangles (J.A. Johnson, unpublished mapping).

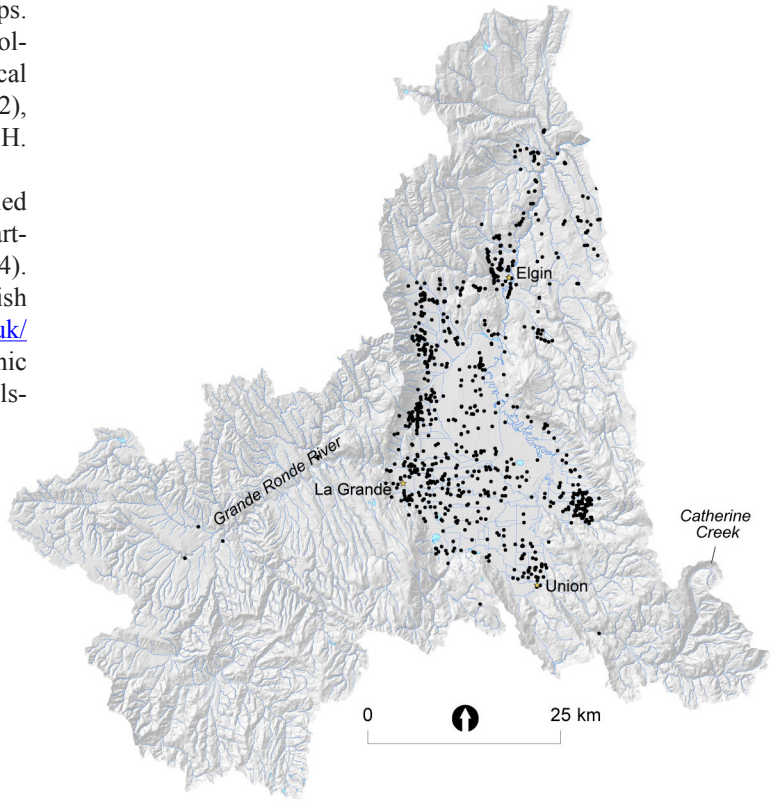

Figure 3. Locations of water wells that provided logs used in this study. Most wells are located in Grande Ronde Valley proper. All locations are approximate. Well logs are available through the Oregon Department of Water Resources (http://www.wrd.state.or.us/OWRD/GW/index.shtml).

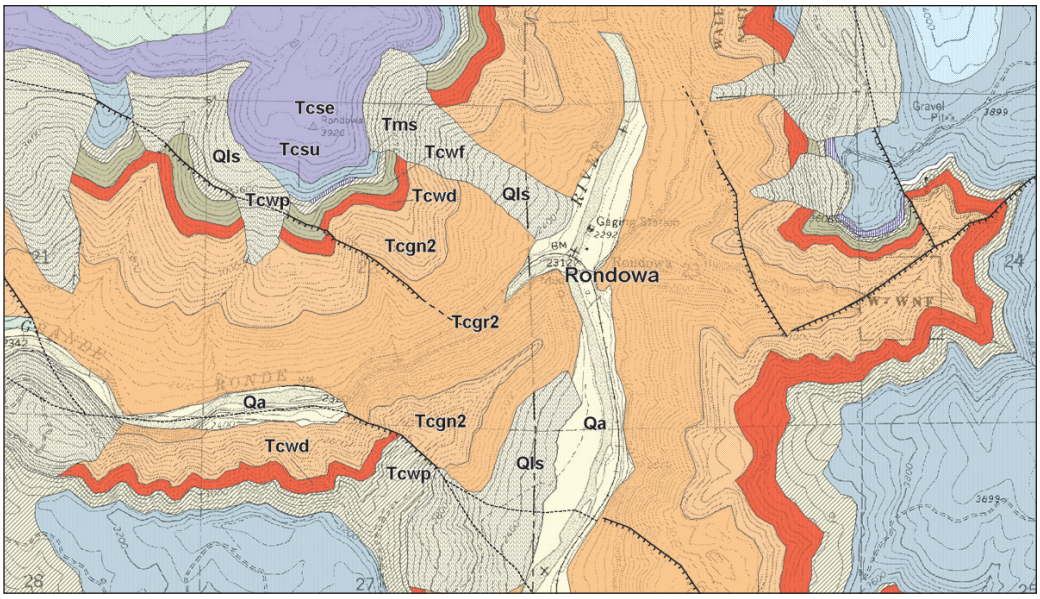

Figure 4. Geologic map of the confluence of the Grande Ronde and Wallowa rivers showing the geology at 1:24,000 scale. Here the Grande Ronde Basalt is separated into two units (Tcgn2 and Tcgr2) using magnetic polarity measurements. The Wanapum Basalt is separated into three units: Tcwd (Dodge member), Tcwf (Frenchman Springs member), and Tcwp (Powatka member). The Saddle Mountains Basalt is divided into two units: Tcsu (Umatilla member) and Tcse (Eden member). Each member is assigned a unique identifier in the geologic map database.

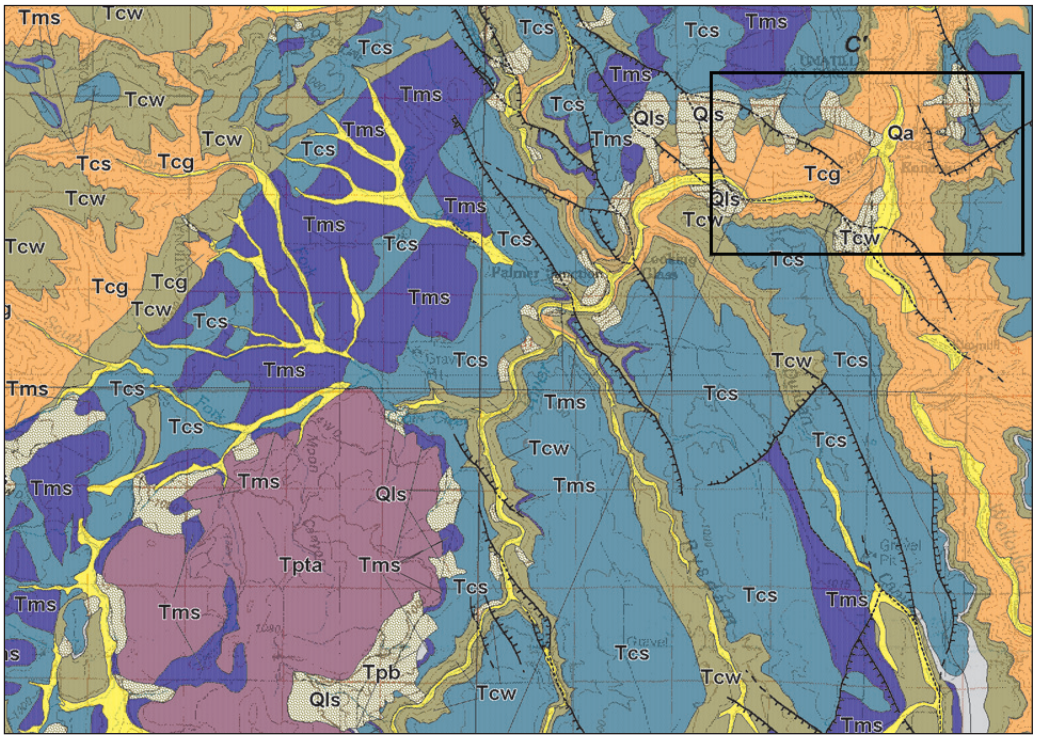

Figure 5. Geologic map of the same area shown in Figure 4 (black outline) showing geology at 1:100,000 scale. Tms includes sediments interbedded with Tcs flows.

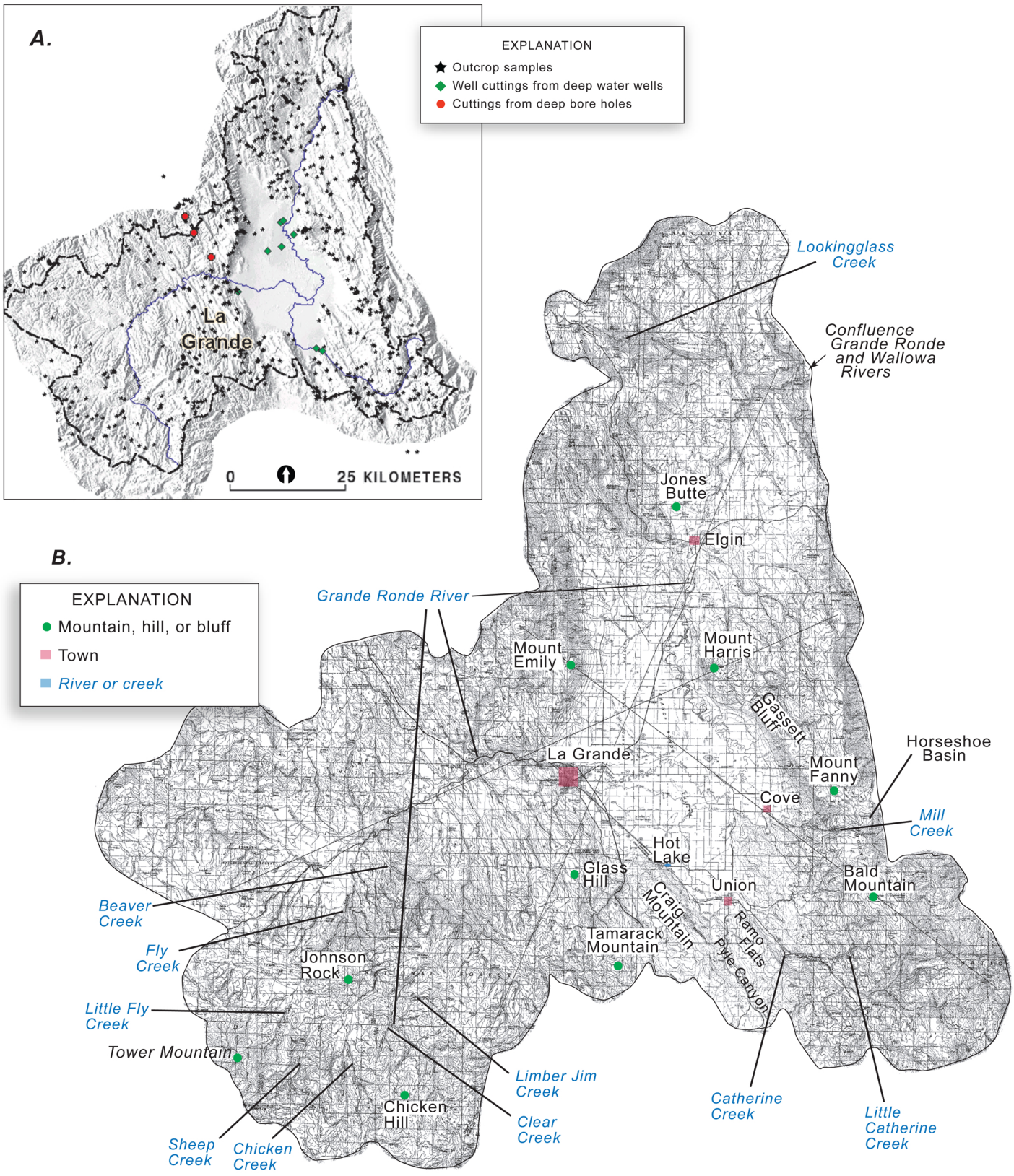

Figure 6. (A) Whole-rock XRF sample locations. Outcrop samples shown as stars. Well cuttings from deep water wells shown as green diamonds. Cuttings from deep bore holes shown as red circles. (B) Location map for geographic places mentioned in sections “Explanation of Map Units” and “Structure.”

EXPLANATION OF MAP UNITS

The upper Grande Ronde basin suite of volcanic, volcaniclastic, intrusive, metamorphic, and sedimentary rocks ranges in age from Permian to Holocene. Many middle Cenozoic stratigraphic units are discontinuous and commonly interbedded; thus contact relations can be uncertain. Widely separated units are grouped on the basis of apparent stratigraphic position, lithology, and chemical composition. Unit names follow local stratigraphic nomenclature if available; where formal rock names do not exist, informal names are given on the basis of composition or well-exposed type section.

Geochemical compositions of all rocks sampled in the map area for this study and from previous publications can be found in the spreadsheet and database files in the Appendix folder on this CD. Whole-rock XRF sample locations for outcrop and well cuttings can be found in Figure 6A, on the map plate, and in the GIS file set. Figure 6B shows geographic locations named in the text. Map units are grouped as follows:

UPPER CENOZOIC SURFICIAL AND VALLEY-FILL DEPOSITS

Qa	Alluvium
Qe	Eolian sand, loess, and ash
Qal	Lacustrine and alluvial plain deposits
Qfd	Fluvial fan delta deposits
Qf	Alluvial fan deposits
Qcf	Colluvium and talus deposits
Qls	Landslide deposits
Qg	Glacial deposits
QTt	Terrace deposits
QTs	Fluviatile and lacustrine deposits

A page-size geologic map of the Upper Grande Ronde Basin is located on page 65.

The Appendix beginning on page 62 briefly describes the data on this CD:
- Geologic data
- Geochemical data
- Water well data

CENOZOIC VOLCANIC AND SEDIMENTARY ROCKS

Powder River Volcanic Field

Tpay	Andesite and dacite
Tpta	Trachyandesite and andesite
Tptb	Basaltic trachyandesite
Tpbo	Basanite and trachybasalt
Tpv	Basaltic andesite and andesite cinder and scoria
Tpa	Andesite and basaltic andesite
Tpd	Dacite
Tpb	Basalt of Little Catherine Creek
Tpi	Basalt, andesite, dacite, and basanite intrusions

Neogene Sedimentary Rocks

Tms	Sedimentary rocks

Columbia River Basalt Group

Tcs	Saddle Mountains Basalt
Tcw	Wanapum Basalt
Tcg	Grande Ronde Basalt
Tci	Imnaha Basalt
Tcv	Vent and hydrovolcanic deposits
Tcd	Columbia River Basalt dikes

Tower Mountain caldera

Tta	Andesite and dacite flows
Ttr	Rhyolite
Ttt	Welded ash-flow tuff
Ttd	Porphyritic lava of Chicken Creek
Ttba	Basalt, basaltic andesite, and andesite
Ttvs	Volcaniclastic deposits of Limber Jim Creek
Ttb	Basalt and basaltic andesite

Tertiary subvolcanic intrusions

Ttbi	Mafic intrusions
Ttri	Rhyolite intrusions
Ttdi	Dacite, andesite intrusions

Lower Cenozoic sedimentary rocks

Teg	Conglomerate, sandstone, and siltstone

MESOZOIC INTRUSIVE ROCKS

Wallowa batholith

Kwt	Tonalite and granodiorite
Kwi	Trondjemite of Catherine Creek

Bald Mountain batholith

KJbt	Granodiorite and tonalite
KJbg	Granite
KJbi	Mafic and intermediate intrusions
KJm	Metamorphosed inclusions

MESOZOIC AND PALEOZOIC ROCKS

Wallowa terrane

TRws	Undifferentiated volcanic and clastic sedimentary rocks
TRPwc	Clover Creek Greenstone

Baker terrane

TRPbe	Elkhorn Ridge Argillite
TRPba	Amphibolite and metamorphosed intrusive rocks

UPPER CENOZOIC SURFICIAL AND VALLEY-FILL DEPOSITS

Upper Miocene to Holocene sedimentary units are found throughout the upper Grande Ronde basin. Largest accumulations are in the Grande Ronde and Indian valleys. Surficial units include alluvial-plain, fluvial fan-delta, glacial, and eolian deposits, plus fringing landslides, terraces, debris flows, and alluvial fans (Figure 7). Map units include:

Qa **Alluvium (Holocene and upper Pleistocene)**—Gravel, sand, and silt deposited in active stream channels and on flood plains. Mainly gravel and channel-sand deposits but includes overbank sand, silt, and clay deposits on low terraces along the Grande Ronde River. Locally includes alluvial fan deposits too small to map separately at the mouths of small tributary streams, and channel-sand, silt, and clay deposits in abandoned distributary channels and sloughs on the Grande Ronde River fan. Also locally includes overbank deposits of water-lain ash as much as 3 m thick. Holocene and late Pleistocene ages based on presence of circa (ca) 6,700 yr BP Mazama and ca ~10,700 yr BP Glacier Peak ashes (Cochran, 1988). Local stratigraphy is complex. Cochran (1988) documented five alluvial aggradation–stable surface–erosion cycles in Ladd Canyon over the last 11,000 years.

Qe **Eolian sand, loess, and ash (Holocene and upper Pleistocene)**—Mainly wind-deposited sand and loess. Includes local accumulations of white, air-fall ash. In Grande Ronde Valley, wind-blown sand has accumulated to thicknesses of 15 m along Sand Ridge, an undulating and vegetated surface of north-trending longitudinal dunes. Light brown, wind-blown silt as thick as 5 m locally mantles land surfaces north of Sand Ridge. The alluvial plain south of Sand Ridge is interpreted as the deflation basin from which the sand and loess were derived. Accumulations of white air-fall ash 0.5 to 1 m thick occur as erosional remnants along stream channels, in landslide sag ponds, and on timbered uplands. In most upland areas, the ash is intermixed with loess and forms a light brown soil. Unit includes Mazama and possibly older ash-fall deposits. The Mazama ash is Holocene, whereas the sand and loess deposits are mostly late Pleistocene.

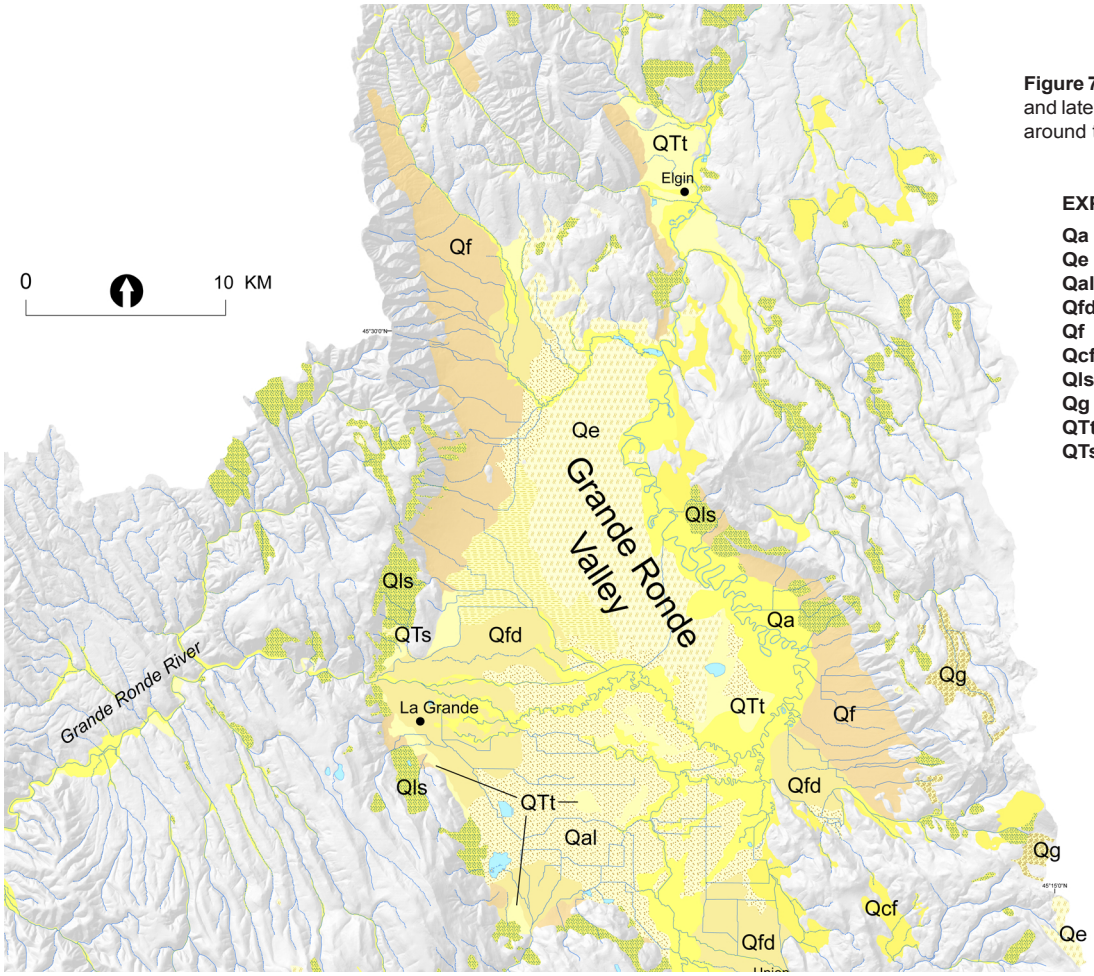

Figure 7. Shaded relief map showing Quaternary and late Tertiary sedimentary units located in and around the margins of Grande Ronde Valley.

EXPLANATION

Qa	Alluvium
Qe	Eolian sand, loess, and ash
Qal	Lacustrine and alluvial plain deposits
Qfd	Fluvial fan delta deposits
Qf	Alluvial fan deposits
Qcf	Colluvium and talus deposits
Qls	Landslide deposits
Qg	Glacial deposits
QTt	Terrace deposits
QTs	Fluviatile and lacustrine deposits

Qal **Lacustrine and alluvial plain deposits (Holocene (?) and upper Pleistocene)** — Mainly silt, clay, and diatomite deposited in the alluvial plain of Grande Ronde Valley. Includes minor lenses of pebbly, coarse- to medium-grained sand and organic- and diatomite-rich clays. Locally marked by thick black loamy soil (Hot Lake and Conley soils of Dyksterhuis and High [1985]). Indicative of marsh, low-energy fluvial, and shallow lake conditions at time of deposition. Includes marsh deposits at Ladd Marsh. Grades vertically into underlying unit QTs. Unit is less than 10 m thick at Ladd Marsh.

Qfd **Fluvial fan delta deposits (Holocene and upper Pleistocene)** — Subaerial delta plain deposits. Mainly stratified gravel, sand, and silt deposited where the Grande Ronde River and its major tributaries enter Grande Ronde Valley. Locally overlain by overbank silt and fine sand deposits. Unit interfingers with unit Qal in the lower part of the Ladd Creek fan. Below the surface of Grande Ronde Valley the unit grades vertically and laterally into underlying unit QTs. Grades down slope into the valley from coarse gravel with clay, to medium-and fine-grained gravel and sand.

Qf **Alluvial fan deposits (Holocene and Pleistocene)** — Mainly unconsolidated, poorly sorted deposits of coarse boulder gravel, gravel, and sand deposited along mountain range fronts fringing Grande Ronde Valley. Deposits grade down slope from coarse, clay-rich boulder gravel to fine- to medium-grained gravel, sand, and silt. At La Grande, includes very coarse block breccias with andesite blocks as large as 1 m across that were deposited by rock falls and small debris avalanches. Upper slopes include unstable colluvial wedges of intermixed soil and rock that mantle fault contacts. Includes both active and inactive alluvial fans. Coalescing fans form extensive bajada surfaces (Figure 8) that extend along the east and west margins of Grande Ronde Valley. On the west side of the valley the northern end of the bajada surface has been deeply incised by modern active stream channels.

Qcf **Colluvium and talus (Holocene and upper Pleistocene)** — Includes boulder- to gravel-sized angular talus with little or no soil at the base of steep cliff faces and hillslope colluvium of poorly sorted soil and rock. Deposits are generally monolithologic and are chiefly derived from cliff-forming Powder River Volcanic Field units. Unit is mapped only where both thick enough and extensive enough to mantle the underlying bedrock. Deposits vary from meters to tens of meters thick. Formed chiefly by gravity and periglacial processes (frost heaving and solifluction). May grade down slope into alluvial fan deposits and laterally into colluvial landslide and debris flow deposits.

Qls **Landslide deposits (Holocene and Pleistocene)** — Unconsolidated, chaotically mixed masses of rock and soil. Terrain is typified by sloping hummocky surfaces marked by closed depressions, springs and wet seeps, scarps, and cracks and crevices. Active or recently active landslides have tilted trees and bent tree trunks. Commonly traceable upslope to headwall scarps or slip surfaces. Unit includes rock fall, mudflow and debris flow deposits. Bedrock landslides in the map area typically form where coherent lava flows overlie tuffaceous sediment. Includes composite landslides along the Grande Ronde River that are as large as 7 km^2 in area. The composite landslides commonly consist of individual slides of different ages that form coalescing masses. Includes landslides of colluvium, rapidly emplaced debris flow deposits, and more deeply rooted bedrock slides. Debris flow deposits down slope of the range front (Figure 9) typically form lobate masses on alluvial fans that are disconnected from the landslide scarp or failure zone. Debris flow deposits along the margins of Grande Ronde Valley apparently formed during catastrophic collapse of high-standing dacite cliffs at Mount Emily and Mount Harris. Older slides are commonly mantled by loess and Mazama ash. Open ground fissures and marginal levees mark younger, active slides, such as those at the north end of Indian Valley, north of Elgin.

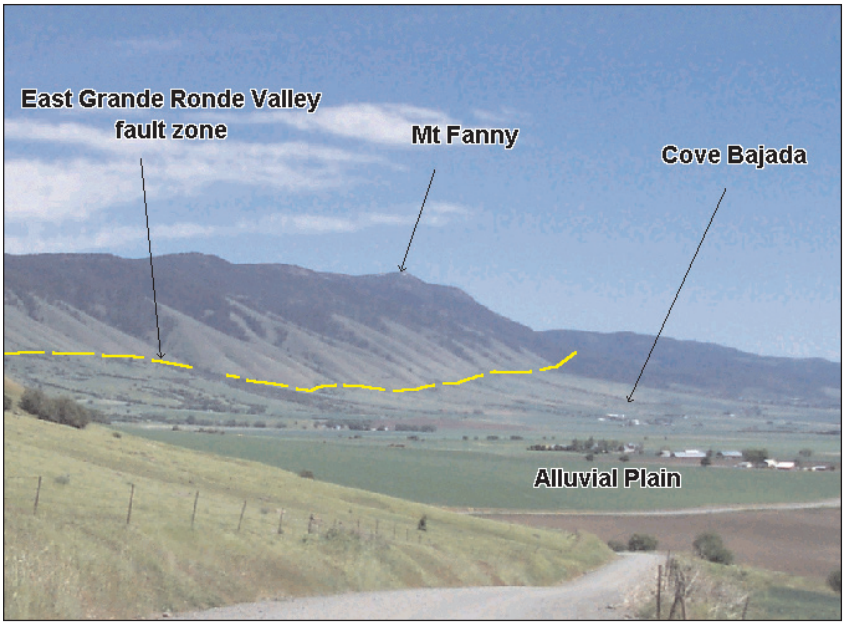

Figure 8. Photograph of the east side of Grande Ronde Valley, showing the Cove bajada, alluvial fan depositis (unit Qf), and the track of the East Grande Ronde Valley fault zone (yellow line). Looking southeast from near the base of Mount Harris.

Qg **Glacial deposits (upper and middle Pleistocene)**—Unconsolidated, poorly stratified deposits of till, coarse gravel, fine silt, sand, and loess, derived largely from granitic rocks of the Bald Mountain and Wallowa batholiths. Till, exposed mainly in lateral moraines along the upper reaches of the Grande Ronde River and Catherine Creek, typically consists of granitic boulders and blocks as large as 150 cm in diameter. Till on the upper reaches of Mill Creek and Indian Creek is made up of large andesite boulders and blocks. Unit includes well-preserved lateral and recessional moraines of the late Pleistocene Pinedale glaciation (10,000–30,000 yr BP) and poorly preserved lateral moraines of the middle Pleistocene Bull Lake glaciation (150,000–200,000 yr BP) (Crandell, 1967; Richmond, 1986; Bilderback, 1999; Geraghty, 1999). Pinedale till forms sharp, topographically distinct glacial features marked by solid granitic boulders, whereas the older Bull Lake till on the Grande Ronde River forms less distinct glacial features marked by grussy soils formed from disintegrating heavily weathered granitic clasts.

QTt **Terrace deposits (Pleistocene and Pliocene (?))**—Unconsolidated to poorly consolidated deposits of gravel, pebbly coarse sand, and medium- to fine-grained sand. In the Sheep Creek area on the headwaters of the Grande Ronde River, includes coarse gravel terraces preserved at two levels: the upper terrace stands 60 m above the modern streambed, whereas the lower terrace is 3 to 10 m above the modern alluvial plain. Along the west side of Grande Ronde Valley, unit includes remnants of a fringing east-sloping terrace that stands 20 to 30 m above the modern valley floor. Includes sinuous, 5- to 12-m-high ridges of fine-grained gravel and sand in the central part of Grande Ronde Valley (Ferns and others, 2002a,b). Includes a 50-m-thick section of medium to coarse volcaniclastic gravel in Indian Valley near Elgin. Possible Pliocene age for the older terraces inferred from Indian Valley gravel that underlies the 2 Ma Jones Butte (Walker, 1979; Bunker and others, 1982). Pleistocene age in part based on a radiocarbon age of 15,280 ± 180 yr BP from a mammoth tooth recovered atop the terrace gravel at the Eastern Oregon University campus (Ferns and others, 2001).

QTs **Fluviatile and lacustrine deposits (Pleistocene, Pliocene, and upper Miocene)**—Poorly consolidated and poorly exposed deposits of clay, silt, sand, and gravel in alluvial-plain, fan-delta, stream-channel, and alluvial-fan deposits. Unit includes all sediment between the top of the Powder River Volcanic Field and the base of late Pleistocene and Holocene geomorphic landforms including locally present black organic-rich clay, pale red paleosol, white diatomite, and white air-fall tuff. In Grande Ronde Valley, the unit is more than 560 m thick and consists mainly of alluvial plain deposits of sandy silt and clay with thin interbeds of sand and fine-grained gravel. Drillers' logs from water wells throughout the valley show that Grande Ronde Valley sediment coarsens upward from alluvial-plain clay and silt to stream-channel and fan-delta gravel and laterally to clay-rich alluvial fan gravel along the valley's margins. Base of the unit in the northern Grande Ronde Valley is marked by peaty clay and fine sand indicative of marsh and bog environments (Van Tassell and others, 2001). Lower late-Miocene isochron age of 7.5 ± 0.11 Ma from glass shards in water-lain ash recovered from 472 m depth (Ferns and others, 2001). Pliocene age based on fish fossils, diatoms, and a $^{40}Ar/^{39}Ar$ age of 3.1 ± 0.3 Ma from glass shards in water-lain ash recovered from 110 m depth (Van Tassell and others, 2000, 2001).

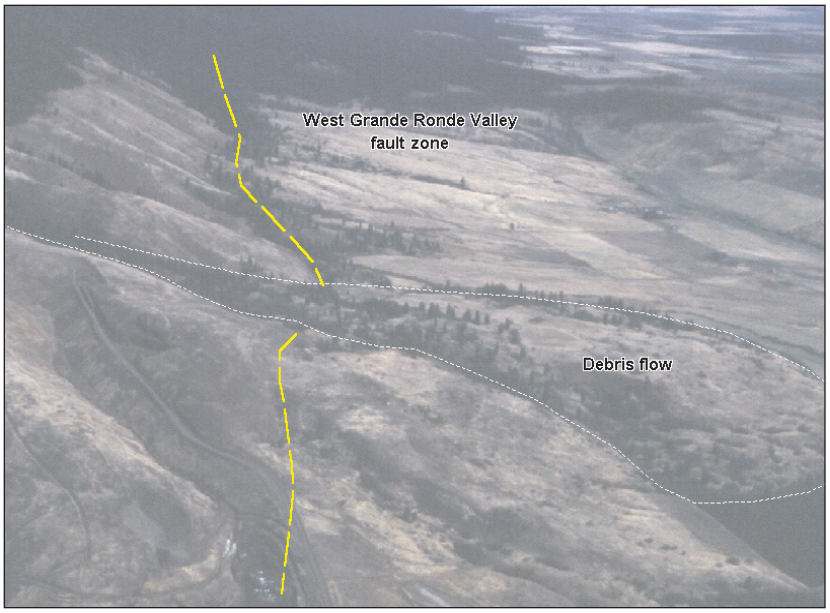

Figure 9. Aerial photograph looking north from above La Grande of the track of the main West Grande Ronde Valley fault (yellow line) and debris flow (white dashed line).

CENOZOIC VOLCANIC AND SEDIMENTARY ROCKS

The bulk of the bedrock in the upper Grande Ronde basin comprises three distinct Cenozoic volcanic suites: the Powder River Volcanic Field, the Columbia River Basalt Group, and the Tower Mountain caldera (see Appendix). The middle-Miocene to Pliocene Powder River Volcanic Field, centered on Grande Ronde Valley, includes calc-alkaline and alkaline lava (Figures 10 and 11) erupted from small shield volcanoes and stratovolcanoes. Middle-Miocene Columbia River Basalt, the oldest rock exposed in most of the middle and northern parts of the basin, is a regionally extensive series of tholeiitic flood lavas that extend across northern Oregon and southern Washington from the Snake River to the Pacific coastline. The late-Oligocene Tower Mountain caldera is a large rhyolite eruptive center that forms the part of the highlands along the southwestern margin of the basin (Ferns, 2002).

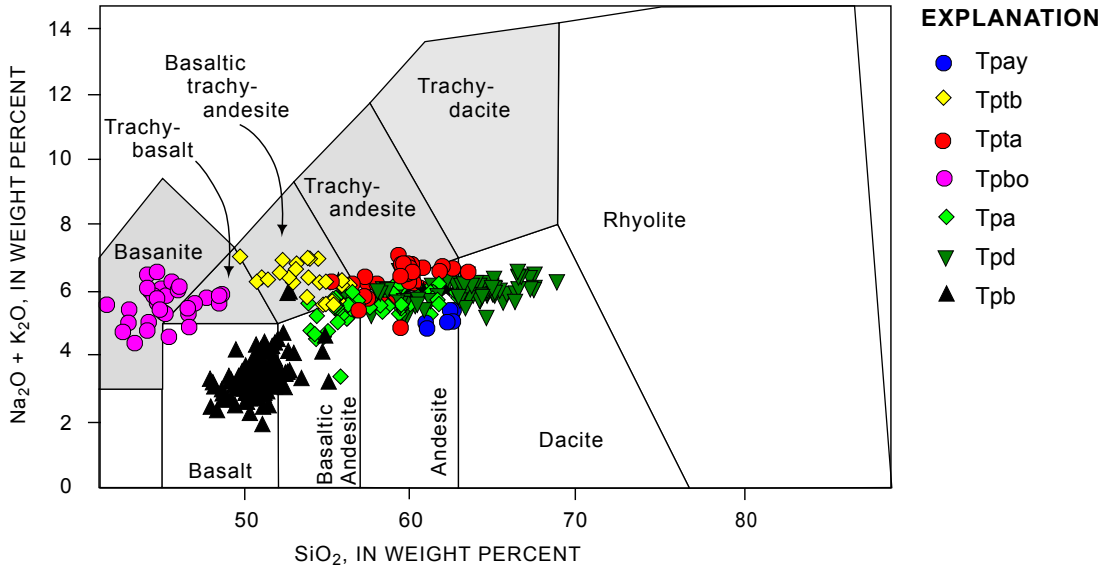

Figure 10. Total alkali vs. silica (TAS) diagram for Powder River Volcanic Field lavas. Youngest flows (Tpay) at Jones Butte and Tamarack Mountain are high-silica andesites. Note that the phyric flows from the small volcanoes in the north end of the field (Tptb and Tpta) are richer in K_2O and Na_2O than the large, aphyric flows in the south (Tpa and Tpd).

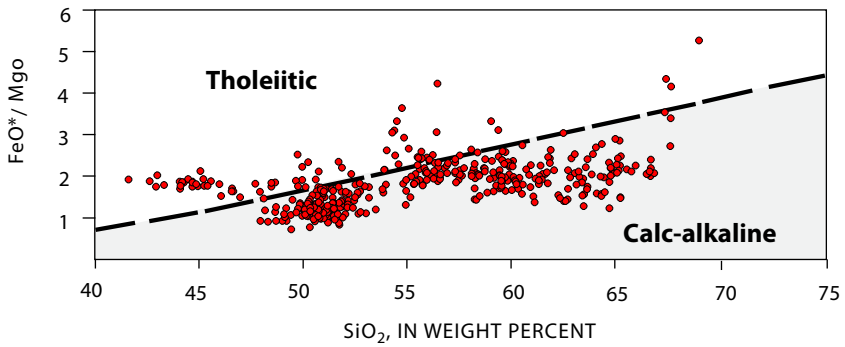

Figure 11. FeO*/MgO vs. SiO_2 plot of Powder River Volcanic Field lavas shows an overall calc-alkaline trend. Although the low-silica flows plot in the tholeiitic field, the overall trend is strongly calc-alkaline. Calc-alkaline/tholeiite trend from Miyashiro (1974). (See Appendix file `XRF_UGRB_Cenozoic.xls` on this CD.)

Powder River Volcanic Field (Middle Miocene to Early Pleistocene (?))

Lava flows that range from dacite to basalt in composition erupted from small volcanic vents form the Powder River Volcanic Field (PRVF) (Bailey, 1990; Ferns and others, 2001, 2002a). Powder River Volcanic Field flows are exposed along the margins of Grande Ronde Valley over an area of about 825 km^2, reaching combined thicknesses of as much as 400 m. (See "Geologic History" section, Figure 48 for distribution in map area.) Water well logs indicate that the floor of Grande Ronde Valley is underlain by a similar thickness of similar lava flows. The base of the field possesses a series of olivine basalt lava flows (Tpb) as much as 100 m thick. The olivine basalt is locally and intermittently underlain by tuffaceous fluviatile sediment that contains interbedded silicic tuff breccia and obsidian clast gravel. The olivine basalt is overlain by an interfingered series of dacite (Tpd), andesite, basaltic andesite (Tpa), and basanite (Tpbo) lava flows. The andesite and dacite are thick accumulations of chiefly very fine grained, aphyric lava from local eruptive centers. Although several small basaltic andesite cinder cones (Tpv) occur along the southern margin of Grande Ronde Valley, the thick masses of andesite and dacite lavas that presumably mark eruptive centers to the east are notably lacking related pyroclastic deposits. Mount Harris, the most notable of the east margin vents, possesses a central dacite spire (Figure 12). Dacite lava flows, possibly flow domes, cover areas as large as 50 km^2 up to 130 m thick. Most Tpd and Tpa lavas display calc-alkaline affinities (Figure 10). Younger intracanyon flows of olivine-rich basanite and trachybasalt (Tpbo) lap around the dacite highs in the Indian Creek area, east of Grande Ronde Valley. The Tpbo lava flows are basanites and trachybasalts that may locally interfinger with dacite and andesite lava flows. The northern part of the Powder River Volcanic Field is defined by a number of small late-Miocene domes and shield volcanoes (Tpta), herein referred to as the Elgin Volcanic Complex. Most of the Elgin volcanoes are small, covering less than 5 km^2, and many consist of a single trachyandesite (Tpta) or basaltic trachyandesite (Tptb) lava flow. Similar small late-Miocene basaltic-trachyandesite and trachyandesite volcanoes are exposed west of Grande Ronde Valley in the Sugarloaf Mountain region (Kienle and others, 1979; Ferns and others, 2001). Pliocene volcanism is represented by Jones Butte and Tamarack Mountain, two very small, aphyric andesites that, although separated by Grande Ronde Valley, are remarkably similar in chemical composition to the late-Miocene andesites.

Tpay Andesite and dacite (Pliocene and early Pleistocene (?))—Fine-grained gray to pinkish-red, high-silica andesite and dacite lava. Includes a pale red to pinkish gray, vesicular hornblende dacite at Jones Butte and a gray trachytic andesite at Tamarack Mountain. The Jones Butte dacite forms 120-m-high rounded hill in Indian Valley (Figure 13). The top of Jones Butte has been intensely altered by vapor phase mineralization. Thin section shows blocky feldspar and oxide-rimmed hornblende crystals set in a matrix of altered glass; hornblende phenocrysts are almost totally replaced by opaque iron oxide minerals. The Tama-

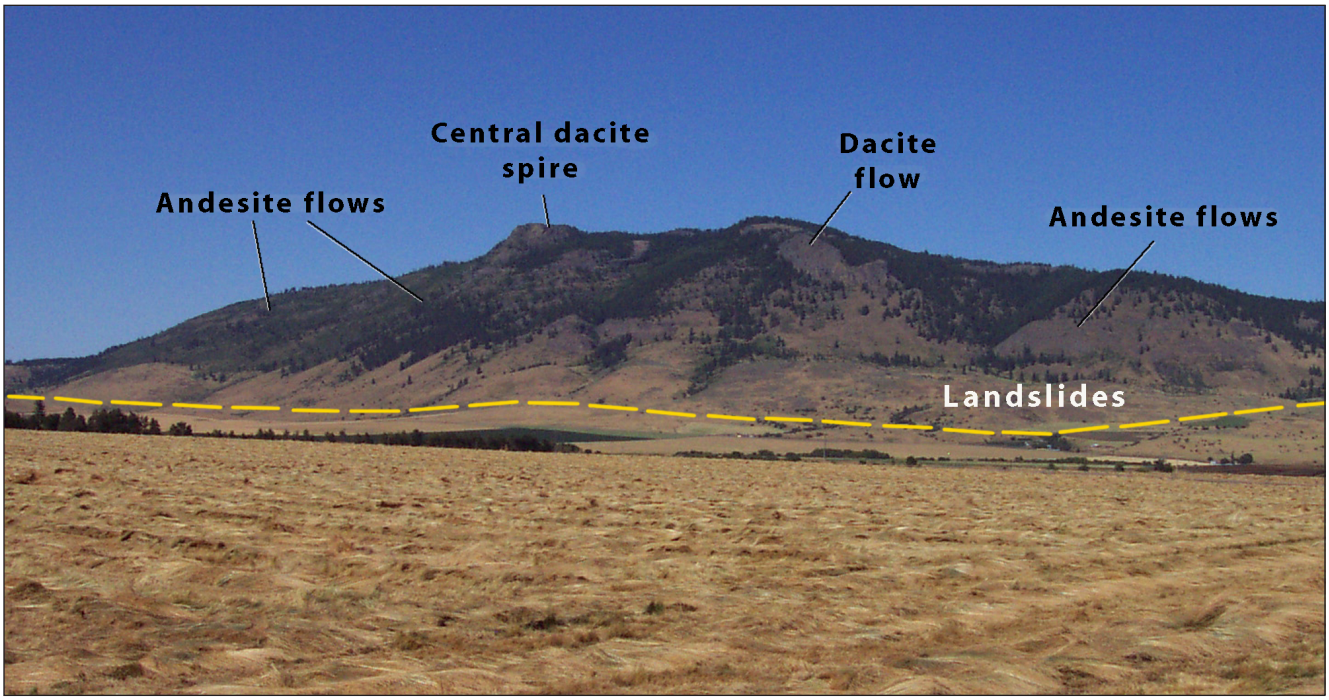

Figure 12. Mount Harris volcano, looking east from Sand Ridge. Mount Harris is a small stratovolcano that rises above northeast Grande Ronde Valley. Dashed yellow line shows approximate trace of the East Grande Ronde Valley fault zone.

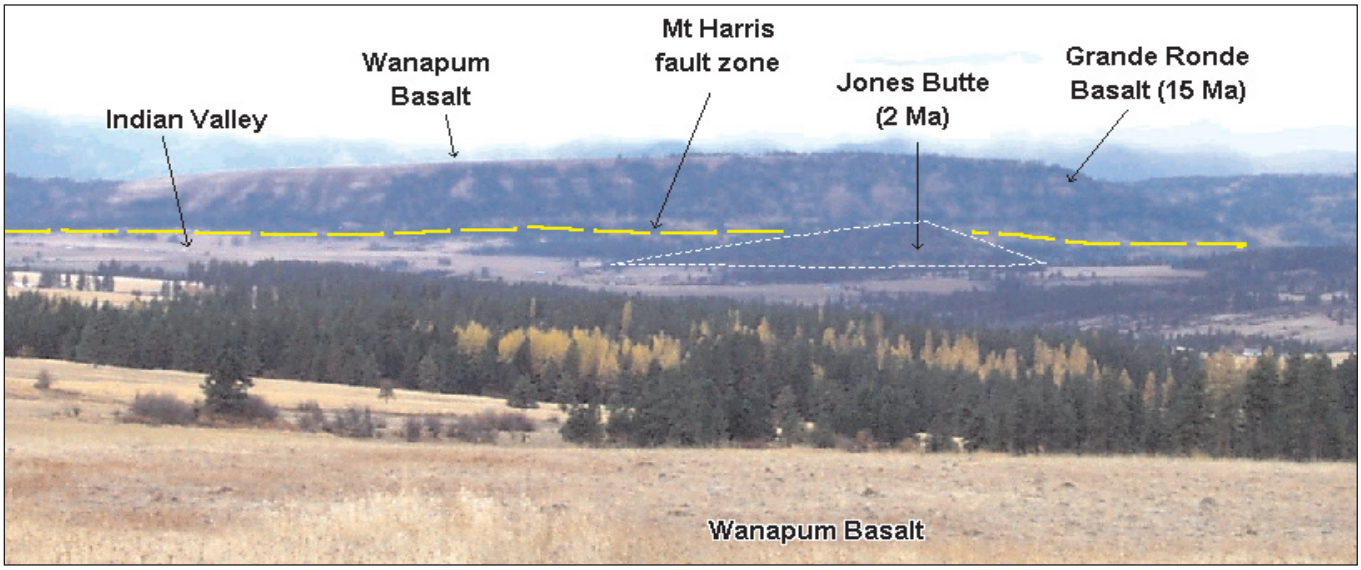

Figure 13. Photograph of the late Pliocene volcano at Jones Butte in Indian Valley looking west from Cricket Flat. The Mount Harris fault zone, shown by the yellow dashed line, separates Indian Valley from an uplifted block of older Grande Ronde and Wanapum Basalt flows.

rack Mountain andesite is a 100-m-thick platy intracanyon flow that forms a low-relief table. In thin section, orthopyroxene and plagioclase phenocrysts are set in a trachytic groundmass of plagioclase and brown interstitial glass. The andesite and dacite, ranging from 61.02 to 62.68 weight percent SiO_2, are markedly high in alumina and display somewhat similar compositions (see Appendix). Rock unit is Pliocene in age on the basis of an $^{40}Ar/^{39}Ar$ isotope age of 3.18 ± 0.15 Ma for the andesite of Tamarack Mountain (Ferns and others, 2001) and a K-Ar radiometric age of 2.0 ± 0.8 Ma for Jones Butte (Bunker and others, 1982) (Figure 13).

Tpta Trachyandesite and andesite (upper Miocene)—Light bluish-gray to gray, aphyric to porphyritic trachyandesite and andesite lava flows that form small, broad buttes extending from Green Mountain, west of Mount Emily, through Elgin and east to Stubblefield Mountain. Unit consists of small (< 1 km^2) lava flows and small shield volcanoes. Lavas are typically fine grained, flow foliated, and have small, irregularly shaped vesicles. Some, such as Stubblefield Mountain, have hornblende phenocrysts. Fine-grained pilotaxitic textures, common in thin section, display a mat of aligned plagioclase needles wrapping rotated and partially resorbed orthopyroxene, clinopyroxene, or olivine microphenocrysts. Includes andesites and trachyandesites with 57.31–62 weight percent SiO_2 (see Appendix). Late Miocene age on basis of stratigraphic position and a $^{39}Ar/^{40}Ar$ isochron age of 5.7 ± 0.9 Ma for the Rock Wall flow north of Elgin.

Tptb Basaltic trachyandesite (upper Miocene)—Light bluish-gray to gray, fine-grained aphyric to porphyritic basaltic trachyandesite lava flows. Lava is typically flow-foliated, markedly porphyritic with black amphibole phenocrysts as long as 8 mm, and commonly has small, irregularly shaped vesicles. Unit forms small, broad buttes that extend from Sugarloaf Mountain, west of Mount Emily, to Indian Creek, southeast of Elgin. Unit consists of small (< 1 km^2) lava flows and small shield volcanoes. Lava flows are commonly trachytic, with green clinopyroxene and plagioclase phenocrysts, as long as 3 mm. Relict amphibole phenocrysts are commonly replaced by opaque iron oxides, and oxide masses are in places rimmed or cored by small clinopyroxene crystals. Ranges from 51.05 to 54.55 weight percent SiO_2; 15.55 to 17.49 weight percent Al_2O_3; and 6.24 to 6.96 weight percent $Na_2O + K_2O$. Late Miocene age on basis of stratigraphic position and K-Ar ages of 6.54 ± 0.14 Ma; 7.26 ± 0.11 Ma; and 7.32 ± 0.15 Ma (Kienle and others, 1979) for the small shield volcanoes near Sugarloaf Mountain.

Tpbo Basanite and trachybasalt (upper or middle Miocene)—Dark bluish gray to very dark gray, aphanitic to glassy, olivine-phyric lava flows. Fresh black surfaces are distinguished by 4 to 12 percent clear yellow olivine phenocrysts 0.5 to 3 mm across. Weathered surfaces typically bluish gray or reddish gray. Individual flows are as thick as 80 m and weather to form blocky, talus-strewn slopes (Figure 14). Includes at least four different locations, including basanite flows at Horseshoe Basin on the east side of Grande Ronde Valley and at Glass Hill on the southwest side of the valley, and a trachybasalt flow exposed at Phys Point, between Cove and Union. Rock is difficult to break, rings like a bell on impact, and forms conchoidal fractures. In thin section the basanite typically contains as much as 10 percent euhedral olivine crystals 0.5 to 3 mm across and 7 percent iron/titanium oxides set in a microcrystalline groundmass of

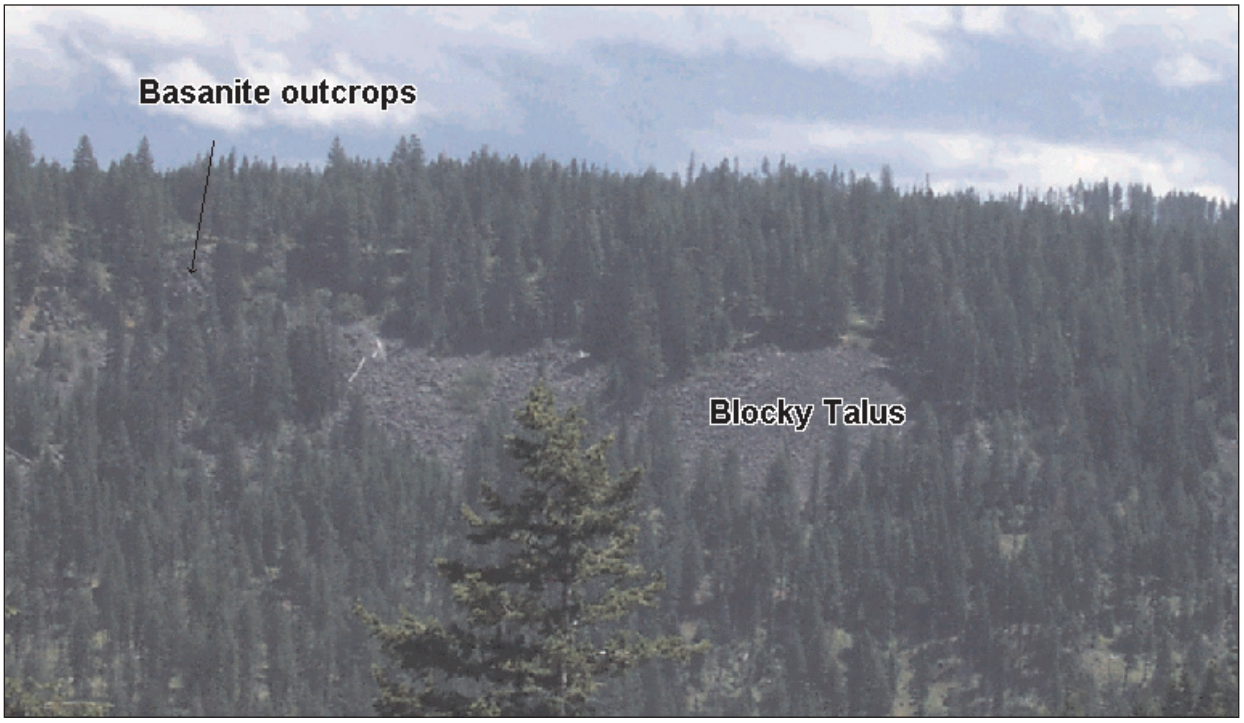

Figure 14. Photograph of the basanite of Horseshoe Basin, looking southeast from near the headwaters of Clarks Creek. Dark gray blocky talus is characteristic of this unit.

intersertal to intergranular plagioclase, FeTi oxides, clinopyroxene, alkali feldspar, and biotite. Distinguished chemically (Figure 11) by low silica (41.61 to 48.45 weight percent SiO_2) and high titanium and high total alkalis (2.49 to 3.49 weight percent TiO_2 and 5.57 to 6.26 weight percent K_2O + Na_2O). Stratigraphic position is not everywhere clear; the Horseshoe Basin lavas form an intracanyon flow in an older paleotopographic surface and in places overlie Tpd dacite flows. In other places the Horseshoe Basin lavas are topographically below Tpd dacite flows. Middle Miocene age on basis of plateau $^{40}Ar/^{39}Ar$ age of 10.85 ± 0.18 Ma for the Horseshoe Basin flow and a plateau $^{40}Ar/^{39}Ar$ age of 11.6 ± 0.4 Ma for a vent-related flow near South Baldy (McConnell and others, 2003). Includes the basanite of Horseshoe Basin (McConnell and others, 2003), the "Bell Tone" basanite of Ferns and others (2002b), and the Glass Butte black olivine basalt of Barrash and others (1980).

Tpv **Basaltic andesite and andesite cinder and scoria (upper or middle Miocene)**—Poorly to moderately well-bedded vent deposits of brick-red to reddish-gray scoria, lapilli, and volcanic bombs. Angular lithic clasts average 1–10 cm across but are as large as 80 cm. Spindle bombs are also as long as 80 cm. Unit includes three partially eroded cinder cones near Ramo Flat, southeast of Union, that are aligned parallel to a northwest-trending fault system. The north cinder cone is over 70 m high and is cut by a massive, 10-m-high, highly resistant plagioclase-phyric basaltic-andesite dike on its northwest flank. Southern flanks of the cones are mantled by thin basaltic-andesite lava flows (Tpa).

Tpa **Andesite and basaltic andesite (middle Miocene)**—Lava flows vary from dark gray, very fine to medium grained, porphyritic, vesicular lava flows, to gray, platy jointed, aphyric to light- to medium-gray fine-grained lava flows. Porphyritic flows have 1 to 2 percent plagioclase 2 to 5 mm across. A 180-m-thick flow-on-flow sequence of red-weathering andesite forms the base of the Mount Harris volcano (Figure 12). Includes andesite flows at the base of Gasset Bluff (McConnell and others, 2003), 180 m of red-weathering andesite and dacite flows at the base of the Mount Harris volcano, andesite flows southwest of La Grande, and basaltic andesite flows associated with the Ramo Flat cinder cones (Tpv). In thin section, characterized by blocky plagioclase set in either a hyalophitic or pilotaxitic groundmass. Some Mount Harris flows contain orthopyroxene microphenocrysts, whereas Ramo Flat flows contain olivine and orthopyroxene microphenocrysts. Unit is chiefly andesite but ranges in composition from basaltic andesite to low-silica dacite, with 53.88 to 63.00 weight percent SiO_2 (see Appendix). Radiogenic argon measurements of a Ramo Flat flow produced a maximum $^{40}Ar/^{39}Ar$ age of 12.0 ± 0.17 Ma for a sample that did not yield either a plateau $^{40}Ar/^{39}Ar$ or isochron age. Bailey (1990) reported a total fusion $^{40}Ar/^{39}Ar$ age of 13.0 ± 0.1 Ma for an andesite flow at Sawtooth Crater; located southeast of the upper Grande Ronde River basin.

Unit includes the "glassy basalt" unit of Barrash and others (1980), the andesite unit of Bailey (1990), the basaltic andesite of Ramo Flat, and the andesite and basaltic andesite units of Ferns and others (2001, 2002a).

Tpd **Dacite (middle Miocene)**—Very light bluish-gray to light pinkish gray, aphyric to sparsely porphyritic lava flows and domes. Stony rock is commonly peppered with finely disseminated iron oxides. Outcrop varies from bold rounded bouldery cliffs to platy flows. The platy parts are characterized by steeply dipping, closely spaced, subhorizontal to subvertical partings (Figure 15) and weather readily to small angular chips. Unit includes early massive flows that are as thick as 130 m and extend over areas as large as 90 km^2. Includes domes and plugs that form the cores of volcanoes such as Mount Harris. Source vents have been identified only at Mount Harris; elsewhere, eruptive sites may correspond to low knolls that mark thickened accumulations of lava flows. Columnar joints more than 1 m across commonly mark interiors of thick flows, such as those exposed at Mount Emily and Point Prominence. Coarse, matrix-supported, vitrophyre-block breccias are locally exposed at the base of the Mount Emily flow, which in places possesses a vesicular flow top. In hand sample, platy flows are pale blue gray and aphyric with millimeter- to centimeter-scale pink and white striping parallel to parting planes that resulted from vapor-phase crystallization of feldspar and hornblende microphenocrysts. In thin section the flows typically contain disseminated microphenocrysts of Fe-Ti oxide and/or clinopyroxene set in a very fine grained pilotaxitic groundmass of plagioclase, clinopyroxene, orthopyroxene, and Fe-Ti oxide crystals. On the east and south sides of Grande Ronde Valley the unit comprises two or more flows that reach more than 250 m in aggregate thickness. Near Mill Creek a thin, black, vesicular, glassy aphyric dacite flow crops out between two thick aphanitic stony dacite flows. Near Ladd Canyon the unit contains at least two separate flows that are locally separated by thin (0.5 m) lithic sandstone (Barrash and others, 1980). Dacitic in composition, with SiO_2 ranging from 61.70 to 68.96 (see Appendix). Age is middle Miocene on the basis of five $^{40}Ar/^{39}Ar$ age plateau ages: 1) summit plug of Mount Harris, 11.86 + 0.12 Ma; (McConnell and others, 2003) 2); top of Mount Fanny, 11.8 + 0.18 Ma (McConnell and others, 2003); 3) Dunns Bluff, 12.10 + 0.10 Ma, 4) a black glassy aphyric dacite flow near Medical Springs, 12.02 + 0.2 Ma; and 5) Mount Emily, 13.38 ± 0.24 Ma (Ferns and Madin, 1999).

Tpb **Basalt of Little Catherine Creek (middle Miocene)**—Flow-on-flow sequences of vesicular fine- to medium-grained olivine basalt flows. Generally medium to light gray with 8–10 percent olivine as large as 4 mm across. Commonly characterized by a diktytaxitic texture with olivine phenocrysts set in an open-textured groundmass of coarse feldspar laths, but includes fine-grained flows that have subophitic to intersertal groundmasses of feldspar, clinopyroxene, FeTi oxides, and olivine. Weathers to compact rounded boulders in a granular soil. Individual

Figure 15. Dacite exposures in Little Valley showing typical folded appearance in the upper, platy part of the flow as contrasted to the more massive, blocky weathering interior of the flow. Individual dacite flows are as much as 100 m thick.

basalt flows are typically 2–10 m thick. In the valley, well cuttings show that the flows are commonly separated from one another by fine-grained sediment and soil. A 70-m-thick flow measured from well cuttings may represent intracanyon or multiple flows with no obvious compositional or temporal break between flows. The 1-m-thick pillow lava on Indian Creek rests on a yellow hydroclastic breccia. Unit thickness ranges from 5 m in the west, where a single flow is exposed near Starkey (Figure 16), to more than 150 m (based on drill cuttings) in Grande Ronde Valley at La Grande. Unit ranges in chemical composition from about 48 to 52 percent SiO_2. Bailey (1990) noted three geochemical variants, including 1) high-alumina olivine tholeiite, 2) low-titanium and low-phosphorous olivine tholeiite, and 3) high-titanium and high-phosphorous olivine tholeiite. Analyses of water-well cuttings show that flows at the top of the unit contain more phosphorous and titanium than those at the base of the unit. Hooper and Swanson (1990) included the PRVF basalt in the Columbia River Basalt Group but noted a higher P_2O_5/TiO_2, Al_2O_3, and Sr and lower Fe than Columbia River Basalt Group flows with the same MgO content. These basalt flows are locally separated from underlying Grande Ronde Basalt by a thin layer of tuffaceous sediment, ash-flow tuff, or cobble gravel. Where overlain by units Tpd or Tpa, the unit has tendency to form large landslides. Lowermost flows have reversely polarized thermal remnant magnetism; uppermost flows possess normal polarity. Middle Miocene on the basis of $^{40}Ar/^{39}Ar$ whole rock ages of 13.3 ± 0.8, Ma, 13.7 ± 0.1 Ma, and 14.4 ± 0.2 Ma determinations on flows 20 km southeast of the map area (Bailey, 1990). North of Elgin, Tpb olivine basalt flows overlie and underlie the Umatilla member of the Saddle Mountains Basalt. (See Geologic History section, Figure 47, for distribution in map area.) Includes the diktytaxitic basalt unit of Barrash and others (1980), the basalt of Cricket Flat (Hooper and Swanson, 1990), the Levi flow of Shubat (1979), and the basalt of Red Ridge (Madin, 1998).

Tpi **Basalt, andesite, dacite, and basanite intrusions (middle Miocene)**—Dikes and sills including gray, hackly jointed, hornblende-phyric basaltic trachyandesite and dacite; bluish black, olivine phyric basanite; aphyric dacite; and olivine basalt. A 30-m-thick basaltic trachyandesite sill is exposed below the summit of Mount Emily on the west side of Grande Ronde Valley. In thin section the Mount Emily sill contains small clinopyroxene crystals and as much as 2 percent euhedral hornblende crystals up to 5 mm in length set in a trachytic groundmass of feldspar and granular clinopyroxene crystals. A 30-m-thick, columnar-jointed hornblende-dacite sill and a 400-m-long hornblende-dacite dike are exposed 5 km and 4.5 km northeast, respectively, of Cove. The sill and dike have 7–10 percent seriate hornblende as long as 1 cm. A columnar-jointed dacite dike at Mill Creek, southeast of Cove, sheds 15- to 30-cm-diameter, 5-m-long columns. The unit includes nearly all of the lava types in the Powder River Volcanic Field (see Appendix).

Figure 16. Olivine basalt flow of Basalt of Little Catherine Creek (unit Tpb) has a massive columnar-jointed interior capped by hackly jointing. Yellow line separates lava flow from the underlying coarse, rounded fluvial gravels (unit Tms). Photograph taken along the road near Starkey.

Neogene Sedimentary Rocks

Although generally described as being separate from the Columbia River Basalt Group (Walker, 1990), Neogene sedimentary and silicic volcaniclastic interbeds are an important component of the middle- to late-Miocene stratigraphy of northeastern Oregon. In the northern part of the basin, sedimentary interbeds separate members of the Saddle Mountains Basalt, the uppermost formation in the Columbia River Basalt Group. In the southern part of the basin, similar interbeds separate Powder River Volcanic Field flows from the underlying Grande Ronde Basalt. Map unit Tms, described below, includes Neogene sedimentary rocks that were deposited following the last Wanapum Basalt eruption.

Tms **Sedimentary rocks (early Pliocene(?) to middle Miocene)**—Weakly indurated, tuffaceous and arkosic gravel, sand, and silt, and intercalated ash-flow tuffs of limited extent. Map unit includes sedimentary rocks deposited between eruptions of the last Wanapum Basalt flow of the Columbia River Basalt Group and the last Powder River Volcanic Field flow. More localized members occur as interbeds within both the Saddle Mountains Basalt (Tcs) and the Powder River Volcanic Field. Generally separated into members on basis of stratigraphic position (Stoffel, 1984) and geographic distribution (Walker, 1990; Ferns and others, 2001), with the assumption that the modern basins were middle Miocene depositional centers. Where capped by lava flows, the unit readily forms landslides. Commonly exposed only in recent road cuts. Also preserved in small, disconnected basins where mantled by coarse terrace and alluvial-fan gravel deposits (Farooqui and others, 1981). Water well logs indicate that the upper part of the unit north of Elgin, where the rock consists largely of tuffaceous and arkosic, fine-grained sandstone and siltstone, is more than 150 m thick. Northern part of unit correlated by Stoffel (1984) with the Ellensburg Formation of Smith (1901). Southern part of unit extends southwest of the map area into the lower Powder River Valley where unit thickens to 150 m (Walker, 1990). Middle Miocene to Pliocene age on the basis of stratigraphic position. Typical exposures include:

- **Sediment of La Grande** (Ferns and others, 2001) overlies the Grande Ronde Basalt (Tcg) and crops out beneath an olivine basalt flow at the base of the Powder River Volcanic Field. Includes tuffaceous siltstone, mudstone, fine-grained tuffaceous and arkosic sandstone, diatomite, and rhyolitic lithic tuff. The lowermost member is laterally extensive and possesses mudflow breccias, rhyolitic-lithic ash-flow tuff, and air-fall tuff. (The chemical composition of the tuffs is 75.38–75.74 percent SiO_2, 13.01–14.02 percent Al_2O_3, and 5.5–5.53 percent K_2O.) Middle Miocene on the basis of stratigraphic position above the 15.54 ± 0.1 Ma ferroandesite of Fiddlers Hell.
- **Squaw Creek interbed** (Ross, 1978) overlies Wanapum Basalt (Tcw). Where exposed between the top of the Wanapum Basalt and base of the Saddle Mountains Basalt (Tcs) at Lookingglass Creek, the Squaw Creek member forms a 30-m-thick sequence of fine-grained, tuffaceous sandstone, diatomite, and vitric air-fall tuff. As at La Grande, the lowermost member is laterally extensive and is marked by mudflow breccias, lithic rhyolitic ash-flow tuff, and air-fall tuff. Middle Miocene, on the basis of stratigraphic position beneath the basalt of Umatilla (13.64 ± 0.17 Ma).
- **Rhyolitic lithic tuff** is exposed beneath basal Powder River Volcanic Field olivine basalt flows (Tpb) west of Elgin and on Cricket Flat east of Elgin (Carson, 2001). Upper part of the unit at Elgin is overlain by the 5.7 ± 0.9 Ma trachyandesite flow at the Rock Wall and the 2 Ma andesite at Jones Butte.
- The **Cricket Flat** exposures contain broken metaquartzite cobble gravel, presumably derived from the older Tertiary gravel exposed at Jim White Ridge, in the headwaters of the Minam River, as well as the rhyolitic lithic tuff above.
- **Tuffaceous siltstone and diatomite** are exposed beneath basal Powder River Volcanic Field olivine basalt flows located in the extreme southern part of the basin.
- **Tuffaceous sandstone and obsidian clast gravel** are exposed beneath the base of the Saddle Mountains Basalt near Tollgate, west of the map area.
- **Starkey member** (Ferns and others, 2001), a 100-m-thick sequence of interbedded, weakly indurated, coarse-grained tuffaceous sandstone, siltstone, and pre-Tertiary-clast, gold-bearing, pebble conglomerate. The Starkey gravel contains well-rounded quartzite cobbles presumably derived from older Tertiary gravel at Camp Carson. The olivine basalt flow (Tpb) at the base of the Powder River Volcanic Field is locally exposed near the base of this member. A 1- to 5-m-thick rhyolite lithic ash-flow tuff crops out above Grande Ronde Basalt (Tcg) flows at the base of the Starkey member near Spring Creek (Ferns and others, 2001).
- The **Menatchee Creek** (Stoffel, 1984) and **Grouse Creek** (Ross, 1978) **interbeds** in the northern exposures of the unit are marked by 1- to 4-m-thick lignite coal beds.
- Also in this unit are the **sediment of Camp Creek** (McConnell and others, 2003) and the **Grouse Creek interbeds** of Ross (1978).

Columbia River Basalt Group (Middle and Late Miocene)

Tholeiitic flood basalts form the most extensive sequence of flows in the upper Grande Ronde River basin (Figure 17; see also "Geologic History" section, Figures 44–48). The Columbia River Basalt Group (CRBG) covers over 164,000 km^2 with a combined volume of more than 175,000 km^3 (Tolan and others, 1989). CRBG members exposed in the map area are the Saddle Mountains, Wanapum, Grande Ronde, and Imnaha Basalts. Individual CRBG members were mapped on the basis of lithology, stratigraphic position, chemistry (Figures 18 and 19; Appendix), thermal remanent magnetic polarity, and petrography following the work of Swanson and others (1979, 1981), Reidel and others (1989), Hooper and Swanson (1990), and Ferns and others (2001).

Tcs **Saddle Mountains Basalt (upper and middle Miocene)**—Bluish gray to dark bluish black, aphyric and plagioclase phyric, fine- to medium-grained iron-rich basaltic trachyandesite and trachyandesite. Weathers to large blocks and readily forms talus slopes and landslides. Includes two separate units, the basalt of Eden and the basalt of Umatilla The basalt of Eden is a porphyritic holocrystalline flow marked by conspicuous feldspar phenocrysts as long as 0.5 cm and clear green olivine phenocrysts as much as 0.2 cm in diameter. The basalt of Umatilla is a gray to blue-black, fine- to medium-grained holocrystalline flow that typically weathers to pale yellow brown and pale orange brown. (See "Geologic History" section, Figure 48 for distribution in map area.) This unit varies markedly in thickness; it is as thick as 60 m locally. Goethite-filled vesicles are commonly found at the base of the Umatilla flow. Each flow is underlain by tuffaceous and arkosic sediment and readily forms

	Member of CRBG	Age (approximate)	Polarity
MIOCENE Middle	Saddle Mountains Basalt	14.5-8.5 Ma (10 units)	R, N, R
	Wanapum Basalt	15.6-14.5 Ma (4 units)	N, R
MIOCENE Lower	Grande Ronde Basalt	16.1-15.0 Ma	R, N, R, N
	Picture Gorge Basalt	14.6-15.8 Ma	R, N
	Imnaha Basalt	16.5-16.1 Ma	R, N

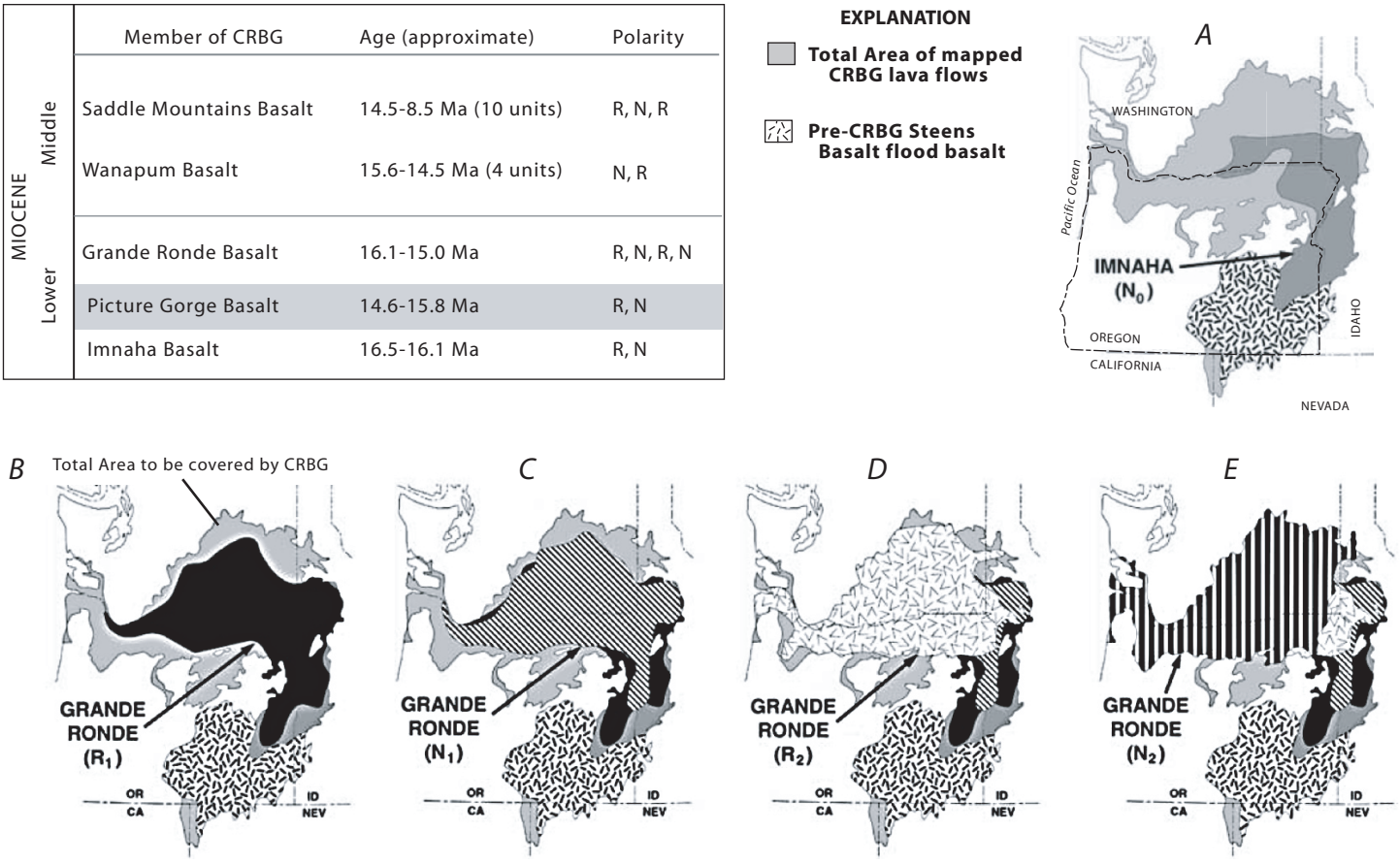

Figure 17. Map showing approximate extent of the Columbia River Basalt Group (CRBG) across parts of Oregon, Washington, and Idaho from Camp and Ross (2004). Chart shows the relative ages of CRBG members (Swanson and Wright, 1981); Picture Gorge Basalt (gray) is not found in the map area. (A–E) Coverage of the Imnaha and Grande Ronde members through time Camp and Ross, 2004). The pale gray area is the final total coverage of the basalts. The stippled area shows the coverage of Steens Basalt, considered to be a precursor to the CRBG.

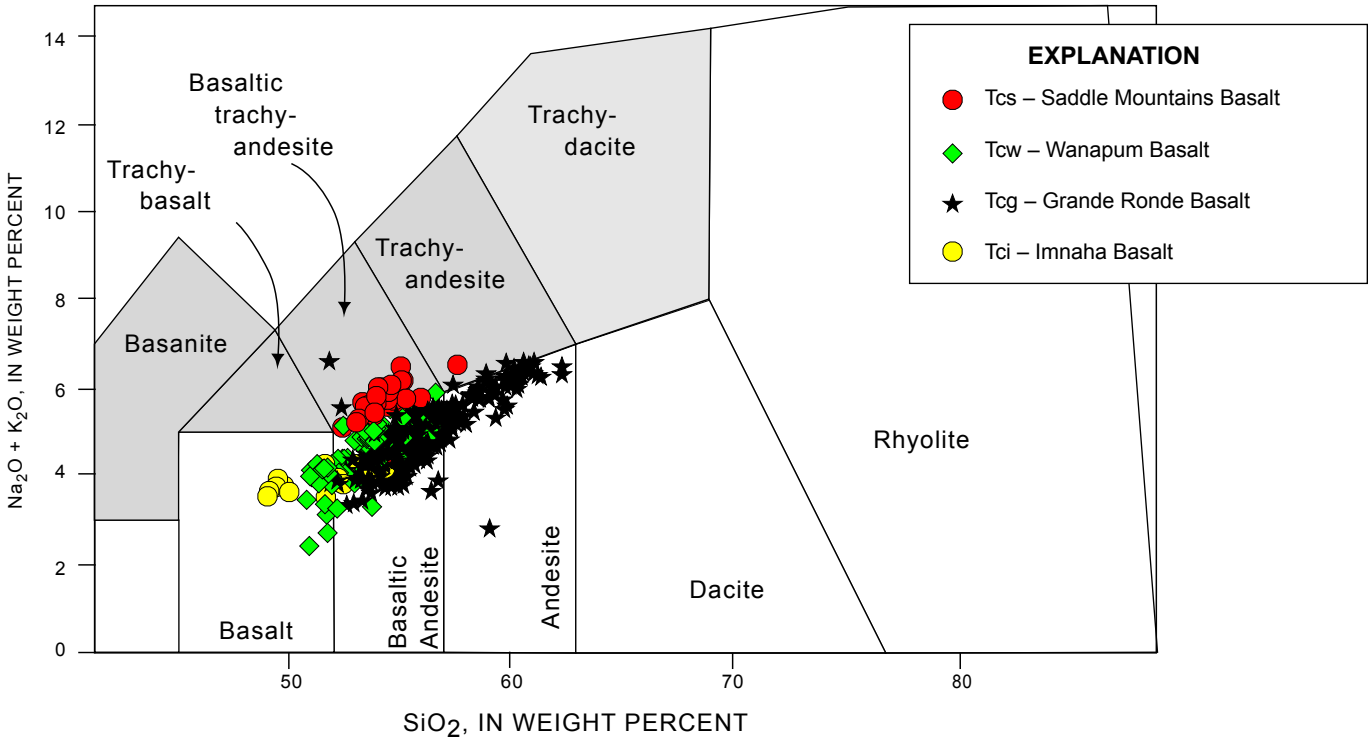

Figure 18. (above) Total alkali versus silica (TAS) diagram for the Columbia River Basalt Group. Fields are from Le Maitre and others (1989). (See Appendix file `XRF_UGRB_Cenozoic.xls` on this CD.)

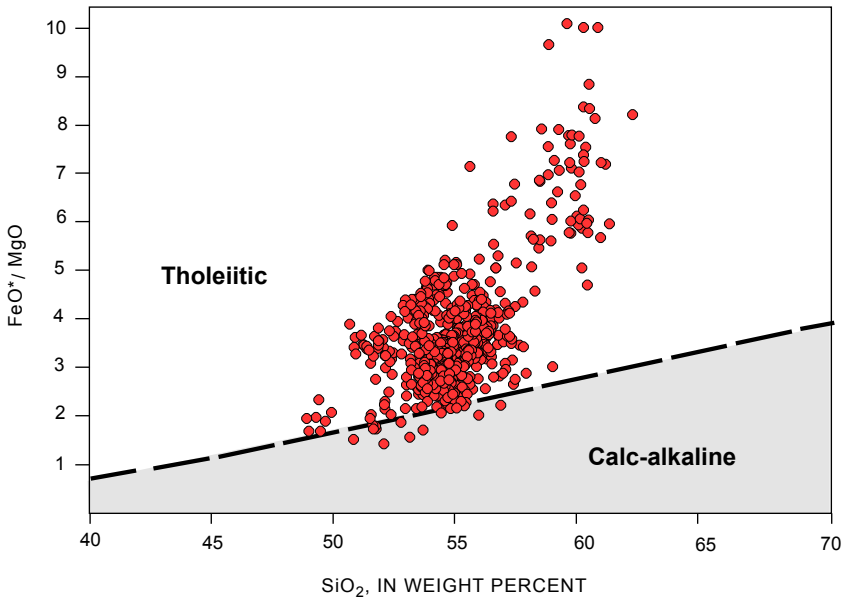

Figure 19. (left) FeO*/MgO versus SiO_2 diagram showing the strong iron enrichment trend that defines the tholeiitic nature of the Columbia River Basalt Group. Tholeiitic and calc-alkaline fields are from Miyashiro (1974).

landslides. The basalt of Eden is an iron-rich basaltic trachyandesite with relatively high potassium, phosphorous, and barium (>2 weight percent K_2O, >1.4 weight percent P_2O_5, >1,800 ppm Ba). The basalt of Umatilla ranges in composition from iron-rich trachyandesite to iron-rich basaltic trachyandesite marked by high potassium and phosphorous and especially high barium (>2.5 weight percent K_2O, >1 weight percent P_2O_5, >3,000 ppm Ba). Both flows display normal remanent magnetic polarity. North of Elgin, the basalt of Umatilla, the oldest member of the Saddle Mountains Basalt, interfingers with the basalt of Little Catherine Creek (Tpb), the oldest member of the Powder River Volcanic Field. Middle Miocene on basis of stratigraphic position and $^{36}Ar/^{40}Ar$ – $^{39}Ar/^{40}$ Ar isochron age of 13.64 ± 0.17 Ma for the basalt of Umatilla. An $^{39}Ar/^{40}Ar$ plateau age could not be determined for the Umatilla sample due to excess radiogenic argon.

Tcw **Wanapum Basalt (middle Miocene)**—Light bluish gray, grayish brown, and dark bluish gray, iron-rich basalt and basaltic andesite lava flows as thick as 130 m. Four petrographically and chemically distinctive units include, from youngest to oldest, the basalt of Powatka, the basalt of Frenchman Springs, the basalt of Lookingglass, and the basalt of Dodge. The basalt of Powatka is a light bluish-gray, platy, medium- to fine-grained aphyric basaltic andesite that is commonly deeply weathered and seldom forms good outcrops; thins to less than 5 m in thickness to the west. The underlying Frenchman Springs consists of thin, grayish black, fine- to medium-grained aphyric basalt flows that are marked by orange-red or red weathering rinds; thickens to the west. The basalt of Lookingglass is a black, fine-grained aphyric basaltic andesite that seldom forms good outcrops; thins to the west. The basalt of Dodge consists of grayish brown, medium- to coarse-grained olivine basalt flows, one of which contains distinctive plagioclase phenocrysts as large as 3 cm in length. Dodge flows are commonly deeply weathered, forming grussy outcrops marked by spheroidal weathering core stones; thins to the west. In covered areas the basalt of Dodge is commonly marked by springs and wet seeps. The basalt of Powatka is an iron-rich basaltic andesite with notably high phosphorous (≥1.2 weight percent P_2O_5). Frenchman Springs flows have high titanium (≥ 3.00 weight percent TiO_2). The basalt of Lookingglass is an iron-rich basaltic andesite marked by moderate phosphorous (~ 0.8 weight percent P_2O_5). The basalt of Dodge is marked by low titanium (≤1.5 weight percent TiO_2) and potassium (≤0.5 weight percent K_2O). Geographic distribution of the Lookingglass and Powatka flows indicates that they erupted from buried vents within the quadrangle. The Frenchman Springs eruptive center is probably marked by the Frenchman Springs dike complex mapped by Kuehn (1995) in the headwaters of the Walla Walla River. The feeder dike for the Dodge flow is located to northeast of Rondowa (Hooper and Swanson, 1990). All members display normal remanent magnetic polarity. The Frenchman Springs member is generally considered to be about 15.3 Ma (Tolan and others, 1989).

Tcg **Grande Ronde Basalt (middle and lower Miocene)**—Flow-on-flow sequence of bluish-black aphyric to sparsely plagioclase-phyric, medium-grained iron-rich basaltic-andesite and andesite lava flows. Includes fine-grained, aphanitic, and glassy lavas that are commonly platy or hackly jointed; some thicker flows have columnar jointing. Basalt weathers to orange-brown angular blocks and forms steep slopes. Differential weathering commonly results in distinctive bench topography; easily erodible interflow breccias are marked by bands of trees, and the more resistant flow interiors form continuous cliffs and grass-topped benches (Figure 20). Includes four magnetostratigraphic members that elsewhere have been mapped as separate members (Figure 17) (Swanson and others, 1981; Ferns and others, 2001). Unit is made up of chemically distinctive flow packages that mark either recurring eruptions of a single magma type or successive lobes of a single, long-lasting eruption. Distinctive flow packages are not distributed uniformly over the map area. Top of the unit in the subsurface of Grande Ronde Valley possesses a series of thin (< 15 m thick), chemically distinctive, sparsely plagioclase-phyric, glassy iron-rich andesite flows (ferroandesite of Fiddlers Hell [Ferns and others, 2001]) that are among the most evolved lavas in the Grande Ronde Basalt. Fiddlers Hell flows are marked by relatively high silica (≥ 56 weight percent SiO_2), potassium (≥ 2 weight

Figure 20. Canyon of Lookingglass Creek, showing the typical topography and outcrop pattern formed by stacked Grande Ronde Basalt flows. Massive interiors of flows commonly form shelves whereas tree bands, which here define horizontal strips, commonly mark flow breccias that separate different flows.

percent K_2O) and phosphorus (≥ 0.6 weight percent P_2O_5), and low magnesium (≤ 3 weight percent MgO). The Fiddlers Hell member thins to the north and west. Top of the Grande Ronde Basalt northwest of Elgin possesses a series of thin (<15 m thick), medium-grained, holocrystalline, iron-rich basaltic andesite flows of the Sentinel Bluffs chemical type (Reidel and others, 1989). Sentinel Bluff flows are among the most primitive lavas in the Grande Ronde Basalt and are marked by relatively low potassium, phosphorus, and titanium and by high magnesium. The Sentinel Bluff thickens westward across the northern part of the basin, forming a package of flows up to 150 m thick. Compositions of other flow packages generally fall somewhere between these two chemical types. Unit appears to thicken to the northwest; showing an overall pattern of successive northward younging flows (Hooper and Swanson, 1990). Base of the unit in the southwest part of the basin is locally marked by sparsely olivine-phyric fine-grained lava flows of the Buckhorn Springs chemical type (Reidel and others, 1989; Ferns and others, 2001). Unit disconformably overlies deeply eroded pre-Tertiary units, with flows of both the Buckhorn Springs and Fiddlers Hell types locally filling channels. A 15.54 ± 0.01 Ma $^{40}Ar/^{39}Ar$ age (Madin, 1998) for the ferroandesite of Fiddlers Hell places a middle Miocene limit on the youngest Grande Ronde Basalt flows. Grande Ronde Basalt eruptions occurred between 15.0 and 16.1 Ma (Baksi, 1989; Hooper and others, 2002).

Tci **Imnaha Basalt (lower Miocene)**—Flow-on-flow sequence of black to brownish black and gray, fine- to medium-grained, plagioclase- and olivine-phyric, iron-rich, basalt and basaltic andesite flows. Unit readily weathers to form bare gravelly slopes marked by discontinuous cliffs. Vesicular flow tops commonly marked by zeolite amygdules. Typically holocrystalline with plagioclase phenocrysts as long as 3 cm. Locally includes diktytaxitic and aphyric flows. Outcrops commonly deeply weathered, with spheroidal core stones. Compared to Grande Ronde Basalt flows, they have lower silica (49 to 54 weight percent SiO_2) and high magnesium (4.45 to 6.75 weight percent MgO). Disconformably overlies deeply eroded pre-Tertiary rocks. Includes both normally and reversely polarized flows (Shubat, 1979; McConnell and others, 2002). Hooper and others (2002) consider the Imnaha Basalt to have erupted circa 16.1 Ma.

Figure 21. Indian Rock vent complex. Indian Rock is a cylindrical mass some 400 m in diameter of massive, matrix supported breccias. Indian Rock has been described as a diatreme (Taubeneck, 1980) and may be a hydrovolcanic complex that formed beneath a now eroded palagonitic vent.

Tcv **Vent and hydrovolcanic deposits (middle Miocene)**—Scoria, welded spatter, and cinder deposits. Welded spatter is typically a dense black glass that breaks to a hackly fracture. Elongated vent complexes as much as 70 m high are capped by banded red and black glassy, welded spatter. Unit includes 200- to 400-m-diameter massive cylindrical masses of matrix-supported diatreme breccias (Figure 21) (Taubeneck, 1980). The Indian Rock diatreme breccia is a massively bedded, matrix-supported breccia with vesicular clasts as large as 30 cm across in a matrix that comprises comingled altered gray glass, volcanic rock fragments, and rare plagioclase phenocrysts. Unit also includes bedded brown, yellowish-brown, or orange-brown basaltic scoria and clast-supported cinder breccias with dark gray to black, finely vesiculated lapilli as large as 3 cm in diameter set in a orange matrix of orange palagonite glass. Lapilli are fine grained and sparsely plagioclase-phyric. Analyses of glass and scoria indicate that these are iron-rich basaltic-andesite or andesite Grande Ronde vent complexes that possess relatively high titanium and phosphorous ($\geq$ 2.4 weight percent TiO_2; $\geq$ 0.4 weight percent P_2O_5). The scoria and welded spatter mounds overlie flows displaying normal remanent magnetic polarity. Stratigraphic position suggests that the spatter mounds may be a vent complex related to the Winter Water flows of Reidel and others (1989, 1996).

Tcd **Columbia River Basalt dikes (middle and lower Miocene)**—Bluish-black to black dikes. Generally blocky weathering and hackly jointing. Includes both Grande Ronde and Imnaha Basalt dikes on the headwaters of Catherine Creek (Figure 22), Grande Ronde Basalt dikes on the upper Grande Ronde River, and a dike at the summit of Tower Mountain that may be a feeder for Picture Gorge Basalt flows exposed to the west of the basin. Individual dikes commonly form vertically freestanding outcrops with horizontal columnar joints.

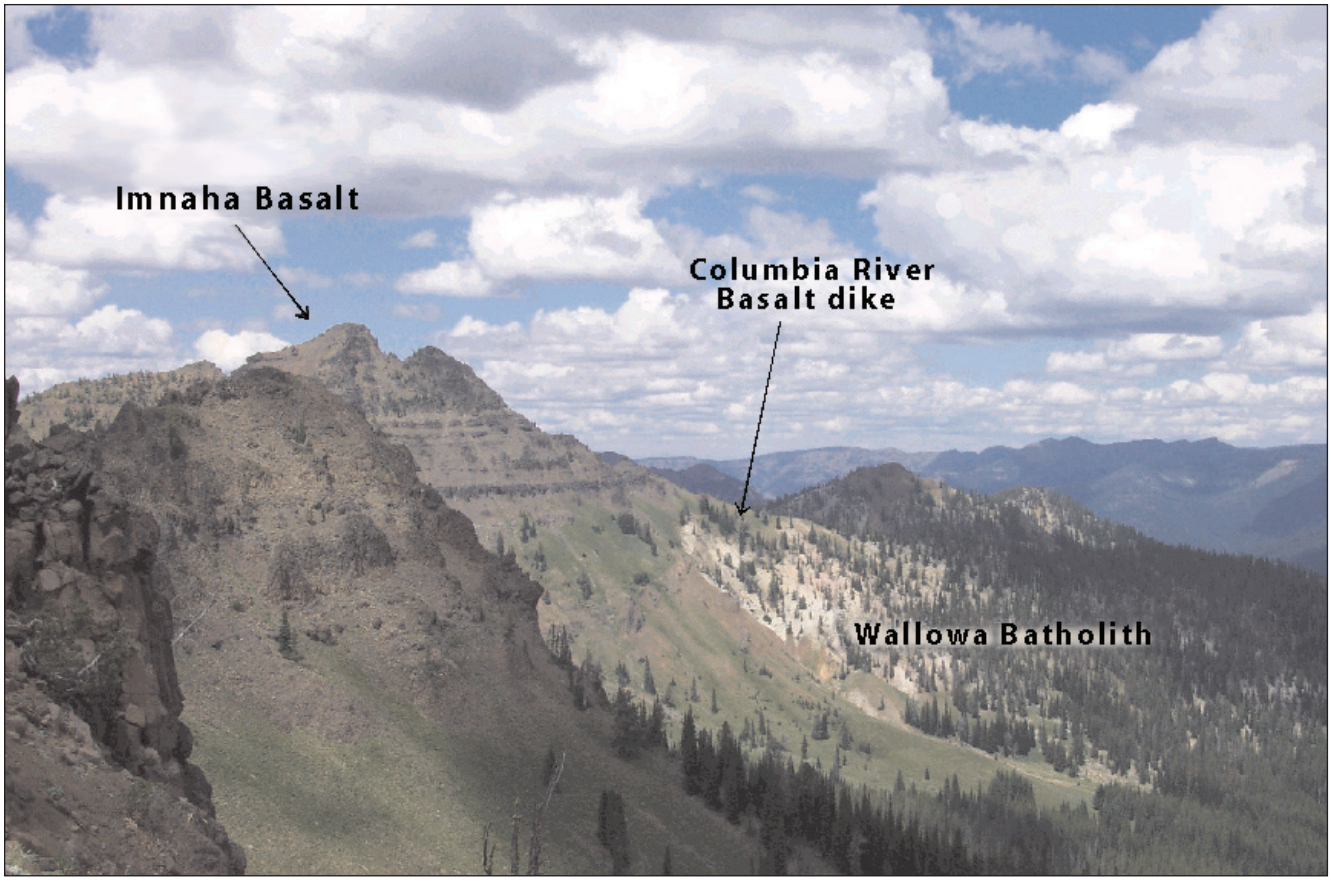

Figure 22. High Hat. View north on the divide between Catherine Creek and the headwaters of the Little Minam River. Here Imnaha Basalt flows, marked by the horizontal bands, fill a paleocanyon cut into the deeply weathered Wallowa batholith. Columbia River Basalt feeder dikes form vertical, dark outcrops.

Tower Mountain Caldera (Lower Miocene and Oligocene)

Volcanic rocks exposed near the headwaters of the Grande Ronde River are part of the large late Oligocene Tower Mountain caldera (Ferns and others, 2001; Ferns, 2002). The Tower Mountain caldera is the northernmost of a string of large rhyolite eruptive centers that formed in eastern Oregon during the late Oligocene and early Miocene (Ferns, 2002). Robinson and others (1990) identified volcaniclastic rocks from this caldera and considered them to be coeval with the eastern facies of the John Day Formation. The resurgent core to the 14-km-wide caldera is a highlands composed of lithic ash-flow tuff and subvolcanic rhyolite and dacite intrusions and is fringed by dacite, andesite, and basalt lava flows and dacitic and rhyolitic breccias and ash-flow tuffs (Figures 23 and 24). The caldera margin is defined by an arcuate belt of rhyolite domes and flows (Ferns and others, 2001) and possesses prominent gravity and aeromagnetic anomalies (Ferns, 2002). Mapped lithologic units include:

Tta **Andesite and dacite flows (lower Miocene)**—Gray, flow-foliated, platy and massive, aphyric and porphyritic andesite and dacite lava flows. Flows are irregular in shape and reach thicknesses greater than 140 m. Includes the dacite of Johnson Rock, andesite of Chicken Hill, and rhyodacite of Sheep Creek of Ferns and others (2001). The Johnson Rock flow has a micaceous luster due to partially resorbed biotite phenocrysts. The Chicken Hill and Sheep Creek flows are each porphyritic with plagioclase, hypersthene, and augite phenocrysts. Unconformably overlies volcaniclastic breccias, ash-flow tuff, and porphyritic lava flows. Early Miocene age is based on 22.4 + 0.16 Ma whole-rock $^{40}Ar/^{39}Ar$ radiometric determination for the Johnson Rock flow (Ferns, 1999; Ferns and others, 2001).

Ttr **Rhyolite (upper Oligocene)**—White to yellowish-gray, flow-banded, platy porphyritic and aphyric domes and lava flows. Unit includes an arcuate flow-dome complex that was emplaced along the southern margin of the Tower Mountain caldera. Steeply dipping matrix-supported and clast-

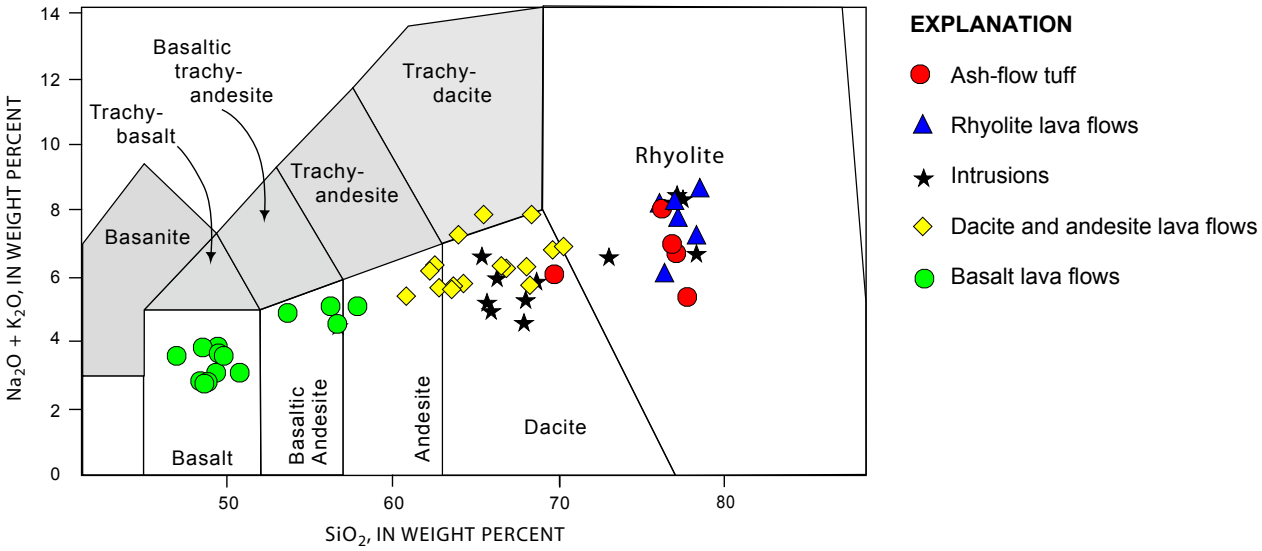

Figure 23. Total alkali versus silica (TAS) diagram for lava, tuff, and intrusions associated with the Tower Mountain caldera.

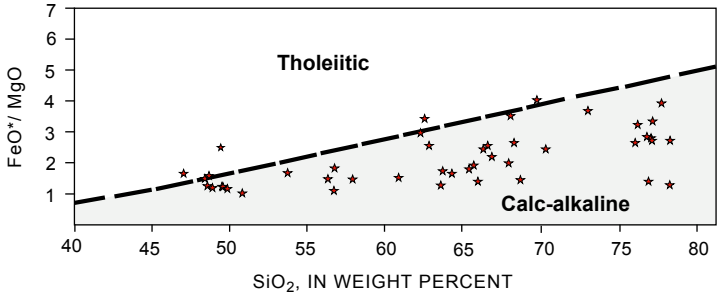

Figure 24. FeO*/MgO versus silica diagram for lavas of the Tower Mountain caldera, showing calc-alkaline trend. Tholeiitic and calc-alkaline fields are from Miyashiro (1974)

supported tuffaceous, rhyolite-clast breccias and complexly folded flow-banded rhyolite lava define individual dome margins. Dome margins are locally marked by steeply dipping perlitic zones as wide as 50 m that contain massive pale red-brown and light-green lithophysal lenses. Dome interiors are marked by platy white rhyolite. In hand sample, the porphyritic varieties commonly show a mottled texture due to presence of 2 to 5 percent plagioclase and potassium feldspar phenocrysts 1 to 3 mm across. Groundmass comprises quartz, potassium feldspar, and plagioclase and is commonly spherulitic. Aphyric rhyolites commonly contain partially zeolitized spherulites in a similar groundmass. Although the contact between the rhyolite domes and the caldera-fill ash-flow tuff (unit Ttt) is steep and generally poorly exposed, the rhyolites appear to have been emplaced following the ash-flow eruption. Rhyolite flows overlie non-welded ash-flow and air-fall tuff at the top of unit Ttvs. Unit includes porphyritic dome complexes along Fly Creek and the Grande Ronde River that intrude dacite lava flows north and east of the caldera margin (Ferns and others, 2001). The dome complex on the Grande Ronde River is coarsely porphyritic, with about 10 percent plagioclase and quartz phenocrysts as large as 5 mm in diameter. Interpreted as a shallow intrusion into the lahars of unit Ttvs on the basis of a zone of intensely bleached, brecciated rhyolite (Ferns and others, 2001). The domes of this unit are high-silica rhyolites, with 75–78 weight percent SiO_2. Upper Oligocene age on the basis of K-Ar age of 28.10 + 1.5 Ma on anorthoclase from a porphyritic rhyolite (Fiebelkorn and others, 1983; Ferns and others, 2001).

Ttt **Welded ash-flow tuff (upper Oligocene)**—Unit includes unwelded to moderately welded high-silica rhyolite and dacite ash-flow tuffs. Most of the volume of this unit is gray, white, light-gray, and pale-yellow lithic ash-flow tuff (Figure 25) deposited in the core of the Tower Mountain caldera. The lithic tuff contains as much as 15 percent lithic clasts of porphyritic dacite clasts, 5 percent phenocrysts of plagioclase and quartz with minor amounts of potassium feldspar and altered biotite, and flattened pumice clasts as much as 15 cm in length. Commonly intensely altered and recrystallized to a felted mat of fine-grained quartz and potassium feldspar. Unit is over 100 m thick in the central part of the map area and is considered to be a caldera fill sequence of ash-flow and air-fall tuffs. Unit includes a thin, crystal-rich, dacitic ash-flow tuff that crops out locally beneath the overlying andesite (Tta) and dacite (Ttd) lava flows. The dacitic tuff is about 25 m thick with a devitrified upper welded zone marked by light-gray tuff with subhorizontal flattened fiamme; lower zone is poorly exposed and consists of devitrified white to pale orange tuff. Welded zone has 2 to 5 percent plagioclase phenocrysts as large as 2 mm in diameter and highly altered, skeletal green hornblende phenocrysts rimmed with opaque oxide minerals. The caldera-fill lithic ash-flow is high-silica rhyolite with 77 percent SiO_2 (see Appendix). The dacite tuff contains 69.71 weight percent SiO_2 (Ferns, 1999). Although found only in outcrop east of Little Fly Creek, welded tuff float occurs below unit Tta on the headwaters of Chicken Creek.

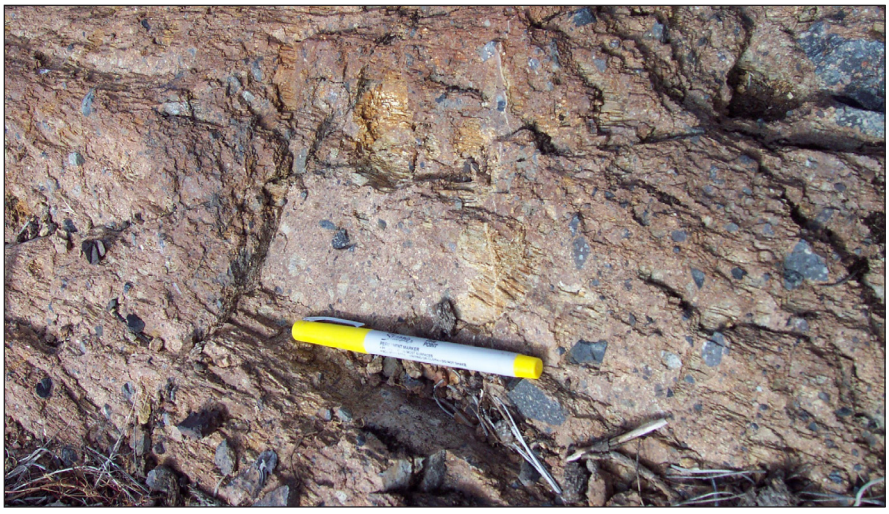

Figure 25. Photograph of lithic tuff (Ttt) within the Tower Mountain caldera. Here the intracaldera tuff is densely welded and exhibits flattened fiamme. Pale clasts are aphyric rhyolite; dark gray, angular lithic clasts are porphyritic dacite.

Ttd **Porphyritic lava of Chicken Creek (upper Oligocene)**—Massive gray, purplish-gray, and bluish-gray porphyritic andesite and dacite lava flows. Conspicuously porphyritic, with as much as 15 percent phenocrysts to 7 mm in length, and as much as 2 percent xenoliths as large as 5 cm in diameter. Three phenocryst assemblages include 1) plagioclase, hypersthene, and augite; 2) plagioclase, olive green hornblende, and hypersthene; and 3) plagioclase, quartz, hypersthene, and augite. Holocrystalline xenoliths comprise hypersthene, augite, and plagioclase. Individual flows commonly grade upward from a coarsely plagioclase-phyric basal vitrophyre into massive, platy jointed stony lava. Flow tops and margins are marked by coarse, clast-supported breccias. At least three separate flows are exposed, each containing phenocrysts set in a variably altered, glassy groundmass. Unit includes flow-banded dacite lava flows with about 5 percent plagioclase phenocrysts as large as 2 mm in diameter, and underlying 1- to 2-m-thick tuffaceous conglomerates and lithic breccias. Compositions range from high-silica andesite to dacite (63–68 weight percent SiO_2) (Ferns, 1999; Ferns and Taubeneck, 1994). Unit is more than 300 m thick and locally interfingers with underlying pyroclastic deposits of unit Ttvs. Oligocene on basis of K-Ar age of 28.8 Ma on a porphyritic hornblende-phyric andesite on Sheep Creek (Fiebelkorn and others, 1983).

Ttba **Basalt, basaltic andesite, and andesite (upper Oligocene)**—Platy, grayish-red to grayish-black, sparsely phyric basalt, basaltic-andesite, and andesite lava flows that locally fill channels within unit Ttvs. Includes 1) hyalopilitic to pilotaxitic olivine- and plagioclase-phyric flows with granular clinopyroxene microphenocrysts; 2) plagioclase- and augite-phyric andesite; and 3) bluish-black olivine basalts that contain ophitic clinopyroxene. Compositions (Figures 23 and 25) range from about 49 to 56 weight percent SiO_2 (Ferns and Taubeneck, 1994).

Ttvs **Volcaniclastic deposits of Limber Jim Creek (upper Oligocene)**—Mainly debris flow deposits locally interbedded with and underlying porphyritic dacite and andesite flows of unit Ttd. Unit consists of coarse, matrix- and clast-supported, tuffaceous breccia largely composed of angular to subrounded clasts of porphyritic andesite and dacite. Along the southern flank of the Tower Mountain caldera, unit grades from matrix-supported rhyolite-clast breccias to matrix and clast-supported dacite porphyry clast breccias (Figure 26). Locally contains casts of logs as large as 2 m in diameter. Unit thickens to the east, where over 225 m of interbedded breccias and tuffaceous conglomerates are exposed along Limber Jim Creek (Ferns and Taubeneck, 1994). Unit includes a gray or light gray, hackly jointed, crystal-lithic, hornblende-bearing tuffaceous breccia with porphyry clasts as large as 5 cm in diameter. Consists mainly of poorly sorted, massive-bedded breccia exposed adjacent to massive exposures of Ttd lavas. Includes primary debris-flow deposits associated with Ttd lava flows. Unit locally includes medium grained, tuffaceous conglomerates made up of rounded dacite, andesite, and rhyolite clasts. Eastern-most exposures on Beaver Creek consist mainly of massive tuffaceous siltstone. Age of unit based on stratigraphic association with unit Ttd.

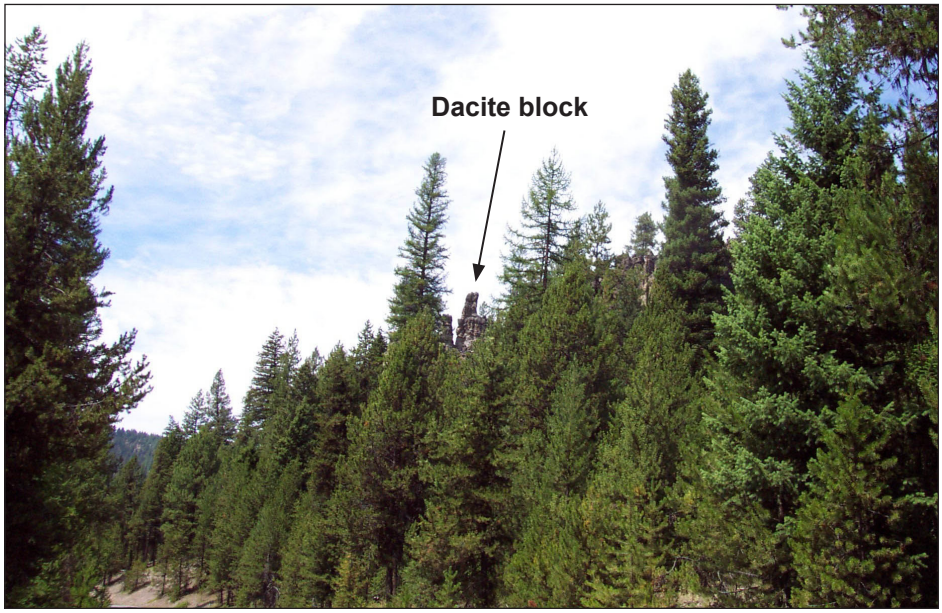

Figure 26. Volcaniclastic deposits of Limber Jim Creek commonly form cliffs and spires. Dacite capstones protect some spires, forming a hoodoo topography that is commonly masked by dense forest cover. These exposures are exposed along the upper Grande Ronde River.

Ttb **Basalt and basaltic andesite (Oligocene)**—Mainly brownish-gray to brownish-black, fine-grained, vesicular olivine basalt flows. Unit includes widely separated chemically and petrographically distinct flows locally exposed beneath unit Ttvs. Flow compositions range from potassium- and titanium-rich alkali olivine basalt flows (47.37 weight percent SiO_2, 4.6 weight percent TiO_2, 1.59 weight percent K_2O) to low-potassium olivine basalt flows (48.38 weight percent SiO_2, 1.30 weight percent TiO_2, 0.33 weight percent K_2O) (Ferns and Taubeneck, 1994). Individual flows are generally hyalophitic with subophitic clinopyroxene. Commonly altered or deeply weathered, with thick spheroidal weathering rinds and zeolite- and/or calcite-filled vesicles. Overlain by unit Ttvs and overlies various pre-Tertiary units. Oligocene on basis of $^{40}Ar/^{39}Ar$ radiometric age of 29.80 ± 0.39 Ma for a flow in the Anthony Butte quadrangle (Ferns and others, 2001; Madin and Taubeneck, 2003).

Tertiary Subvolcanic Intrusions

Ttbi **Mafic intrusions (lower Miocene to upper Oligocene)**—Basalt and basaltic andesite dikes and sills. Mainly black to grayish-black, aphyric to glomeroporphyritic dikes. Glomerocrysts have plagioclase and clinopyroxene. Includes a 100-m-wide, 1.25-km-long, east-west-trending dike near the headwaters of Sheep Creek.

Ttri **Rhyolite intrusions (lower Miocene to upper Oligocene)**—Aphyric to plagioclase-phyric rhyolite dikes and small intrusions that are locally columnar jointed. The dikes are white to light gray on fresh surfaces, are commonly finely laminated, and weather to shades of light purple. Contain as much as 5 percent plagioclase phenocrysts and rare mafic phenocrysts altered to fine-grained mass of chlorite and biotite. Groundmass in places altered to fine-grained mat of quartz, biotite, and potassium feldspar. Small, irregularly shaped, high-silica rhyolite (77 percent SiO_2) stocks intrude the caldera fill sequence (Ttt) and a small, west-northwest-trending swarm of rhyolite dikes cuts across the caldera margin. Within the caldera, rhyolite intrusions are commonly intensely silicified and cut by cryptocrystalline quartz seams less than 1 mm thick. Age of unit based on intrusive relationships within the caldera.

Ttdi **Dacite and andesite intrusions (lower Miocene to upper Oligocene)**—Mainly dikes and small plugs of hornblende-phyric dacite that intrude the caldera fill tuffs of unit Ttt, plus aphyric to slightly plagioclase-phyric, bluish-gray silicic andesite and dacite intrusions exposed east of the caldera, and coarsely porphyritic intrusions with as much as 15 percent phenocrysts of hornblende, plagioclase, quartz, and potassium feldspar as large as 6 mm across. Unaltered dikes and small plugs of hornblende-phyric high-silica dacite form massive to columnar-jointed, gray to light-bluish-gray outcrops. Irregularly shaped, platy jointed, subvolcanic intrusions exposed on Little Fly Creek contain less than 1 percent plagioclase and hypersthene phenocrysts 1 to 2 mm in length. A small, unaltered hornblende-phyric rhyodacite plug is exposed east of the caldera margin (Ferns, 1999). Most of the intrusions are dacites with 65 to 69 weight percent SiO_2. Many dikes within the caldera are hydrothermally altered; alteration assemblages range from chlorite + carbonate to potassium feldspar + biotite. Thin argillic alteration zones and pyritic seams occur along small faults and joints in the large Chicken Creek intrusion.

Lower Cenozoic Sedimentary Rocks

Teg **Conglomerate, sandstone, and siltstone (lower Oligocene (?), Eocene, or Paleocene (?))**—Compositionally heterogeneous unit that includes conglomerate, siltstone, and sandstone. Poorly exposed and only moderately lithified. Best exposures are in the old hydraulic placer mine workings in the Elkhorn Mountains at Camp Carson, where a basal, gold-bearing boulder conglomerate fills channels cut into underlying pre-Tertiary units. The 2- to 6-m-thick basal conglomerate, locally referred to as the Carson Wash (after Lindgren, 1901), possesses well-rounded metamorphic quartzite boulders as large as 60 cm in diameter in a quartz- and feldspar-rich sand matrix that contains pink translucent garnet and placer gold and weathers to light orange. The conglomerate is overlain by at least 8 m of tuffaceous sandstone, finely laminated, dark organic-rich silt and mudstone, and 12 m of matrix-supported, tuffaceous chert-clast conglomerate. An upper conglomerate contains clasts 1 to 10 cm across of bluish-black chert and argillite and deeply weathered white tuff and rhyolite. Through much of the map area this unit is poorly exposed and is mapped on the basis of quartzite boulders or black chert pebbles. Locally includes tuffaceous sedimentary rocks that may be distal facies of members of the overlying Tower Mountain Volcanic Field. Lava flow and tuffaceous units of the Tower Mountain Volcanic Field unconformably overlie the unit. Eocene/Paleocene age is based on interpretation that the unit is a high-energy river-channel deposit associated with the deltaic sandstones of the Herren Formation of Shorey (1976) that crops out in two localities on the north flank of the Blue Mountains.

MESOZOIC INTRUSIVE ROCKS

Two large Mesozoic intrusions, the Wallowa batholith and the Bald Mountain batholith, are exposed in the headwaters of the upper Grande Ronde River basin. Both batholiths are composed of smaller individual intrusions that are chemically and petrographically distinct (Figure 27; Appendix). The composite Wallowa batholith (Taubeneck, 1964, 1987) forms the core of the Wallowa Mountains and underlies the area at the headwaters of Catherine Creek. The Bald Mountain batholith (Lindgren, 1901; Taubeneck, 1957, 1995) forms the core of the Elkhorn Mountains at the headwaters of the Grande Ronde River.

Wallowa Batholith (Early Cretaceous and Late Jurassic(?))

Composite intrusion that contains four separate compositionally zoned plutons, each ranging in composition from tonalite to granodiorite. Unit includes the westernmost exposures of the tonalitic Wallowa batholith and a small satellite intrusion exposed along Catherine Creek.

Kwt **Tonalite and granodiorite of the Wallowa batholith (Early Cretaceous)**—Gray to light gray, medium-grained granodiorite and tonalite, best exposed in the ridges at the head of Catherine Creek (Figure 28). According to Taubeneck (1995), main area of exposure belt along the headwaters of Catherine Creek comprises two compositionally zoned plutons that range in composition from tonalite to granodiorite (Units 2 and 3 of Taubeneck [1987]). Tonalite phases are typically fine to medium grained and are composed largely of quartz, plagioclase, and hornblende. Interstitial biotite and potassium feldspar are common. Deeply weathered tonalite exposed in road cuts and mine workings at the confluence of the South and North forks of Catherine Creek intrudes calcareous sediment and appears identical to the main intrusive mass exposed in the Wallowa Mountains. Geochemical analyses of several samples indicate that they are typical of calc-alkaline tonalites (67.27 to 67.6 weight percent SiO_2; 15.80 to 16.09 weight percent Al_2O_3; 2.58 to 2.75 weight percent K_2O, and 3.61 to 3.63 weight percent Na_2O). The main tonalite phase of the Wallowa batholith is early Cretaceous on the basis of U-Pb (zircon) ages of ~137 Ma (Walker, 1986).

Kwi **Trondjemite of Catherine Creek (Early Cretaceous or Late Jurassic)**—Gray, fine- to medium-grained trondjemite and diorite exposed in a road cut downstream of Catherine Creek State Park (Ferns and others, 2002a). The intrusion is poorly exposed and largely altered with mafic minerals replaced by chlorite. Pegmatites with pink potassium feldspar and quartz are found as float. Considered to be a trondjemite on the basis of mineralogy and chemistry (65.13 weight percent SiO_2; 17.02 weight percent Al_2O_3; 1.70 weight percent K_2O, and 4.39 weight percent Na_2O). Age is unknown. Trondjemite composition indicates the Catherine Creek intrusion may be younger than the main Wallowa batholith. Johnson (1995) and Johnson and others (1995) indicated that undeformed trondjemite intrusions in the Blue Mountains are generally younger than the more common tonalite and granodiorite intrusions. Older trondjemites are generally deformed and metamorphosed. It is unclear whether the extensive alteration in the Catherine Creek intrusion is due to weathering or hydrothermal alteration.

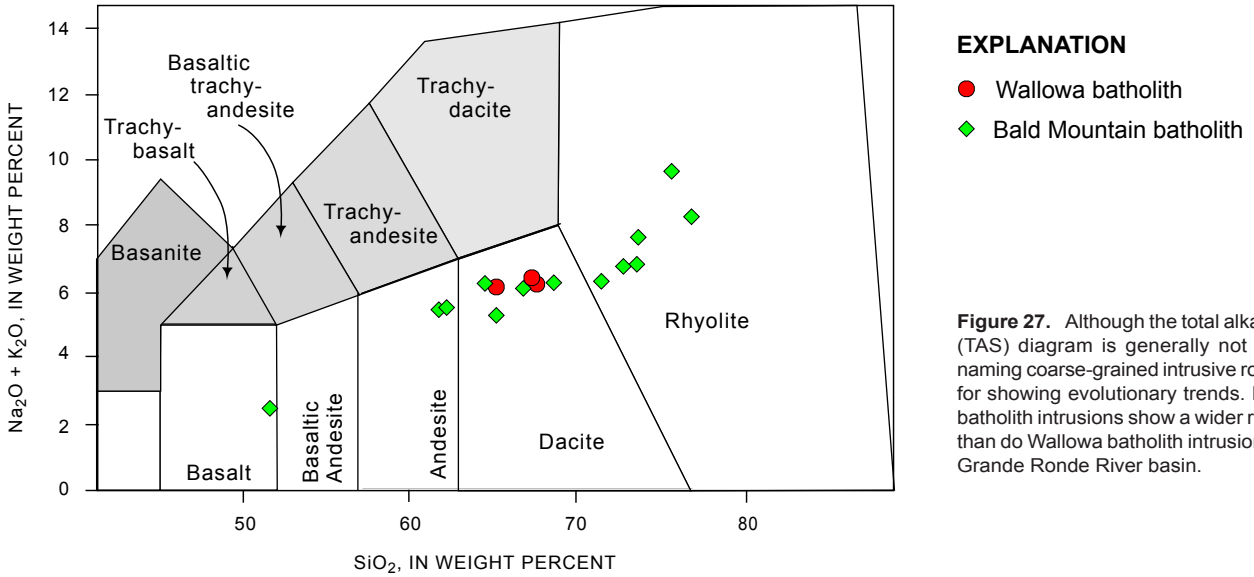

Figure 27. Although the total alkali versus silica (TAS) diagram is generally not applicable for naming coarse-grained intrusive rocks, it is useful for showing evolutionary trends. Bald Mountain batholith intrusions show a wider range of values than do Wallowa batholith intrusions in the upper Grande Ronde River basin.

Figure 28. Looking east into the Wallowa batholith near the headwaters of Catherine Creek. Note contrast in topography and vegetation between the distant rugged glaciated core of the batholith and the grass-covered benches of Grande Ronde Basalt in the foreground.

Bald Mountain Batholith (Early Cretaceous and Late Jurassic)

The Bald Mountain batholith is a composite intrusion. The main phase, the Elkhorn pluton (Taubeneck, 1995), ranges in composition from tonalite to granodiorite. The Bald Mountain batholith smaller intrusive masses of gabbro, diorite, quartz diorite, granite, and lamprophyre that are mapped separately on the basis of composition. Also includes highly metamorphosed inclusions of older country rock that are entrained along intraplutonic contacts. For detailed descriptions of individual intrusions and inclusions, see Taubeneck (1995).

KJbt Granodiorite and tonalite (Early Cretaceous and Late Jurassic)—White to light-gray, medium- to coarse-grained, hypidiomorphic-textured biotite-hornblende tonalite and granodiorite. Commonly forms rounded, hummocky outcrops mantled by grussy soil. Best natural exposures occur in glaciated uplands. Includes the Elkhorn pluton, the largest intrusion in the Bald Mountain batholith, as well as several small satellite intrusions, including the granodiorite of the Indianna Mine Road, the granodiorite of Beaver Meadow, and the tonalite of North Fork. The Elkhorn pluton is a single intrusion that constitutes about 93 percent of the Bald Mountain batholith (Taubeneck, 1995). The Elkhorn pluton is chiefly a medium-grained, pale-gray granodiorite with biotite and euhedral hornblende. The granodiorite of the Indianna Mine Road is deeply weathered, light gray to white, and medium-grained; it contains small, scattered biotite flakes that define a distinct foliation (Taubeneck, 1995). The granodiorite of Beaver Meadow is medium-grained, light gray, and characterized by scattered megacrysts of potassium feldspar as large as 2.5 cm across (Taubeneck, 1995). The tonalite of North Fork is a light gray, medium-grained mass that intrudes amphibolite and metasediment just north of the North Fork of Anthony Creek. Also in this unit are several small, poorly exposed granodiorite and tonalite intrusions in the Guard Station inlier that are noteworthy as they include pinkish-white to light-gray biotite granodiorites that contain both biotite and muscovite (Taubeneck, 1995; Ferns and Taubeneck, 1994). Late Jurassic and Early Cretaceous age derived from limited radiometric age determinations. Walker (1989) reported a U/Pb zircon age of ~143 Ma for an early gabbronorite phase of the Bald Mountain batholith that is exposed at the headwaters to the North Fork of the John Day River. Armstrong and others (1977) reported K-Ar ages from biotite and hornblende that range from 134 ± 4 Ma to 159 ± 5 Ma (recalculated by Fiebelkorn and others, 1983) and a whole-rock Rb-Sr isochron age of 147 ± 17 Ma for the Bald Mountain batholith.

KJbg Granite (Early Cretaceous or Late Jurassic)—White, grayish white, and pale yellowish white granite stocks that intrude and are peripheral to the Bald Mountain batholith. Includes the granite of Clear Creek (Ferns and Taubeneck, 1994; Taubeneck, 1995), the granite of Anthony Butte, the leucogranite of Dutch Creek (Taubeneck, 1995; Madin, 1998), the leucogranite of Trail Creek (Taubeneck, 1995), and the granite of Isham Spring (Taubeneck, 1995; Madin and Taubeneck, 2003), plus several small, poorly exposed granites situated west and north of the main mass of the Bald Mountain batholith. Granites and granodiorites are generally white to shades of yellow-white and are recognized by their pink to white potassium feldspar crystals. The Clear Creek and Anthony Butte granites intrude the main tonalite phase of the Elkhorn pluton. The granite of Clear Creek forms a white to pale-pinkish white outcrop at the confluence of Clear Creek and the Grande Ronde River. The Clear Creek intrusion contains several small muscovite-biotite-orthoclase pegmatite and aplite dikes. The granite of Anthony Butte is white to light-gray, medium grained, contains porphyritic potassium feldspar megacrysts as long as 3.5 cm (Figure 29), and commonly weathers to a yellow-white and orange gruss. The leucogranite of Dutch Creek is deeply weathered, pale grayish-white, and contains quartz, plagioclase, orthoclase, and less than 2 modal percent biotite. The granite of Isham Spring is medium grained, light gray, and marked by small, scattered biotite flakes that define a distinct foliation (Taubeneck, 1995). The granite of Isham Springs intrudes schistic metasedimentary rocks of unit TRPe.

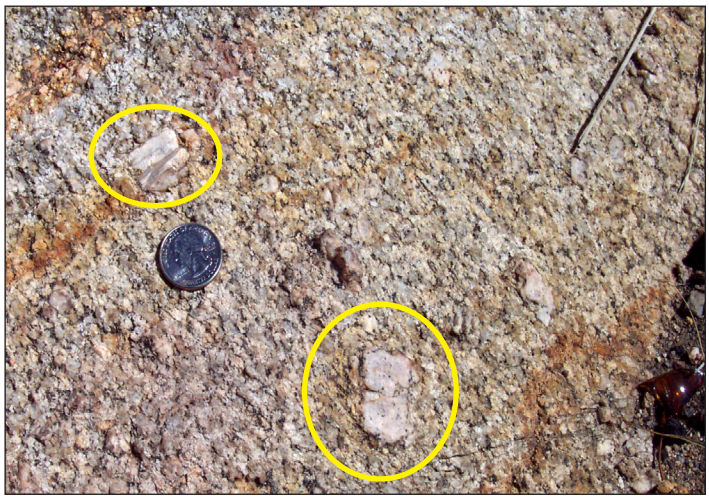

Figure 29. Photograph of the Anthony Butte granite. Potassium feldspar megacrysts are circled in yellow. Groundmass is composed of quartz, plagioclase, biotite, and potassium feldspar. Potassium feldspar crystals are found only in the more silicic phases of the Bald Mountain batholith.

KJbi Mafic and intermediate intrusions (Early Cretaceous and Late Jurassic)—Dark-gray, gray, and greenish-black intermediate and mafic intrusions associated with the Bald Mountain batholith. Quartz diorite is gray to grayish-white and contains both hornblende and biotite crystals. The lamprophyre is coarse-grained and contains equant, poikilitic hornblende crystals 2 to 3 cm long with intergrown green clinopyroxene, orthopyroxene, and olivine crystals. Most intrusions are quartz diorites, including the quartz diorite of Wolf Creek, the Boundary quartz diorite, a small, unnamed intrusion in the Guard Station inlier, and several large inclusions enclosed by the granite of Anthony Butte (Taubeneck, 1995). The quartz diorite of Wolf Creek is gray, medium-grained quartz diorite composed of aligned tabular, deformed plagioclase crystals set in an interstitial groundmass of quartz and potassium feldspar. The Boundary quartz diorite unit is gray, medium-grained quartz diorite characterized by a greenish-gray gruss. Unit includes a small lamprophyre stock exposed along the Rainbow Mine Road and a small quartz-gabbro intrusion exposed in the Guard Station inlier. The quartz gabbro is gray, medium-grained, and contains hornblende, augite, plagioclase, and strained quartz crystals. The lamprophyre is considered to be a late mafic intrusion into the Elkhorn pluton; the quartz diorites and quartz gabbro appear to be precursors to the pluton. The quartz diorites predate the latest granitic intrusions. For example, the Wolf Creek intrusion (KJbi), which encloses large quartz diorite inclusions, is cut by the granite of Anthony Butte, and the boundary intrusion is cut by the leucogranite of Dutch Creek (KJbg) (Taubeneck, 1995).

KJm Metamorphosed inclusions (Early Cretaceous and Late Jurassic)—Unit consists of masses of pyroxene- and hornblende-bearing country rock that are entrained along intra-plutonic contacts within the Bald Mountain batholith. Includes thermally metamorphosed ultramafic, metavolcanic, and metasedimentary rocks that are presumed to have been originally part of the Baker terrane. Typically gneissic in texture with well-defined compositional banding.

MESOZOIC AND PALEOZOIC ROCKS

Variably metamorphosed Mesozoic and Paleozoic igneous and sedimentary rocks protrude through younger volcanic cover in several widely separated areas at the headwaters of the upper Grande Ronde River basin. Units in the study area include parts of the Baker and Wallowa terranes mapped on the basis of lithology and complex internal stratigraphy (Silberling and others, 1984; Vallier, 1995; Avé Lallemant, 1995). Units include:

Wallowa Terrane (Early Jurassic, Triassic, and Permian)

Fine-grained calcareous sediment, epiclastic siltstone and sandstone, tuff, lava flows, and subvolcanic intrusions exposed in the Catherine Creek drainage are part of the Wallowa terrane, a late Paleozoic and early Mesozoic island arc complex that is best exposed in the Wallowa Mountains and Hells Canyon areas east of the study area. Wallowa terrane units exposed in the upper Grande Ronde River basin include:

TRws **Undifferentiated volcaniclastic and clastic sedimentary rocks (Triassic (?))**—Mainly bluish-gray to light gray argillite and siltstone. Unit is heterogeneous and includes bluish-black calcareous argillite, feldspar-bearing tuffaceous argillite, volcaniclastic sandstone, limestone, and volcaniclastic breccia. Seldom forms outcrop, readily weathers to rounded slopes mantled by angular rock fragments. Commonly thinly bedded (1 to 50 cm) and marked by fracture cleavage. Considered to be correlative with the Lower Sedimentary Series of Smith and Allen (1941) on the basis of lithology and apparent stratigraphic position. Triassic age on the basis of fossil localities in similar-appearing strata exposed near Medical Springs (Bostwick and Koch, 1962).

TRPwc **Clover Creek Greenstone (Triassic or Permian)**—Mainly dark-green to dark bluish-gray, metamorphosed volcanic, subvolcanic intrusive, and volcaniclastic rocks that weather to shades of dark brown. Heterogeneous unit contains a wide range of metamorphosed volcanic rocks, including quartz keratophyre, quartz keratophyre tuff, spilite, diabase, and meta-andesite. Very poorly exposed, weathers to form rounded hills. Typically sheared and chloritized where exposed along roads in the south. Part of the Clover Creek Greenstone of Gilluly (1937), which contains both Permian and upper Triassic strata.

Baker Terrane (Triassic, Permian, Pennsylvanian, and Devonian (?))

The Baker terrane is largely composed of a complicated mix of Paleozoic and Triassic igneous, sedimentary, and metamorphic rock (Bishop 1984). Exposures along the upper Grande Ronde River include internally disrupted, fine-grained siliceous deep-water sediment of the Elkhorn Ridge Argillite and large, internally disrupted slabs of metamorphosed island-arc volcanic rocks. See Appendix for analyzed rocks (samples 529–539). Mapped units include:

TRPbe **Elkhorn Ridge Argillite (Triassic, Permian, Pennsylvanian and Devonian (?))**—Mainly dark-bluish-black to black siliceous argillite and chert. Unit is heterogeneous and includes carbonaceous argillite, feldspar-bearing tuffaceous argillite, and ribbon chert. Generally forms massive jagged outcrops with steeply dipping layers. Stratified layers are typically fault- or cataclasite-bounded slabs of steeply dipping, isoclinally folded chert and argillite (Figure 30). Isoclinal fold noses are commonly sheared. Typically mantled by shallow soils containing abundant angular chips of chert and argillite. Many exposures in the map area show thermal metamorphism due to nearby Mesozoic intrusions. Contact aureoles along the Bald Mountain batholith are marked by recrystallization of chert to coarser-grained banded quartz-

Figure 30. Exposure of Elkhorn Ridge Argillite on the Grande Ronde River. Thin to massively bedded cherty argillite that has been sheared and folded along steeply dipping bedding planes.

ites containing biotite and garnet. Hornblende hornfels (hornblende + plagioclase + quartz + diopside) and pyroxene hornfels (orthopyroxene + diopside + hornblende + plagioclase +quartz + biotite) assemblages occur along contacts between argillite and intrusive rocks (Taubeneck, 1995; Evans, 1989). Godwin (1999) reported biotite + andalusite + cordierite and biotite + andalusite + garnet in the contact aureole of the Bald Mountain batholith south of the map area. Regional metamorphic grade for the Elkhorn Ridge Argillite is lower greenschist facies; diagnostic mineral assemblages include biotite + chlorite + white mica and white mica + chlorite + quartz (Ferns and Brooks, 1995; Kays and others, 1987). Chemical analyses for regionally metamorphosed chert collected south of the Bald Mountain batholith show 78.30 to 94.72 weight percent SiO_2, 0.12–0.47 weight percent Al_2O_3, and 0.44 to 1.79 weight percent K_2O (Ken Johnson, written communication, 1998). Unit is structurally disrupted, generally dipping steeply to the south. Permian and Triassic age range on the basis of invertebrate fossils from limestone pods and ribbon chert. Pennsylvanian (Coward, 1983; Ferns and others, 1987: Blome and others, 1986), and possible Devonian fossils have also been reported (Morris and Wardlaw, 1986; Evans, 1989, 1995) from Elkhorn Ridge Argillite exposures to the south.

TRPba Amphibolite and metamorphosed intrusive rocks (Triassic and Permian)—Dark green, green, and yellowish white to light green, fine- to coarse-grained amphibolite and metamorphosed intrusive rock. Heterogeneous unit possesses complexly intermixed intrusive, volcanic, and volcaniclastic sedimentary rocks that have been deformed and metamorphosed. Outcrops are massive and blocky but tend to weather to shallow subcrops marked by 4 cm subangular pieces. Commonly cut by closely spaced, randomly oriented, anastomosing microbreccia zones as much as 5 cm thick. Typical quartz diorites contain hornblende, plagioclase, and quartz crystals. Diorites comprise ophitic green hornblende and andesine; trondjemites are composed largely of oligoclase and quartz. In most exposures, relict magmatic feldspar and hornblende crystals are partially recrystallized. Relict intrusive textures are commonly hypidiomorphic-granular (Evans, 1989). Composition ranges from gabbro to trondjemite. The contact aureoles of younger Mesozoic intrusions have foliated amphibolite in which original magmatic textures have been obliterated. Gneissic layering is defined in intensely metamorphosed metagabbro by light colored, plagioclase-rich layers and dark-colored hornblende and diopside-rich layers (Taubeneck, 1995). Recrystallized to hornblende hornfels (hornblende + plagioclase + diopside + garnet along the margins of the Bald Mountain batholith (Taubeneck, 1995). Intermediate-composition rocks are low-potassium trondjemites; with 58.32 weight percent SiO_2, 15.05 weight percent Al_2O_3, and 0.14 weight percent K_2O. Late Permian Triassic age on the basis of a 244 + 1 Ma ^{206}Pb-^{238}U zircon age from similar rocks along the North Fork of the John Day River (Walker, 1986). Composite unit that includes the TRPa and TRPi units that were mapped at 1:24,000 scale by Madin (1998) and Ferns and Taubeneck (1994).

STRUCTURE

The upper Grande Ronde River basin is part of the Blue Mountains physiographic province (Figure 1), an uplifted, mountainous region with several large, roughly north-trending, fault-bounded valleys and depressions (Figure 31). The basin is largely buried by middle Miocene and younger volcanic rocks. Folds and faults that shape the modern topography developed over the last 15 million years and may be as young as latest Pleistocene (Personius, 1998). Historically, the major younger faults have been viewed as having formed in conjunction with regional movement along the enigmatic Olympic Wallowa lineament (OWL), a topographic lineament that extends from the Olympic Mountains of northwest Washington through northeast Oregon (Hooper and Conrey, 1989; Mann and Meyer, 1993). The OWL was originally defined by Raisz (1945) to include the Wallowa Fault on the northeast side of the Wallowa Mountains and was believed to extend across the northern end of the upper Grande Ronde River basin. The absence of suitably oriented topographic features in the north end of the upper Grande Ronde River basin led Mann (1989) to suggest that the faults that form the OWL are deflected south to form the north and east margins of Grande Ronde Valley, eventually linking through a zone of normal and right oblique faults to the western Snake River plain in Idaho.

The structure of the upper Grande Ronde River basin is complex but can be divided into five sections (Figure 32) on the basis of structural variation: 1) Grande Ronde Valley, 2) western uplands, encompassing the Grande Ronde River and tributary streams entering upstream of Grande Ronde Valley, 3) southern uplands, which includes the headwaters of Catherine Creek drainage and many tributary streams that join the Grande Ronde River in Grande Ronde Valley, 4) eastern block, which encompasses Indian Valley, the Grande Ronde River downstream of Grande Ronde Valley, and tributary streams joining the Grande Ronde River from the east, and 5) northern uplands; which includes the tributary streams that enter Indian Valley from the west.

Grande Ronde Valley

The modern Grande Ronde Valley lies in a fault-bounded depression that is about 40 km on its north-south axis (Figure 33) and 20 miles wide from the town of Cove, on the east side, to La Grande, on the west side. The valley is a graben bounded on the east and west by major fault zones (Hampton and Brown, 1964) and has been described as a pull-apart basin (Gehrels, 1981; White, 1981). The basin floor, as defined by bedrock at the top of lava flows of the Powder River Volcanic Field, is a faulted and tilted surface that plunges to more than 600 m below the valley floor. Water well and geophysical data, including regional gravity and magnetic profiles (AMAX Exploration, Inc., 1975; Ferns and others, 2002a) and a seismic refraction line across the south end of the valley (Ferns and others, 2002a), indicate that the basal sedimentary section dips to the west (Liberty and Barrash, 1998). The southern margin of the valley is defined by irregularly shaped north-sloping uplands that dive beneath the valley fill sequence. The valley's northern margin is defined by irregularly shaped, south-sloping uplands that also dive beneath the valley fill.

The West Grande Ronde Valley (WGRV) fault zone is a 40-km-long and 3-km-wide band of mainly down-to-the-east, subparallel normal faults that possess a strong aeromagnetic gradient (Ferns and others, 2002a). The western margin of Grande Ronde Valley has an abrupt escarpment that stands 770 m above the valley, separating Grande Ronde Basalt flows exposed in the steep sloping escarpment from the more gently sloping bajada surface. Within the West Grande Ronde Valley fault zone, individual north- and northwest-trending faults with vertical offsets up to 700 m can be traced as far as 10 km. Total cumulative vertical displacement along the WGRV fault zone exceeds 1,100 m. Subtle topographic features, including linear range fronts, low linear escarpments on alluvial fans and terraces, faceted spurs, and *Z*-shaped topographic inflections along bedrock-alluvial fan contacts, indicate that surface ruptures along the West Grande Ronde Valley fault zone are Late Quaternary and possibly Holocene in age (Simpson and others, 1993; Personius,

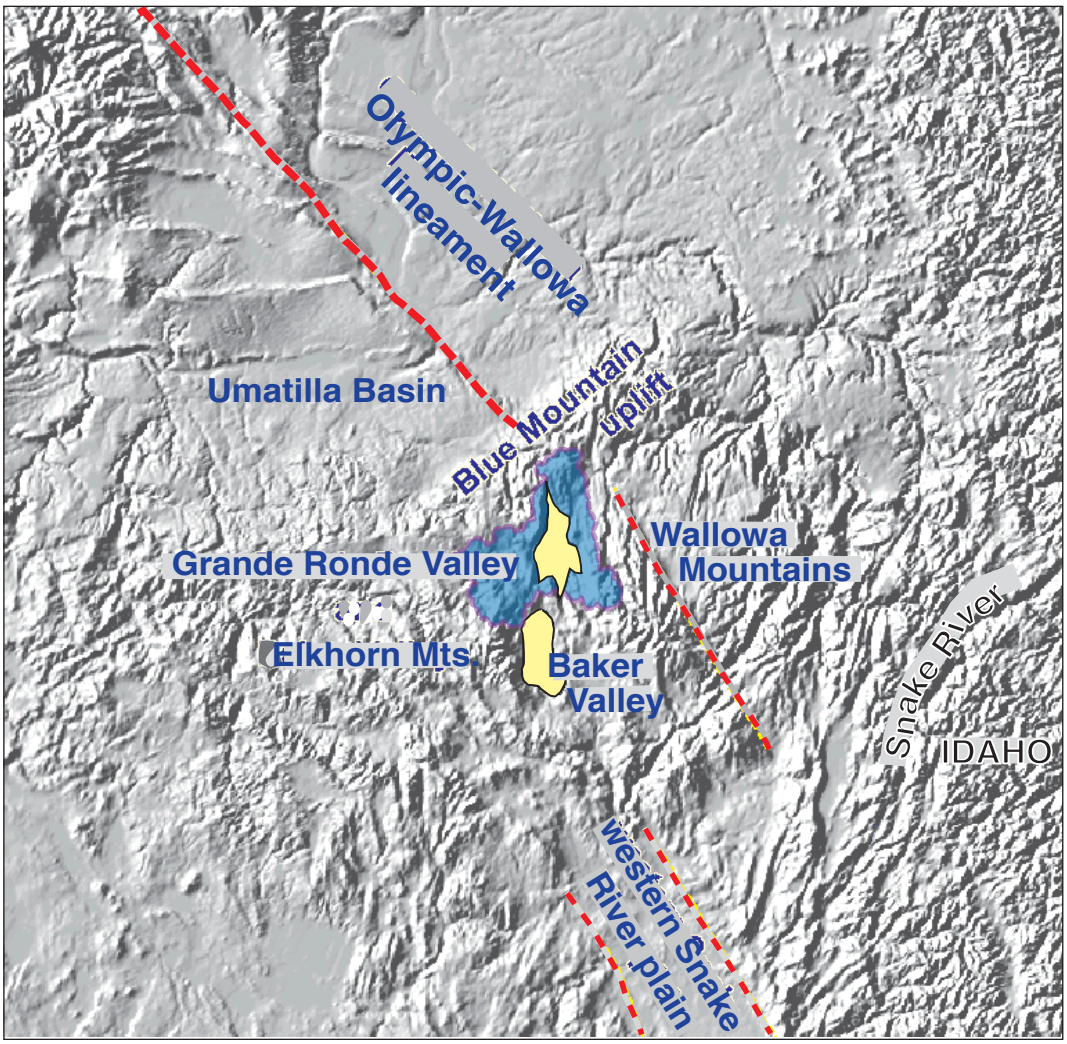

Figure 31. Shaded relief map of northeast Oregon, southeast Washington, and western Idaho, showing how Grande Ronde Valley lies between the Olympic-Wallowa lineament (OWL) and the western Snake River plain.

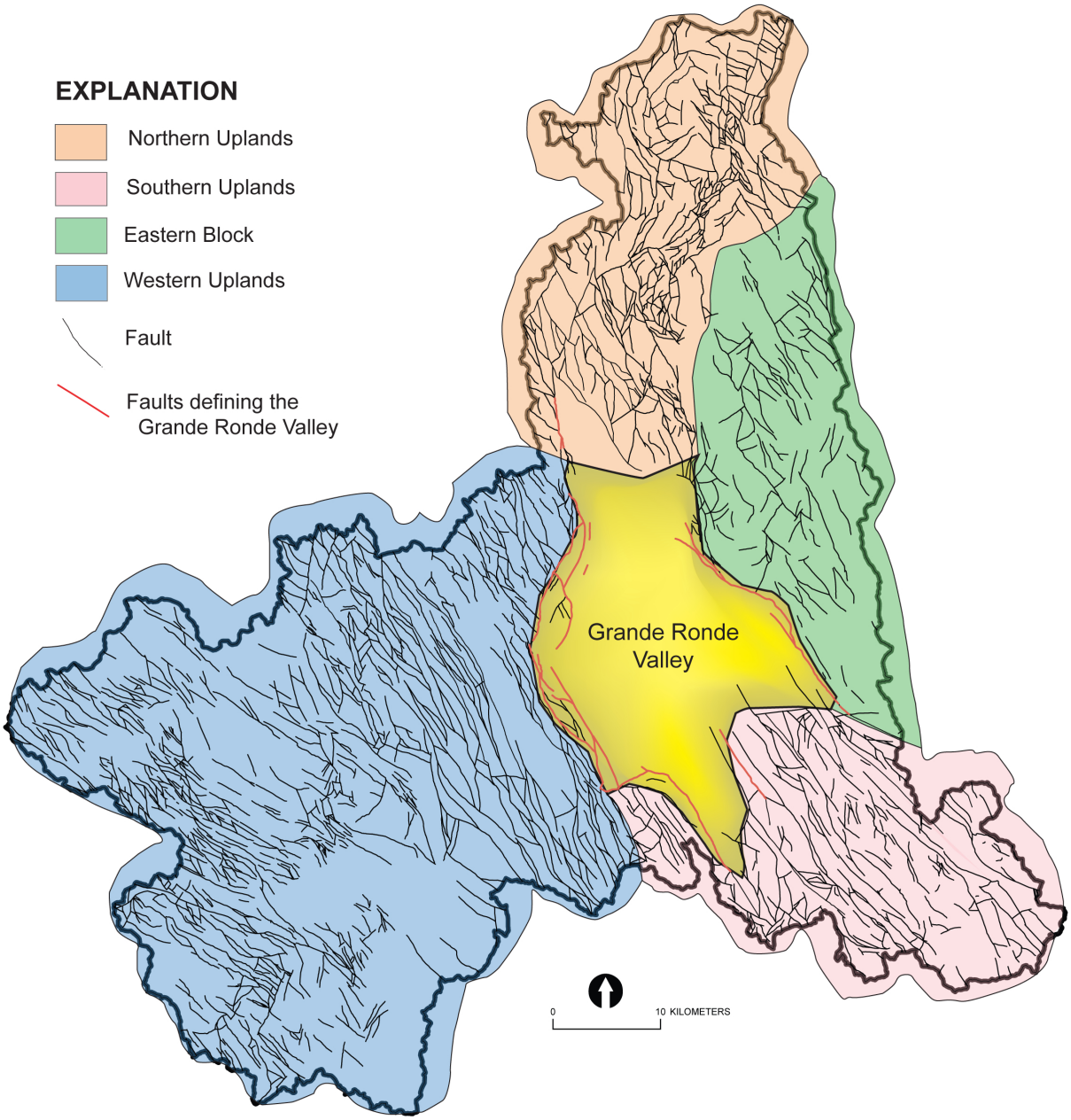

Figure 32. Fault map of the upper Grande Ronde River basin showing the five physiographic regions described in the text: 1) Grande Ronde Valley, 2) western uplands, 3) southern uplands, 4) eastern block, and 5) northern uplands.

1998; Ferns and Madin, 1999). An exposed fault plane in this zone dips 70° to the southeast. The northern part of the WGRV fault zone continues beyond Grande Ronde Valley to the northwest and crosses the crest of the Blue Mountain uplift, where zone loses topographic expression in the deeply eroded upper Umatilla River basin (Figure 31). The southern part of the WGRV fault zone possesses subparallel fault strands that separate rotated blocks of volcanic rocks that dip into the valley. One fault segment, the Taylor Creek fault of Gehrels (1981), crosses into the valley floor south of La Grande beneath Ladd Marsh and trends toward Hot Lake.

The East Grande Ronde Valley (EGRV) fault zone abruptly separates Grande Ronde Basalt flows exposed in the steep sloping escarpment from more gently sloping bajada by as much as 760 m of vertical relief. At least 1,200 m of cumulative down-to-the-west vertical displacement is indicated across the fault zone, which also shows a strong aeromagnetic gradient coincident with the trace of the EGRV fault zone (Ferns and others, 2002a). The fault zone consists of several large-displacement, en echelon faults as long as 20 km and is considered by some to be part of the Olympic-Wallowa lineament (Mann, 1989). The EGRV fault zone is about

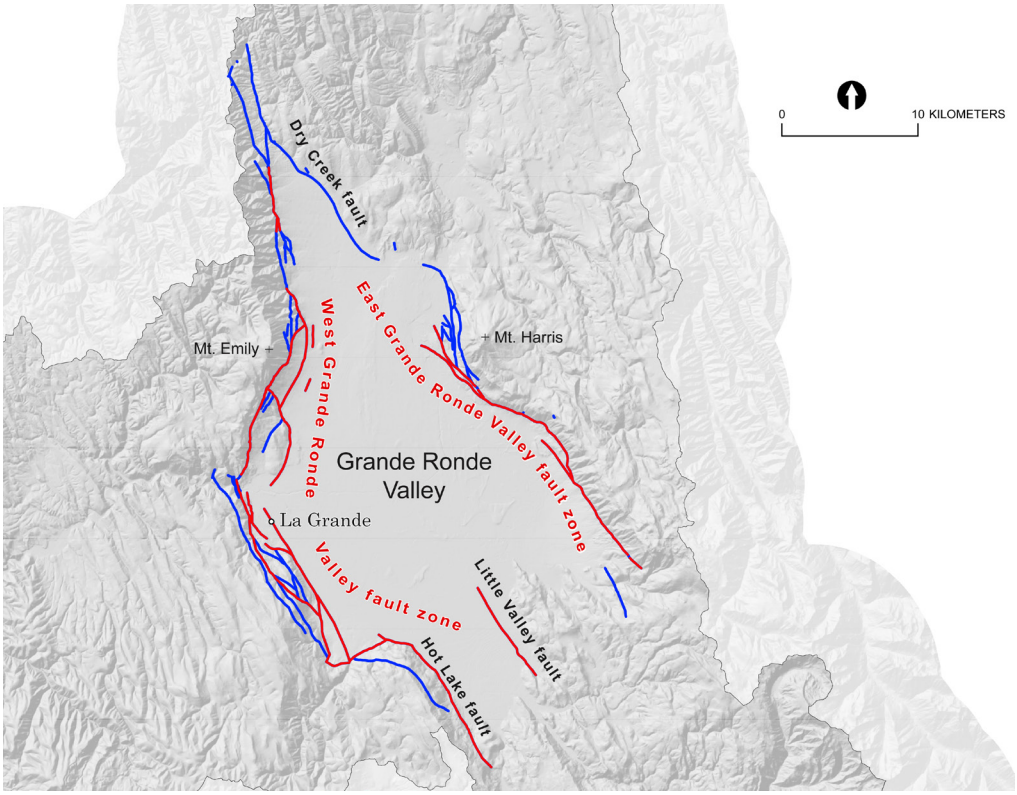

Figure 33. Shaded relief map of Grande Ronde Valley showing the major fault zones and faults (in blue) that define the valley's margins. The Little Valley fault and several segments of the West Grande Ronde Valley and East Grande Ronde Valley fault zones show evidence of probable Holocene movement (in red).

1 km wide and is offset on the south by the east-west-trending Mill Creek fault (White, 1981). The Cove segment of the fault zone consists of a single fault that extends nearly 20 km along faceted spurs that mark the prominent eastern escarpment of Grande Ronde Valley (Simpson and others, 1993; Personius, 1998; V.S. McConnell and others, unpublished mapping). The surface of the upthrown block on the eastern side of the EGRV fault zone dips to the north-northwest and forms a topographic ramp that slopes beneath the Mount Harris volcano. At Mount Harris the Cove and Mount Harris fault segments intersect beneath a large landslide complex at Grays Corner (Simpson and others, 1993; Personius, 1998). Although the landslides at Grays Corner cover a faulted surface and are marked by linear ridges and closed depressions, inset fans do not appear to be offset by faulting (Personius, 1998; Ferns and others, 2002b). North of Mount Harris, the valley margin is marked by a closely spaced series of short-strike-length faults that are considered by Simpson and others (1993) to be segments to the larger EGRV fault zone. Apparent lateral displacement of volcanic units along the base of Mount Harris may indicate as much as 300 m of right-lateral displacement and 450 m of vertical displacement along the southern margin of the Mount Harris fault zone (Ferns and others, 2002b).

The southern margin of Grande Ronde Valley possesses a more topographically subdued, faulted upland that slopes downward to the northwest. Individual fault blocks are generally tilted to the west and bounded by down-to-the-east faults. The most pronounced escarpment along the south margin is formed by the Hot Lake fault (Gehrels, 1981), which swings to the west at Hot Lake, and projects into Grande Ronde Valley on trend with the WGRV fault zone. A seismic profile across the valley east of the Hot Lake fault (Ferns and others, 2002a) indicates that the basin floor north of Union forms a west-dipping surface that dives to more than 300 m below the valley floor. Total displacement along the Hot Lake and companion faults is in excess of 1,000 m. Many of the northwest-trending ridges in the uplands to the south (Figure 36) are bounded by smaller faults that continue into Grande Ronde Valley. Northeast of Union, a sinuous, 1- to 3-m-high scarp of possible Holocene age extends into the valley for 1 km along the projected northern extension of the Little Creek Fault (White, 1981; Gehrels, 1981). The base of the valley fill sediment is vertically offset about 25 m along the Little Creek fault (Ferns and others, 2002a). Seismic profiles and water well data along the south margin show that the volcanic basement underlying Grande Ronde Valley is here broken into a series of west-dipping blocks (Ferns and others, 2002a).

The north margin of Grande Ronde Valley is marked by a southeast dipping homocline that is bounded on the west by the northwest-trending down-to-the-west Dry Creek fault (White, 1981). The homocline is cut by small-displacement, northwest- and northeast-trending faults that do not appear to continue into the valley. The Dry Creek fault continues north and intersects the WGRV fault zone and probably extends eastward beneath valley sediment and links up with the EGRV fault zone.

Western Uplands

The western uplands region is part of the Blue Mountains uplift and includes all of the area drained by the Grande Ronde River upstream from Grande Ronde Valley (Figure 34). Major structural features in the western uplands include 1) northeast-trending folds and faults of the Blue Mountains uplift, and 2) cross-cutting northwest-trending fault zones that break the core of the uplift into a series of shallow basins separated by faulted ridges.

Folds

The Blue Mountains uplift is a broad anticlinorium that forms an extensive upland. The crest of the anticlinorium forms a broad arc that curves to the northwest and forms a gently rolling surface of broad open folds over much of its length. Fold-axis trends range from N. 85° W. to N. 50° E. Anticlinal crests are marked by flat-lying lava flows of the upper Grande Ronde Basalt (N2 of Swanson and others [1979] and Fiddlers Hell members of Ferns and others [2001]). Grande Ronde Basalt flows unconformably overlie an irregular surface of pre-Miocene strata that is exposed locally at the surface along the uplift. The crest of the anticlinorium provides a barrier between the upper Grande Ronde River basin and the Umatilla River basin to the northwest (Figure 31). The upper Grande Ronde River flows eastward along the southeast flank of the anticlinorium, through the axial trough of the Grande Ronde syncline (Hampton and Brown, 1964; Walker, 1973), a bowl-like, concave surface with several monoclinal to synclinal flexures (Barrash and others, 1980). Near Tower Mountain, southwest of the Grande Ronde syncline, north-dipping upper flows of Grande Ronde Basalt lap onto deeply dissected highlands of the Tower Mountain caldera. Farther east, tilted lower Grande Ronde Basalt flows fill canyons of the deeply eroded pre-Tertiary highlands and are sequentially younger to the north.

Northwest-Trending Fault Zones

Northwest-trending fault zones cut across the western uplands and form bold topographic lineaments (Figure 35). The lineaments are characterized by short-strike-length faults that bound northwest-trending shallow structural depressions partially filled by middle- and late-Miocene sediment. In places, the Grande Ronde River and major tributary streams, such as Fly Creek, Beaver Creek, and Meadow Creek, flow parallel to the fault zones. The dominant sense of vertical displacement changes along the length of each fault zone from predominantly down to the southwest to predominantly down to the northeast and then back to down to the southwest. Shifts in sense of displacement occur where the fault zones are disrupted by crosscutting, north-trending, high-angle normal and reverse faults.

The Fly Valley fault zone is a series of short-strike-length faults that form a N. 65° W.-trending zone 60 km long by about 7 km wide (Ferns, 1999; Ferns and others, 2001). Individual fault strands can be traced as far as 8 km with as much as 130 m of vertical offset. More than 400 m of cumulative vertical displacement is apparent where the Fly Valley fault zone parallels the Grande Ronde River. The sense and magnitude of vertical displacement varies along the zone from down to the southwest north of Ukiah to down to the northeast at Lehman Springs, then back to down to the southwest at Fly Valley. Stream gradients change markedly across the Fly Valley fault zone (Ferns and Taubeneck, 1994).

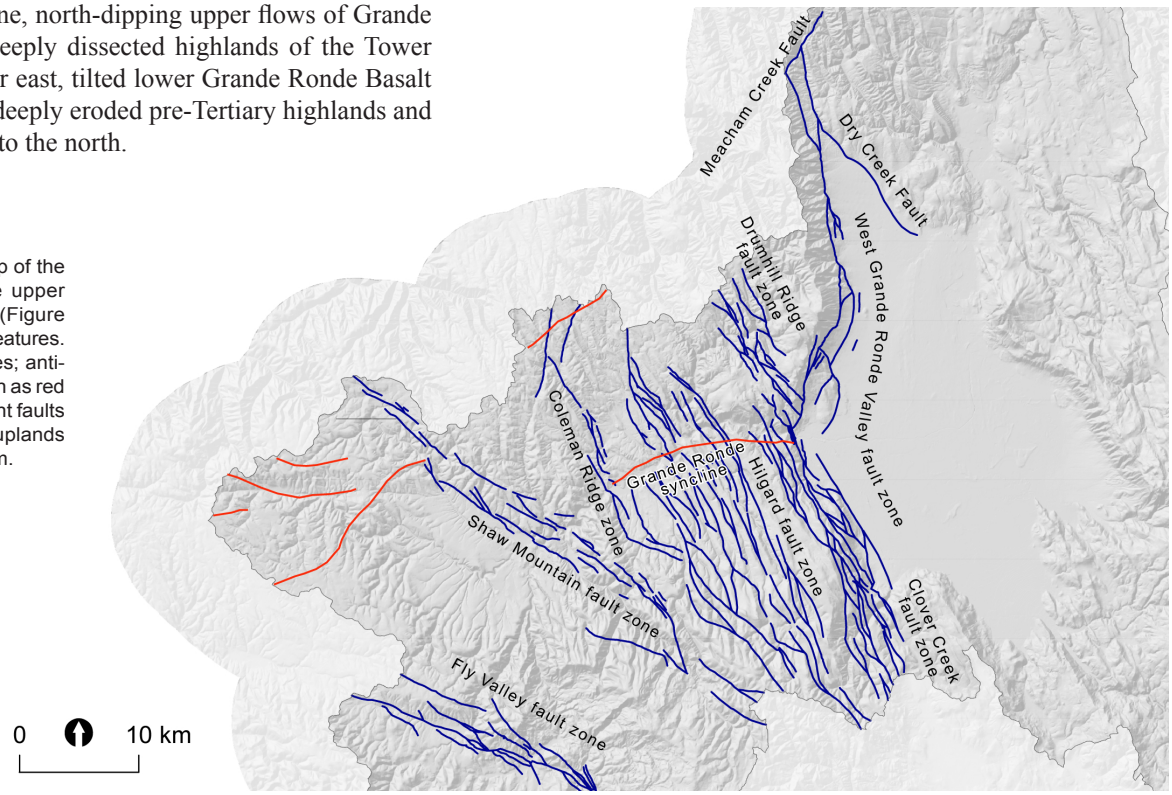

Figure 34. Shaded relief map of the western uplands part of the upper Grande Ronde River basin (Figure 32) showing major structural features. Faults are shown as blue lines; anticlines and synclines are shown as red lines. Many small displacement faults cutting across the western uplands are not shown on this diagram.

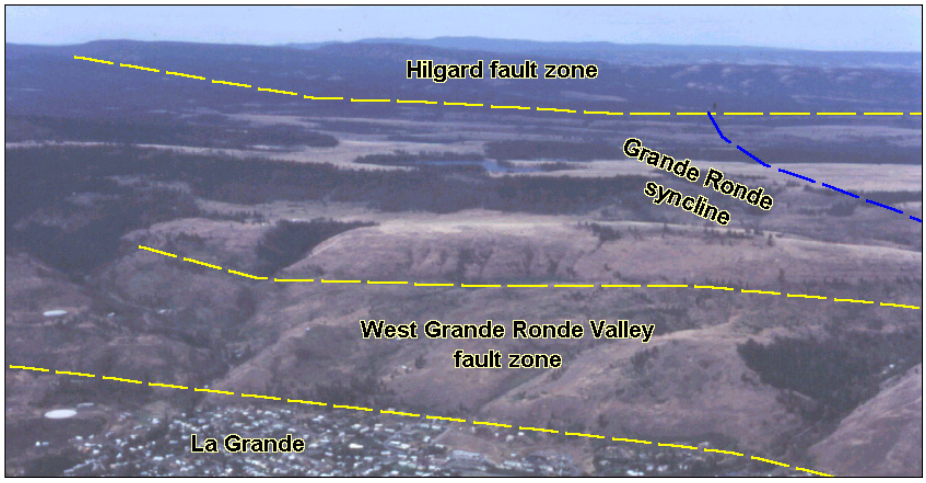

Figure 35. Aerial photograph of the West Grande Ronde Valley fault zone, looking west from above La Grande. Part of the town of La Grande shows at lower left.

The Shaw Mountain fault zone consists of a series of northwest-trending, mostly down-to-the-southwest fault strands. There is at least 365 m of cumulative vertical displacement along the east end of the zone (Madin, 1998). The zone can be traced westward from Shaw Mountain to Beaver Ridge, where it is broken up by a series of short-strike-length, N. 0° to 15° E. normal- and high-angle reverse faults. At Beaver Ridge the sense of relative displacement along the Shaw Mountain fault zone is reversed to down to the northwest. The sense of displacement changes back to down to the southeast on the northern margin of the Starkey basin. Measured dips on fault planes range from 85° to 90°.

The Spring Creek basin is bounded by two fault zones: the N. 35° W. striking Coleman Ridge fault zone on the west, and the Hilgard fault zone on the east (Ferns and others, 2001). Individual fault segments, including the Spring Creek and Coleman Ridge faults (Kienle and others, 1979), may be as long as 7 km with as much as 150 m of down-to-the-northeast vertical displacement. The Coleman Ridge fault zone does not cross the crest of the Blue Mountain uplift but instead merges with a set of down-to-the-west, N. 5° E.-trending faults. The south end of the Coleman Ridge fault zone merges with the north side of the Shaw Mountain fault zone.

The eastern margin of the Spring Creek basin is marked by the N. 35° W.-trending Hilgard fault zone, a group of 5- to 15-km-long faults. The zone includes the Hilgard and Peach Canyon faults of Kienle and others (1979) and the Rock Creek East, Rock Creek West, and Little Coyote Canyon faults of Barrash and others (1980). The general sense of displacement varies along the Hilgard fault zone, shifting from down to the northeast on the southern end of the zone to down to the southwest northward across the axis of the Grande Ronde syncline and then back to down to the northeast closer to the crest of the Blue Mountain uplift. Vertical displacements along individual faults are typically less than 100 m. Some of the shorter splays show evidence of strike-slip displacement (Kienle and others, 1979). Longer faults such as the Peach Canyon fault show changes in sense of relative movement, shifting from down to the northeast north of the Grande Ronde synclinal axis to down to the southwest south of the axis (Barrash and others, 1980). Apparent right-lateral offset is suggested where faults cut the Powder River Volcanics near Glass Hill. The south end of the Hilgard fault zone also merges with the north side of the Shaw Mountain fault zone.

The Drumhill Ridge fault zone, which includes the Drumhill Ridge, Perry, and Wilbur Mountain faults of Kienle and others (1979), consists of a series of normal faults with small displacements that trend N. 35° W. Vertical displacement along individual faults is less than 100 m with most less than 30 m. The dominant sense of vertical displacement shifts from down to the southwest east of Mount Emily to down to the northwest where the zone merges with the West Grande Ronde fault zone. As much as 1 km of dextral displacement may be evident by possible right-lateral offset of a Powder River Volcanics dacite (Tpd) flow east of Mahogany Mountain. Gehrels (1981) cited shallow-plunging striations and mullion structures on nearly vertical fault planes as evidence for right-lateral movement along these faults.

Southern Uplands

The southern uplands region (Figure 36) includes the entire Catherine Creek watershed south of Grande Ronde Valley and is bordered on the west by Ladd Creek and on the east by Mill Creek, southeast of Cove. The topography, which is more subdued than the surrounding topography (Figure 37), is dominated by a series of northwest-trending ridges that slope northward and plunge beneath Grande Ronde Valley sediment. Discontinuous fault zones continuing south from the West and East Grande Ronde Valley fault zones separate the southern uplands from the high-standing Elkhorn Mountains (Figure 31) west of Baker Valley and the Wallowa Mountains to the east. Although most of the topography is fault controlled, some constructional volcanic features are preserved locally.

Bounding Fault Zones

The Clover Creek fault zone is a series of 0° N.- to N. 20° W.-trending faults that are the southern extension of the West Grande Ronde Valley Fault Zone that continues south toward Baker Valley. Vertical displacement along individual faults may exceed 100 m, with the predominant sense of displacement being down to the east. Cumulative down-to-the-east vertical displacement along the Clover Creek fault zone is more than 300 m. Gehrels (1981) reported predominantly vertical dips on slickensides along the Clover Creek fault zone.

The South Baldy fault zone (Figure 36) links the East Grande Ronde Valley fault zone with the Wallowa Fault to the southeast. The South Baldy fault zone consists of a series of N. 25° W.- to N. 45° W.-trending faults with a cumulative down-to-the-southwest vertical displacement of about 300 m, with some individual faults having vertical displacement of more than 100 m. The South Baldy fault zone includes several small grabens, such as the Moss Springs graben (McConnell and others, 2003). Although the primary sense of displacement is vertical, offsets of stream drainages and contacts suggest some right-lateral component of movement (McConnell and others, 2003).

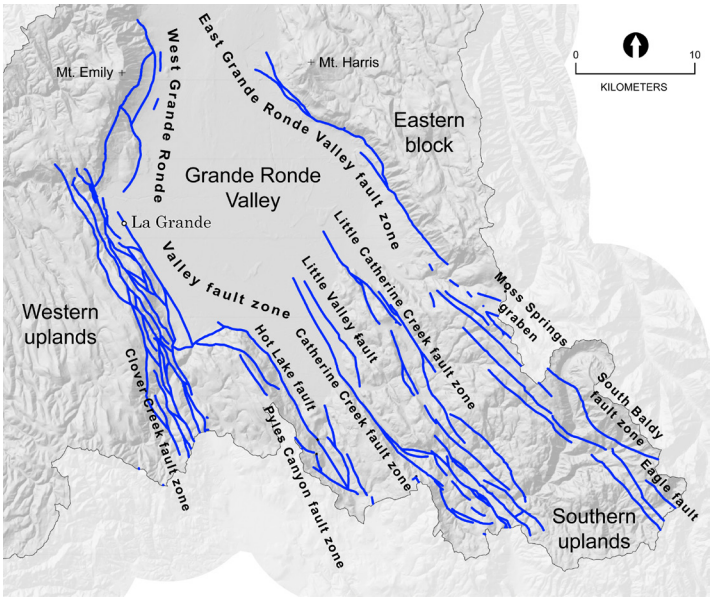

Figure 36. Shaded relief map of the southern uplands part of the upper Grande Ronde River basin (Figure 32) showing major structural features. Faults are shown as blue lines. The Clover Creek fault zone and the South Baldy fault zone form the major bounding structures to the southern uplands.

Northwest-Trending Faults and Cinder Cones

Faults, fault zones, and cinder cones are aligned along a common N. 40° W. to N. 50° W. trend in the southern uplands. Two major fault zones are herein named the Pyles Canyon and Catherine Creek fault zones. Northwest-trending faults near the head of Pyles Canyon can be traced north where they merge with the Hot Lake and other faults of Gehrels (1981). At its northern end, near Hot Lake, the Pyles Canyon fault zone is separated from the Clover Creek fault zone by several east-west trending, low-angle faults that tilt lava flows to the north (Gehrels, 1981). Farther south, along the east face of Craig Mountain, a structurally disrupted zone of massive landslides and steeply tilted, fault-bounded blocks of broken rock (jumbled block unit

Figure 37. View looking northeast from atop the Catherine Creek faulted escarpment across the rolling hills of the southern uplands to the high plateau of the eastern block. The green valley in the foreground is the Catherine Creek drainage. The horizon shows Mount Harris on the left and Mount Fanny on the right.

of Barrash and others [1980]) separates the Hot Lake fault and Craig Mountain faults. The Pyles Canyon fault zone is truncated on the south by a northeast-trending fault zone.

Four basaltic andesite vents on Ramo Flat and a trachybasalt dike to the southeast (Tpv) are aligned along a northwest axis east of the Pyles Canyon fault zone. The three northern vents are deeply eroded basaltic andesite cinder and scoria cones that are surrounded by flows of the Powder River Volcanic Field.

The Catherine Creek fault forms the high escarpment of the lower Catherine Creek drainage. The northwest-trending fault can be traced south into a large landslide, where it is broken up by several west- to northwest-trending faults. The fault crosses an area where there is rapid lateral thinning and thickening of Tertiary volcanic units due to deeply eroded paleotopography. Welded spatter and scoria mounds exposed along both sides of the fault mark locations of Grande Ronde Basalt (Tcg) and Powder River basalt and basaltic andesite vents (Tpv). Although the total amount of displacement is uncertain, the Catherine Creek fault exhibits as much as 210 m of down-to-the-east offset.

Late Pleistocene, and possibly Holocene, movement is indicated along the Little Valley fault, which forms a 1- to 3-m-high, east-facing scarp in fan gravel. The Little Creek fault can bet raced from the valley floor onto the southern uplands, where it splays into two segments (White, 1981). Predominant sense of displacement is down to the east. The southern splay may continue south and link up with the Catherine Creek fault (White, 1981).

The Phys Point, Mill Creek, High Valley, and Little Catherine Creek faults are part of a northwest-trending fault zone herein referred to as the Little Catherine Creek fault zone. The Little Catherine Creek fault zone extends from Grande Ronde Valley to where Catherine Creek makes a 90° turn from southwest to northwest. The sense of displacement along the north end of the zone is predominantly down to the east. The dominant sense of displacement shifts to down to the west farther south along the High Valley and Little Catherine Creek faults. Dextral shifts in stream channels at or near some faults in the Little Catherine Creek fault zone may indicate right-lateral displacement.

Eastern Block

The eastern block (Figure 38) is a northwest-sloping plateau (Figure 39) that encompasses the upper Grande Ronde River basin east of the South Baldy, East Grande Ronde Valley, and Mount Harris fault zones and includes Indian Valley bordered on the north by the Big Hole and Lookingglass fault zones. The higher parts of the block are referred to as the Mount Fanny plateau (McConnell and others, 2003; unpublished mapping). Major streams originating on the Mount Fanny plateau include Indian Creek and Clarks Creek. The lower, northern part of the eastern block is cut by the Grande Ronde River and includes some streams entering from the west.

Most of the relatively undeformed eastern block is formed by a 1° to 4° northwest tilt that culminates in a broad, northeast-trending syncline north of Elgin. Many of the topographic highs on the eastern block are small volcanoes. Some ridges are erosional remnants of intracanyon lava flows. Fault displacements are typically less than 50 m. Structures include northeast-trending folds and faults, and north- to northwest- trending faults and fault zones; however, fault escarpments are relatively uncommon.

Northeast-Trending Folds and Faults

Northeast-trending structures of the eastern block include the Big Hole fault zone and an asymmetric syncline at the north end of the block. A late Miocene or Pliocene andesite flow occupies the synclinal trough. The east limb of the syncline dips gently to the northwest, whereas the west limb dips steeply to the east and is broken by numerous faults. The largest northeast-trending faults lie along the Big Hole fault zone, which possesses a series of down-to-the-east N. 50° E.- to N. 60° E.-trending faults that have a maximum cumulative vertical displacement of 240 m. The amount of offset decreases to the northeast, where the zone terminates against the north- to northwest-trending faults of the Lookingglass fault zone.

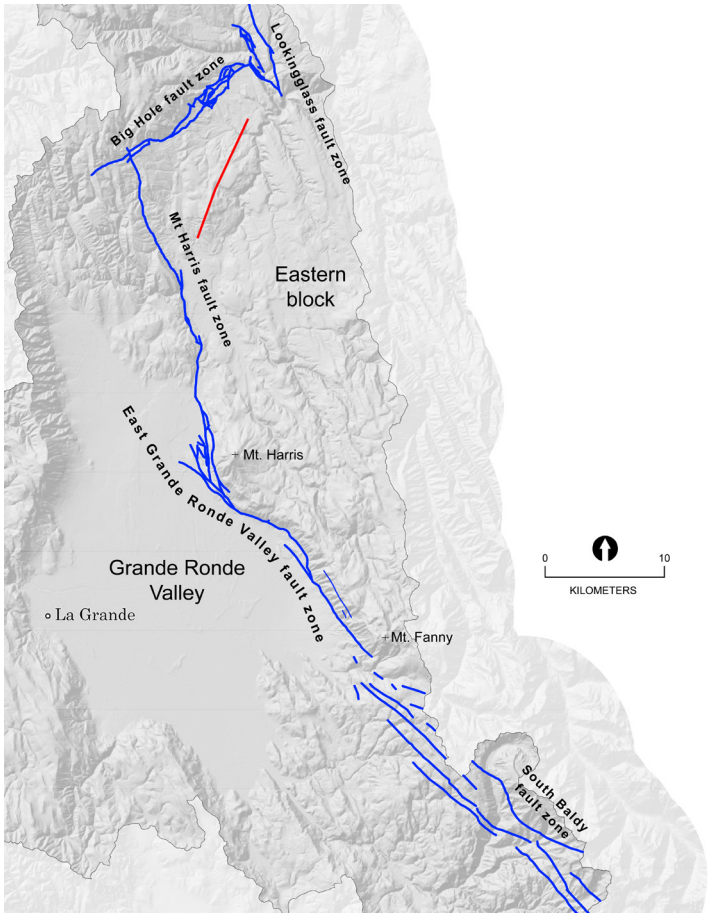

Figure 38. Shaded relief map of the eastern block part of the upper Grande Ronde River basin (Figure 32) showing major structural features. Note the northward tilt to the eastern block evident in Figure 39. Faults are shown as blue lines. Syncline east of Big Hole fault zone is shown as a red line. In contrast to the western uplands, the eastern block is a stable platform cut by relatively few faults.

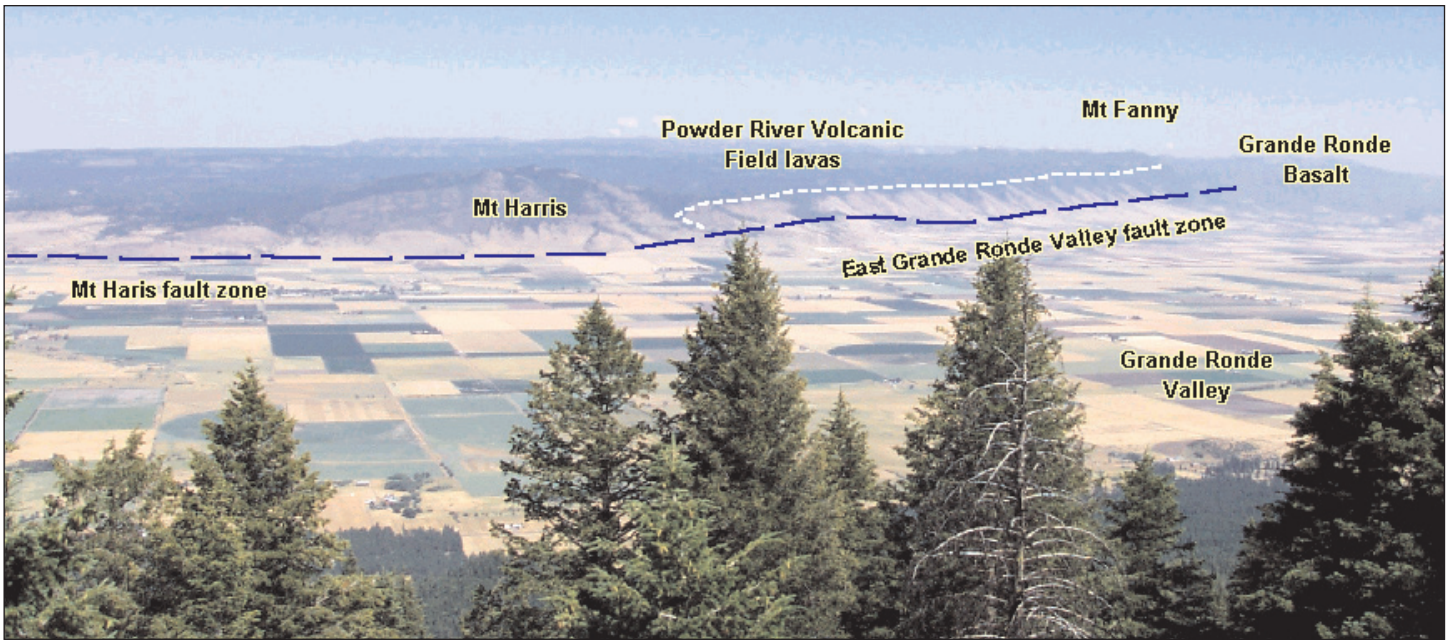

Figure 39. View looking east-southeast across Grande Ronde Valley to the eastern block. The block dips north from Mount Fanny on the right, toward the Big Hole fault zone, out of sight to the left. Dashed white line marks the contact between Grande Ronde Basalt (Tcg) and the base of the Powder River Volcanic Field.

Northeast-trending faults also occur east of Mount Harris, where they truncate against the East Grande Ronde Valley fault zone.

North- and Northwest-Trending Fault Zones

The south end of the Mount Harris fault zone consists of closely spaced, 0° N.- to N. 15° W.-trending, short-strike-length faults that merge with the main East Grande Ronde fault at Mount Harris. These faults form a scissors zone along which the dominant down-to-the-west sense of displacement in Grande Ronde Valley changes to a dominant down-to-the-east sense of motion to the north. The Mount Harris fault zone continues north for about 8 km from Elgin, where it is disrupted by the northeast-trending Big Hole fault zone. Approximately 270 m of cumulative, down-to-the-east vertical displacement is indicated at Elgin where fault planes dip between 60° and 65° to the east.

The Lookingglass fault zone possesses a series of short-strike-length, vertical faults with N. 35° W. to N. 55° W. trends. Lookingglass Creek makes a sharp 80° turn where the Lookingglass fault zone truncates the Big Hole fault zone in an area marked by poor exposures and landslides. Fault displacements along individual faults are typically on the order of a few meters. Although apparent offset is normal, subhorizontal slickenside striations strongly indicate oblique movement. Cumulative west-side-down displacement along the Lookingglass fault zone is about 200 m.

Northern Uplands

All of the Blue Mountains uplift northeast of Grande Ronde Valley is referred to herein as the northern uplands (Figure 40) of the upper Grande Ronde River basin. The northern uplands extend east along the crest of the Blue Mountains from the head of Dry Creek to the head of Jarbidge Creek. Phillips Creek and Lookingglass Creek are the major streams that head in the northern uplands. The northern uplands form a southward tilted ramp that is broken by northwest-, north-, and northeast-trending faults. Major structural features include northeast-trending folds.

Northeast-Trending Folds and Faults

The northern and western uplands are similar and could be considered a single province defined by the Blue Mountain anticlinorium. The crests of the N. 45° E.- to N. 60° E.-trending anticlines are defined by originally flat-lying Saddle Mountains Basalt and Wanapum Basalt flows and intervening sedimentary units. The younger strata conformably overlie a surface of older Grande Ronde Basalt flows.

The northern uplands are cut by N. 0° E.- to N. 40° E.-trending faults) The westernmost of these, the Meacham Creek fault (Kienle and others, 1979), trends N. 30° E. and truncates the West Grande Ronde Valley fault zone. The next major northeast-trending fault to the southeast, the N. 20° E.-trending Pedro Ridge fault, truncates the Big Hole fault zone. The sense of displacement along the Pedro Ridge fault is down-to-the-east. The Bal-

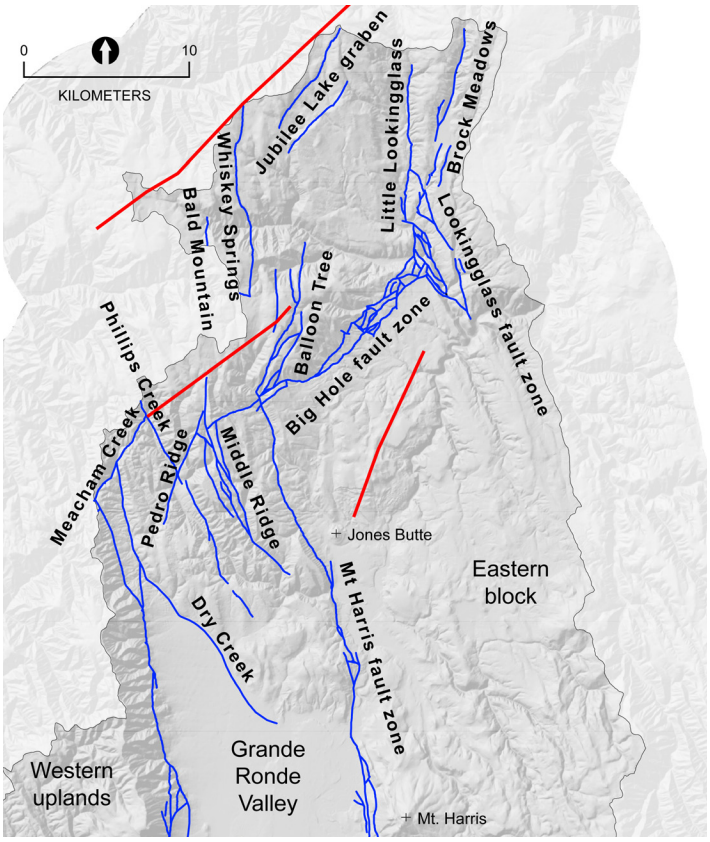

Figure 40. Shaded relief map of the northern uplands part of the upper Grande Ronde River basin (Figure 32) showing the major structural features. Faults are shown as blue lines, folds are red lines.

loon Tree fault zone also trends N. 20° E. and extends north from the Big Hole fault zone, cutting the nose of one of the anticlines. N. 40° E.-trending faults form a small graben along the crest of Blue Mountain uplift farther north at Jubilee Lake. The sense of displacement along the Jubilee Lake fault is down to the west, toward the anticlinal axis. The upthrown block is tilted to the southeast. Still farther east, the Little Lookingglass Creek and Brock Meadows faults trend N. 0° E. to N. 15° E. and cross out of the upper Grande Ronde River basin. Although both faults can be traced for considerable distance along strike, cumulative vertical offset is small and sense of displacement is down to the east (Figure 41). The northwest-trending Lookingglass fault zone truncates the southern ends of the Brock Meadows and Little Lookingglass Creek faults.

Northwest-Trending Faults

Northwest-trending faults cross the anticlinal crest of the Blue Mountains on the west side of the northern uplands. The N. 25° W.-trending Phillips Creek fault truncates the northeast-trending Meacham Creek fault and crosses into the Umatilla River drainage. The Phillips Creek fault dips 85°W with more than 100 m of down-to-the-west displacement. The Middle Ridge fault zone consists of a number of N. 15° W.- to N. 25° W.-trending, down-to-the-east faults that are truncated against the south end of the Big Hole fault zone. The intersection of the Middle Ridge and Big Hole fault zones is complex and forms a transition zone between the eastern block and the northern uplands. A similar fault complex is at the intersection of the northern end of the Big Hole fault zone and the Lookingglass Creek fault zone. There the west end of the Lookingglass Creek fault zone is deflected northward and truncates the southern ends of the Little Lookingglass Creek and Brock Meadows faults.

Large faults within the northern block include several parallel faults that form horsts and grabens. One horst is formed where the Bald Mountain and Whiskey Springs faults cross the upper reaches of Lookingglass Creek. The Bald Mountain fault is a 0° N.- to N. 10° W.-trending structure that has about 185 m of down-to-the-west offset. The Whiskey Springs fault has a N. 10° W. trend and about 125 m of down-to-the-east offset. Both faults cross the Blue Mountain uplift.

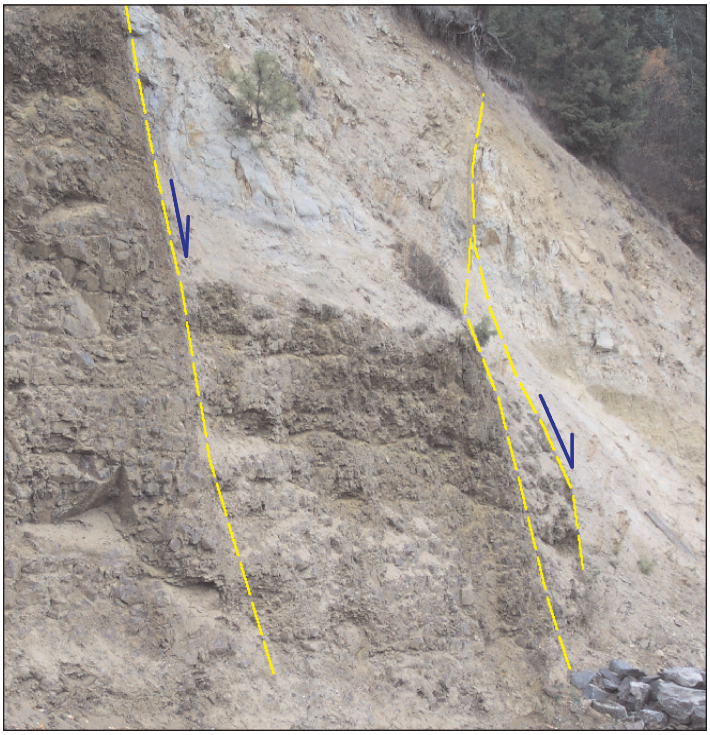

Figure 41. Photograph of fault zone exposed in a road cut near Lookingglass Creek. Here Tms sediments overlie the Powatka member of the Wanapum Basalt. Sense of displacement is down to the northeast. This is one of the faults in the Lookingglass Creek fault zone, many of which display subhorizontal slickensides. Outcrops such as this are quickly mantled by bank debris and small landslides.

GEOLOGIC HISTORY

Rocks exposed in the upper Grande Ronde River basin record a complex tectonic and volcanic history that began 250 million years ago and continues to the present. Although the early pre- and early-Tertiary history of the basin is only partly known because of the limited exposures of rocks older than 15 million years, seven important regional events are recognized (Ferns and others, 2001): 1) deep ocean subduction and island arc volcanism in an tropical environment during the Permian and Triassic, 2) deformation, plutonism, and metamorphism related to the tectonic "docking" of the resulting "exotic" terranes onto the North American continent during the Late Jurassic and Early Cretaceous, 3) uplift and extensive erosion during the Late Cretaceous and Early Tertiary following docking, 4) explosive bimodal continental volcanism in the Oligocene, 5) extensive tholeiitic flood basalt volcanism in the middle Miocene, possibly related to initiation of the Yellowstone hot spot plume, 6) subsequent rift-related calc-alkaline volcanism, and 7) regional uplift and warping along the Blue Mountain anticlinorium accompanied by formation of structural basins and glaciation.

Pre-Tertiary

Fragments of the Baker and Wallowa terranes (Figure 42), two of the five pre-Tertiary exotic terranes in northeastern Oregon recognized by Silberling and others (1984), are exposed in the upper Grande Ronde River basin. All the exotic terranes have undergone significant post-accretion rotation (Wilson and Cox, 1980; Hillhouse and others, 1982); therefore, the relative positions of the terranes are generally described in what is now assumed to be their pre-rotation positions.

The Baker terrane is divided into two subterranes: 1) the northern Bourne subterrane, an accretionary complex dominated by deepwater chert and siliceous argillite, and 2) the southern Greenhorn subterrane, a forearc complex dominated by serpentinite-matrix melange (Ferns and Brooks, 1995). The Bourne subterrane is composed chiefly of Elkhorn Ridge Argillite (Gilluly, 1937), a severely deformed and disrupted sequence of late Paleozoic and early Mesozoic deep-water ocean-floor chert and fine-grained siliceous argillite. The Elkhorn Ridge Argillite is considered to be the

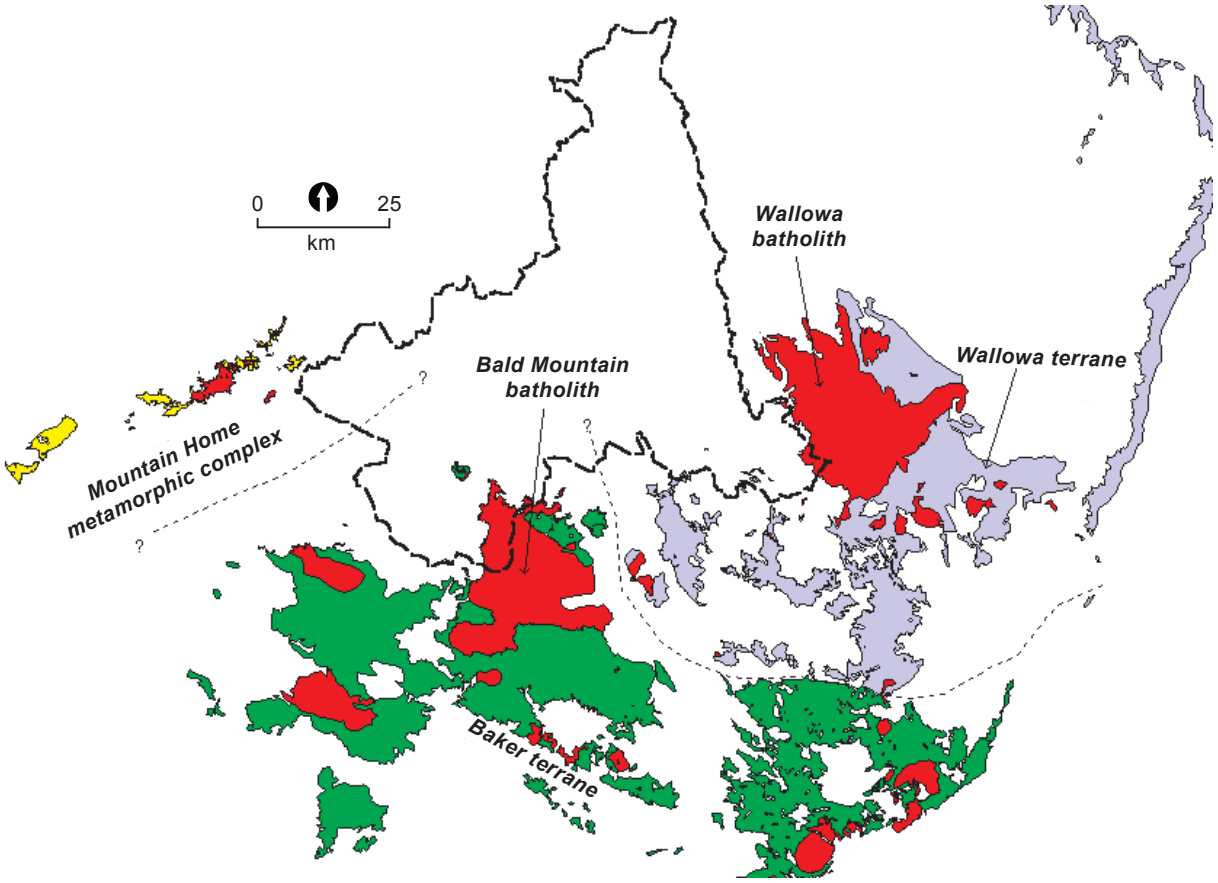

Figure 42. Sketch map showing geographic distribution of accreted terranes and the Bald Mountain and Wallowa batholiths. Mesozoic intrusive rocks shown in red, Wallowa terrane in blue, Baker terrane in green, and Mountain Home metamorphic complex in yellow. Projected trace (dashed line) of the boundary between the Baker and Wallowa terranes is northward beneath Grande Ronde Valley.

accretionary prism part of a Permian and Triassic fore-arc/subduction complex (Dickenson, 1979; Avé Lallemant, 1995; Ferns and Brooks, 1995). Deformation in the accretionary prism is generally considered to have resulted from eastward subduction of oceanic and island arc crust beneath a west-facing Huntington/Olds Ferry volcanic arc, which, following post-accretion rotation, is now exposed southeast of the upper Grande Ronde River basin (Dickenson, 1979; Avé Lallemant, 1995; Ferns and Brooks, 1995).

The Wallowa terrane is a volcanic-arc complex. In the upper Grande Ronde River basin two units are exposed: 1) the volcanic-dominated Clover Creek Greenstone (Gilluly, 1937) on the south, and 2) a volcanic and calcareous sedimentary unit considered to be equivalent to the Lower Sedimentary Series of Smith and Allen (1941) to the north. Although the Lower Sedimentary Series generally unconformably overlies the Clover Creek Greenstone, the two units are in fault contact along a significant northwest-trending fault near Medical Springs. Although not exposed in the upper Grande Ronde Basin, rocks of the Mountain Home Metamorphic Complex mapped west of the study area (Ferns and others, 2001) probably underlie the Grande Ronde Basalt at shallow levels in the western part of the basin. The Mountain Home metamorphic complex and some of the tectonically dismembered fragments of island arc volcanic and plutonic rocks that are intermixed with the Elkhorn Ridge Argillite in the southern part of the La Grande 30′ × 60′ quadrangle may be detached fragments from the Wallowa terrane (Ferns and Brooks, 1995; Avé Lallemant, 1995). If significant post-accretion rotation has occurred (Wilson and Cox, 1980; Hillhouse and others, 1982), the Wallowa arc originally would have been located west of the Baker terrane (Brooks and Vallier, 1978; Brooks, 1979; Dickenson, 1979; Avé Lallemant, 1995). Tectonic dismemberment along the Baker-Wallowa terrane boundary culminated during the late Jurassic as the Wallowa and Olds Ferry terranes collided. This collision resulted in east-directed folding and thrusting along north-south axes (Avé Lallemant, 1995) and tectonic mixing of deep-water ocean-floor and island-arc volcanic and plutonic rocks with shallow-water sedimentary rocks along the terrane boundary (Ferns and Brooks, 1995). The collision was quickly followed by province-wide plutonism and regional amphibolite-facies grade metamorphism in the Mountain Home Metamorphic Complex (Ferns and others, 2001).

Two large intrusive complexes, the Bald Mountain and Wallowa batholiths, were emplaced across major structural discontinuities in the Baker and Wallowa terranes in the Late Jurassic and/or Early Cretaceous. At Mountain Home, sillimanite gneisses, migmatites, and garnet-tourmaline pegmatites were produced when the Carney Butte stock was emplaced (Ferns and others, 2001). Metamorphic mineral assemblages suggest emplacement at pressures somewhat greater than 3.5 kb. The Bald Mountain batholith, the largest and most complex pluton, was emplaced along the boundary between the Baker and Wallowa terranes, whereas the Wallowa batholith was intruded into the Wallowa terrane. Sphalerite geobarometry (Reinthal, 1986) and a contact metamorphic mineral assemblage of andalusite + biotite + garnet (Godwin, 1999) indicate that the Bald Mountain batholith was emplaced at 1- to 2-kb pressure and is therefore the shallowest of the intrusive complexes. Although absolute emplacement ages for the Bald Mountain and Wallowa batholiths are poorly constrained, intraplutonic contact relationships indicate that for each, the most mafic phases (gabbronorite through diorite) were emplaced first, followed by larger tonalite intrusions. Emplacement of small, more-evolved granodiorite and granite magmas generally marked the cessation of Mesozoic intrusive activity. The Bald Mountain batholith displays a general evolution from diorite through tonalite and granodiorite. The Wallowa batholith shows an evolution from gabbro to tonalite and granodiorite. Small satellite intrusions, such as the one on Catherine Creek, are more alumina-rich trondjemites. Work by Johnson and others (1995) indicated that northeast Oregon Mesozoic magmatism can be divided into two episodes: a Late Jurassic–Early Cretaceous tonalite-dominated event and a later Cretaceous trondjemite-dominated episode.

The upper Grande Ronde River basin underwent significant uplift and unroofing of Mesozoic rock through the middle and late Cretaceous. Between 5 and 15 km of overlying rocks was stripped by erosion from above the plutonic complexes. The eroded material was redeposited as sediment in middle- and late-Cretaceous marine basins near Mitchell, 100 km southeast of the basin (Wilkinson and Oles, 1968). Fossiliferous beach sands place the edge of the marine basin a short distance northeast of John Day in the Cenomonian-Turonian epochs of the late Cretaceous (Brooks and others, 1984). During the Paleocene and Eocene, river systems draining the continental interior deposited the thick sequence of deltaic sandstone of the Herren Formation west of the upper Grande Ronde River basin (Fisk, 1986). Detrital muscovite in the Herren Formation was likely derived from an Idaho batholith source (Heller and others, 1985). Farther east, quartzite-boulder-filled channels cut into the Bald Mountain and Wallowa batholiths are all that remain of a westward-flowing river system that once fed the deltaic sequence (Cisneros, 1999). The old channels, which locally contain placer gold, are marked by hydraulic placer pits such as those at Camp Carson and on Jim White Ridge. Percussion-marked quartzite boulders as large as 0.60 m in diameter most likely came from the Proterozoic or lower Paleozoic quartzites of central Idaho (Trafton, 1999).

Tertiary

Tertiary continental volcanism began in northeast Oregon during the Eocene with eruption of the calc-alkaline Clarno Formation. Basalt, basaltic andesite, andesite, dacite, and rhyodacite flows and associated small subvolcanic intrusions were emplaced south of the map area between 33.6 and 40 Ma (Ferns and others, 1982; Brooks and others, 1982, 1984; Lilligren, 1992). Mid-Tertiary

bimodal volcanism in the upper Grande Ronde River basin began with small eruptions of tholeiitic and alkalic basalts circa 29.8 Ma. The first silicic eruptions from the Tower Mountain caldera (Figure 43) sent lahars, pyroclastic flows, and lava flows across Tertiary stream channels cut into older pre-Tertiary bedrock. Later explosive eruptions produced a more than 100-m-thick welded ash-flow tuff that flowed southwest from Tower Mountain. Collapse along arcuate ring fractures produced a subsiding, lithic-tuff-filled cauldron nearly 15 km in diameter. Circa 28 Ma, a series of rhyolite domes was extruded along the arcuate ring fractures. Caldera-fill tuffs were subsequently intruded by porphyritic and aphyric dacite and rhyolite masses, forming a resurgent caldera core complex that today is characterized by a pronounced gravity low. Volcanism ceased at Tower Mountain circa 22 Ma with eruptions of dacite and andesite lava east of the caldera margin.

The northern flank of the Tower Mountain caldera was buried by Columbia River Basalt Group lava flows, a long-lived episode of voluminous basalt outpouring considered to be related to the onset of the Yellowstone Hotspot (Hooper and others, 2002). These middle Miocene tholeiitic flood basalts cover over 164,000 km^2 and reach thicknesses as great as 700 m. Flood basalt magmatism began between 17 and 16 Ma with eruption of basal units of the Imnaha Basalt south of the map area (Hooper and others, 1984). In the map area, early Imnaha Basalt flows erupted from vents along the eastern edge of the basin and flowed northwest onto a highly irregular surface of deeply eroded pre-Tertiary rocks. Although several early Grande Ronde Basalt flows apparently erupted from a small, north-trending dike swarm exposed along the west margin of the Bald Mountain batholith, most of the Grande Ronde flows in the basin apparently erupted from vents located near the east margin of Grande Ronde Valley (Figure 44). In the southeast quadrant of the map area the last Grande Ronde flows formed an onlapping sequence of flows across an actively tilting surface of older Grande Ronde flows and underlying basement rocks. Some tilting was accompanied by vertical movement along the Shaw Mountain fault zone (Madin, 1998).

Grande Ronde volcanism culminated circa 15.5 Ma with eruption of the highly evolved, low-MgO ferroandesites of Fid-

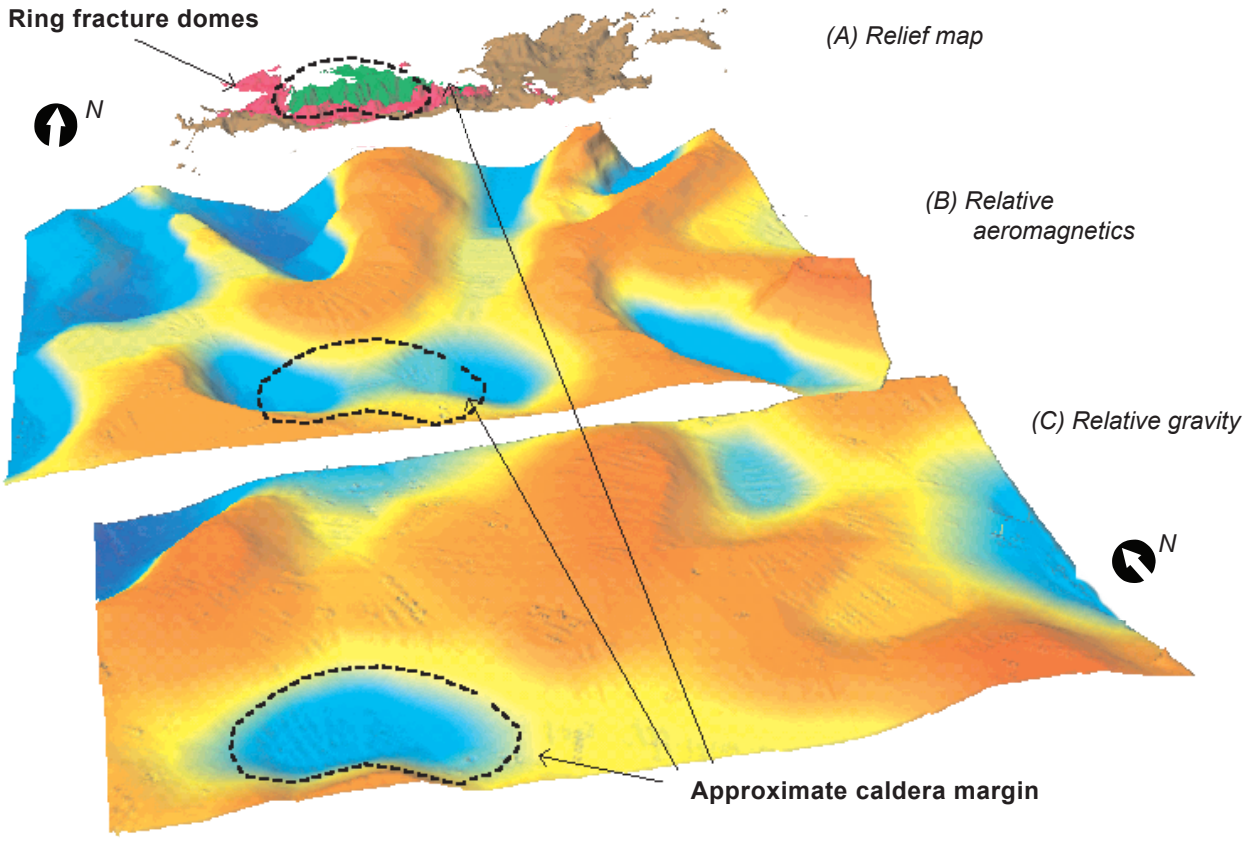

Figure 43. Regional aeromagnetic and gravity map of Tower Mountain caldera. (A) inclined relief map of the caldera with inclined regional (B) aeromagnetic and (C) gravity maps. Caldera fill tuff is shown in green, ring fracture domes in pink, and bordering tuffs, breccias, and lava flows in brown. Aeromagnetic and gravity highs are shown as shades of orange, lows as shades of blue.

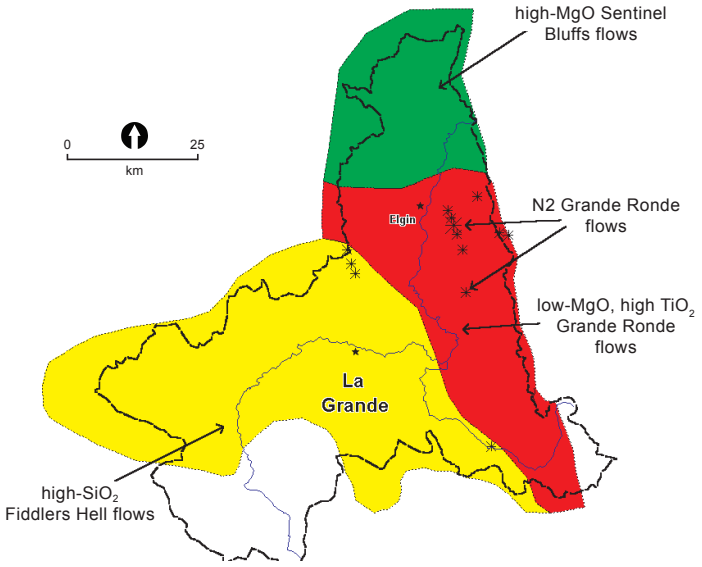

Figure 44. Distribution of late Grande Ronde Basalt flows and vents (N2 of Swanson and others [1979]). The Fiddlers Hell flows erupted from vents along the present-day eastern margin of Grande Ronde Valley and flowed westward. Other low-MgO, high-TiO_2 flows subsequently erupted from vents in the northern part of the basin, where they were buried by still younger high-MgO Sentinel Bluffs flows, which flowed across the northern end of the basin. Locations of Sentinel Bluffs vents are presently unknown.

dlers Hell from vents along the southeast margin of the modern Grande Ronde Valley (Ferns and others, 2001). Diatremes, spatter mounds, and northeast-trending dikes exposed high in the Grande Ronde section at Indian Rock and at Cricket Flat north of Grande Ronde Valley mark the location of other low-MgO Grande Ronde vents. High-MgO flows of the Sentinel Bluffs member (Reidel and others, 1989) that flowed eastward across the northern end of the upper Grande Ronde River basin may be the last of the Grande Ronde Basalt flows to erupt. Although individual Grande Ronde Basalt flows commonly rest directly atop one another, the last Fiddlers Hell and Sentinel Bluff eruptions show evidence for interaction with water. Fiddlers Hell flows locally invade diatomaceous sediment near Wolf Creek Reservoir (Madin, 1998) and Ladd Canyon along the east edge of the La Grande 30′ × 60′ quadrangle (Ferns and others, 2001). Palagonite breccias also occur at the top of the Grande Ronde Basalt near Cricket Flat. Local interactions between flows and water are considered evidence for early development of structural basins atop the Grande Ronde Basalt surface.

Palagonitic flows at the top of the Grande Ronde Basalt are commonly marked by a red, saprolitic soil zone that separates the top of the Grande Ronde Basalt from the basal flows of the Wanapum Basalt. Many Wanapum Basalt flows in the upper Grande Ronde River basin are also deeply weathered and show evidence of interaction with water. Wanapum Basalt volcanism began with eruption of coarsely crystalline, high-MgO, low-TiO_2 olivine basalt flows of the Dodge member from a dike swarm to the east (Hooper and Swanson, 1990). The Lookingglass flow, a fine-grained flow that is chemically and petrographically similar to the more-evolved low-MgO flows exposed at the top of the Grande Ronde Basalt to the south, erupted from a buried source in the northern part of the basin (Figure 45). The Lookingglass eruption was followed by arrival of a single Frenchman Springs flow. The Powatka flow, a more-evolved low-MgO lava that is also very similar to more-evolved low-MgO Grande Ronde Basalt flows, erupted from a now buried source near Cricket Flat. In the northern part of the basin, the upper Grande Ronde Basalt flows and Wanapum Basalt flows are similar. High-MgO flows, including the Sentinel Bluffs Member of the Grande Ronde Basalt and the Dodge and Frenchman Springs members of the Wanapum Basalt, erupted from sources outside of the upper Grande Ronde Basin and flowed westward across the northern part of the basin. More-evolved low-MgO flows, including the Fiddlers Hell Member of the Grande Ronde Basalt and the Lookingglass and Powatka Members of the Wanapum Basalt, erupted from a line of vents located along the eastern margin of the basin. The short hiatus that separates Grande Ronde volcanism (which ended at approximately 15.5 Ma) from the eruption of the first of the Wanapum Basalt flows at 15.3 Ma is marked by saprolitic soils and water-affected basalt. The present-day configuration of the Wanapum flows (Swanson and others, 1981) indicates that the Wanapum lavas flowed across the present-day Blue Mountains axis without impediment, showing that the Blue Mountains uplift postdates Wanapum volcanism. Westward thickening of the Frenchman Springs member can be attributed to paleogeography. The cluster of Frenchman Springs dikes in the northern Umatilla and southern Walla Walla River drainages suggests that the Frenchman Springs volcano was situated to the west of the upper Grande Ronde River basin.

Middle Miocene fluviatile sand and gravel, and thin discontinuous lenses of rhyolitic lithic ash-flow tuff were subsequently deposited in shallow basins extending from the southern part of

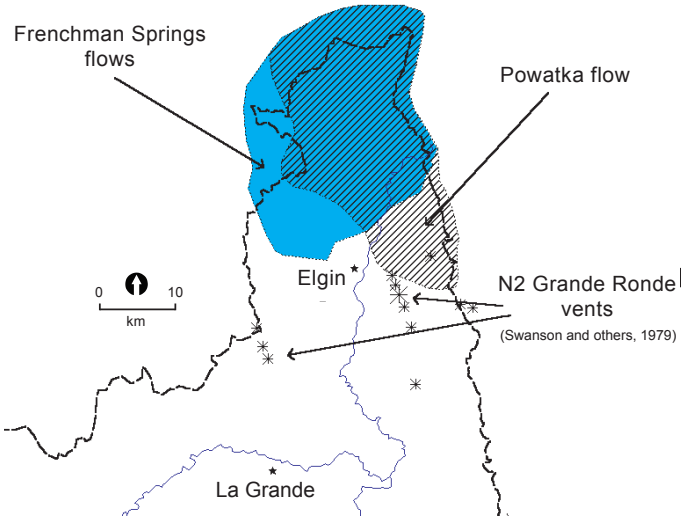

Figure 45. Extent of late Wanapum Basalt flows. Areal extent of the Powatka flow indicates that it probably erupted from a now buried series of vents northeast of Elgin. The Frenchman Springs flows thicken to the west, toward a dike complex exposed on the South Fork of the Walla Walla River. The Frenchman Springs flows exposed in the quadrangle may have flowed eastward from a Frenchman Springs eruptive complex located in that area.

the upper Grande Ronde River basin (Figure 46) north into the Umatilla Basin. The sediments were preserved in 1) structural basins developed atop the Grande Ronde and 2) areas where they were protected by younger overlying volcanic rocks. Isolated, widely separated remnants of presumably once-extensive flows of olivine basalt and ash-flow tuff are preserved between Starkey and La Grande. Although the source for the ash-flow tuff has not been identified, the thickest ash-flow exposures identified are exposed southeast of the basin along the northwest margin of Baker Valley (Madin, 1998). A regionally extensive ash-flow tuff (informally referred to as the tuff of Pleasant Valley) exposed over a large area south and east of Baker Valley may correlate with the La Grande exposures. The source of the tuff of Pleasant Valley is generally considered to be the large rhyolite complex at Dooley Mountain that lies south of Baker Valley (Figure 47) (Evans, 1992). Limited radiometric ages indicate the tuff erupted circa 14.7 Ma to 14.8 Ma (Bailey, 1990; Fiebelkorn and others, 1983). Northward transport directions (Carson and others, 1989) are also indicated by the lithologic makeup of interbedded gravels near Starkey, La Grande, and Elgin (unit Tms). The gravel contains quartzite, blue chert, rhyolite, dacite, and granitic and metamorphic clasts, micaceous sand, and, locally, small amounts of placer gold. The Tower Mountain caldera is the most likely source for the rhyolite and dacite clasts. Nearby exposures of Elkhorn Ridge Argillite are likely southern sources for the blue chert clasts.

The middle Miocene ash-flow tuffs and sedimentary rocks were quickly buried by the first eruptions of the Powder River Volcanic Field. Diktytaxitic olivine basalt (Tpb) flows began erupting about 14.5 Ma (Bailey, 1990), filling local channels and spreading laterally over much of the eastern part of the basin. Deep water wells in Grande Ronde Valley indicate that successive olivine basalt eruptions filled a north-northwest-trending ancestral Grande Ronde Valley with as much as 150 m of olivine basalt. On the west margin of the valley, olivine basalt flows extend laterally over an area of 580 km^2, thinning to the west, where they are interbedded with middle Miocene gravel in the Starkey units (Tms).

In the northern part of the basin, middle Miocene sediment was buried by the first Saddle Mountains Basalt (Tcs) flow, the Umatilla member (Figure 47), which erupted from a source east of the basin (Hooper and Swanson, 1990) circa 13.5 Ma. Continued sedimentation in the northern part of the basin resulted in formation of extensive coal swamps, perhaps in response to initial blockage of a west-flowing ancestral Grande Ronde-Salmon River drainage system by the Umatilla flow (Hooper and Swanson, 1990; Swanson and Wright, 1981). The next youngest Saddle Mountains Basalt flow, the Eden flow, erupted from a source located near the confluence of the Wallowa and Grande Ronde rivers and flowed northeastward into the Lewiston area (Hooper and Swanson, 1990).

Dacite volcanism in the Powder River Volcanic Field (Figure 48) began circa 13.4 Ma with the eruption of the Mount Emily dacite (Tpd) flow located on the west side of Grande Ronde Valley. Continued calc-alkaline volcanism continued through 12 Ma, with formation of a moderate sized stratovolcano at Mount Harris, eruption of large dacite (Tpd) and andesite (Tpa) flows at the top of Mount Fanny, and formation of the small basaltic andesite cinder cones (Tpv) at Ramo Flat. The N. 35° W. trend of the Ramo Flat vents suggests that fault zones within and marginal to Grande Ronde valley may have become active during initial stages of Powder River volcanism (Ferns and others, 2001). Later alkalic eruptions between 10.5 Ma and 12 Ma produced small basanite and alkali olivine basalt flows that filled northwest-trending channels.

Between 10 Ma and 7 Ma, the modern upper Grande Ronde River basin began to take form as the Blue Mountain anticlinorium rose to form a topographic barrier to westward migration of lava flows and sediments (Hooper and Swanson, 1990). By

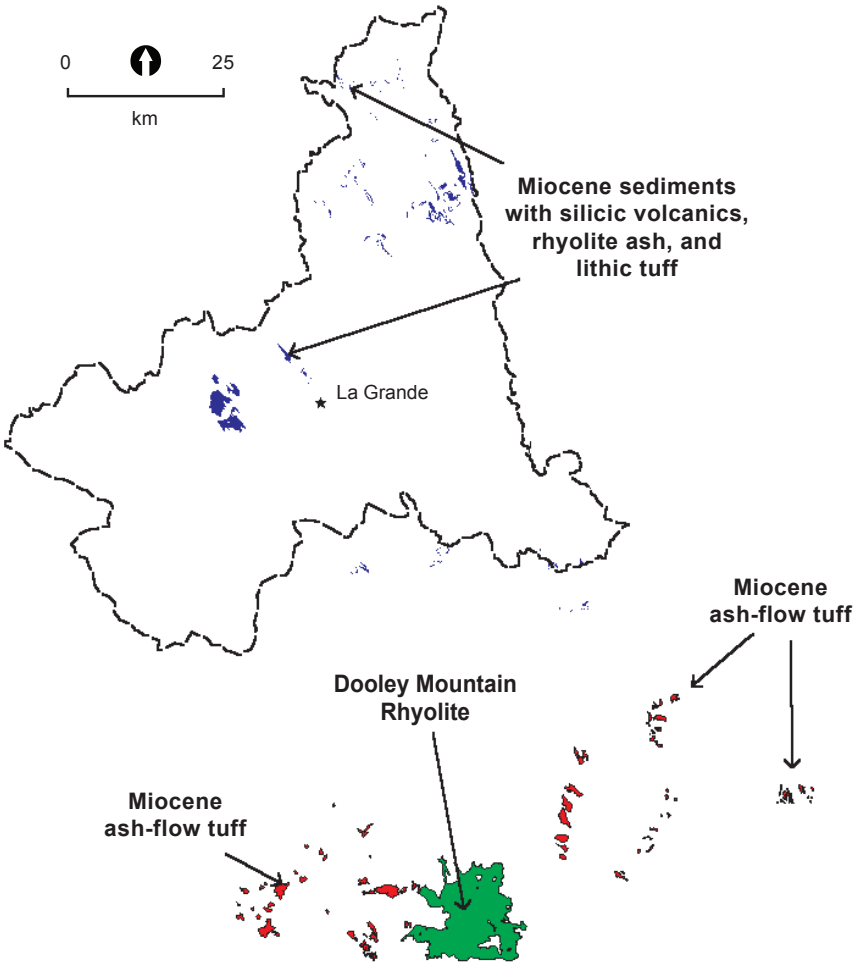

Figure 46. Diagram showing the distribution of middle Miocene sediments (Tms, in blue) that contain rhyolitic tuff and ash. The closest known middle Miocene rhyolite eruptive center is located at Dooley Mountain, shown in green, located over 50 km south of the basin. Ash-flow tuff exposures are shown in red.

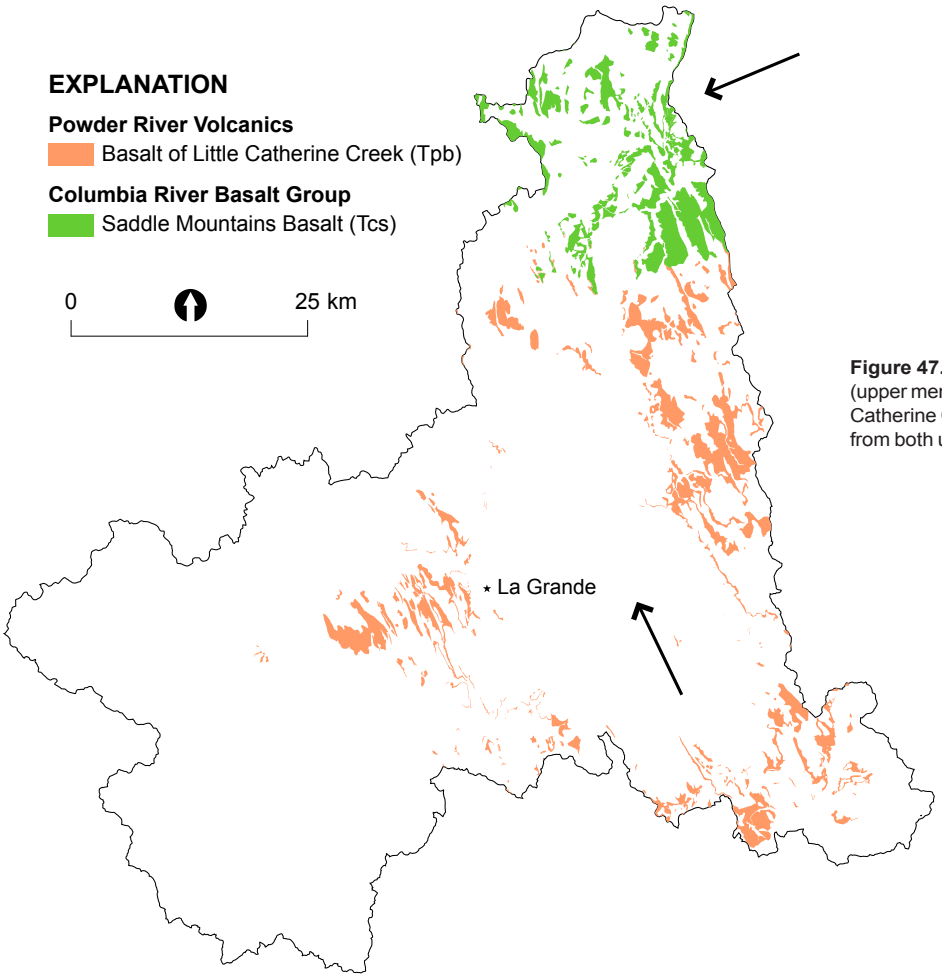

Figure 47. Diagram showing regional distribution of Umatilla basalt (upper member of the Saddle Mountains Basalt) and the basalt of Little Catherine Creek (oldest Powder River Volcanic Field member). Vents from both units are unknown. Arrows show presumed flow directions.

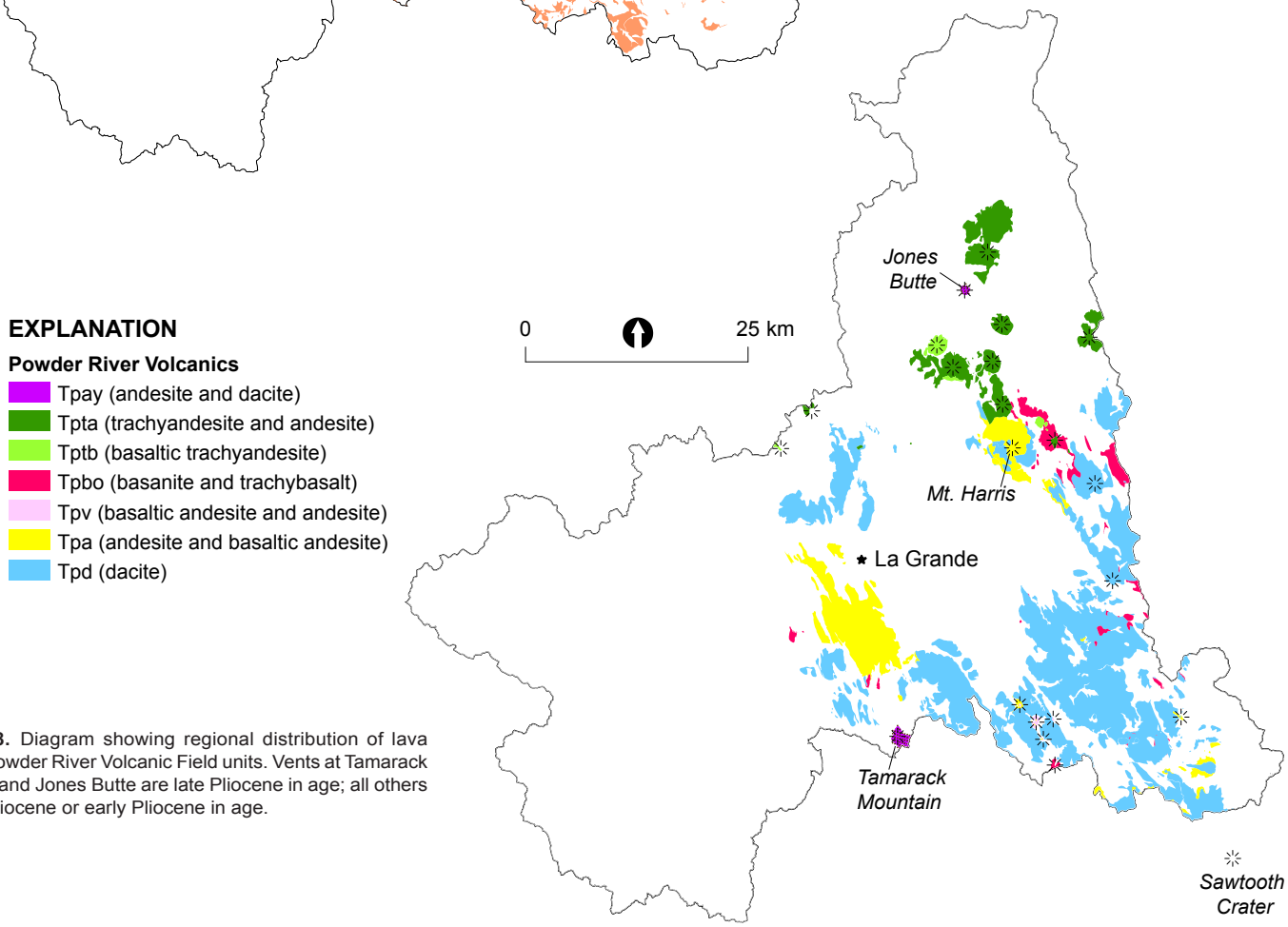

Figure 48. Diagram showing regional distribution of lava flows of Powder River Volcanic Field units. Vents at Tamarack Mountain and Jones Butte are late Pliocene in age; all others are late Miocene or early Pliocene in age.

8 Ma, Grande Ronde Valley was subsiding to form a major, fault-bounded catch basin for air-fall tuffs and fine-grained silts. Post-Grande Ronde Basalt sediments were preserved in basins developed along the Shaw Mountain fault zone. About 7 Ma, small trachybasalt, basaltic trachyandesite, and trachyandesite flows erupted onto the faulted Grande Ronde Basalt highlands west of Mount Emily (Kienle and others, 1979) and at Elgin. Eruptions in both areas formed clusters of small, typically < 1 km^2, compositionally distinct shield volcanoes that formed along northwest-trending fault zones. Major uplift and deformation waned by the middle Pliocene, around 3.2 Ma, when the small high-silica andesite of Tamarack Mountain erupted along the southern end of the Hilgard fault zone. The Tamarack Mountain flow unconformably overrode an older faulted and tilted surface of Grande Ronde and Glass Hill lavas. A young (~2 Ma) high-silica andesite also erupted at Jones Butte (Fiebelkorn and others, 1983) and flowed onto older terrace gravel (Walker, 1979).

Late Miocene, Pliocene, and post-Pliocene subsidence along the eastern edge of the map area resulted in the formation of Grande Ronde Valley. Although Grande Ronde Valley is described as an extensional graben (Hooper and Conrey, 1989) or pull-apart basin that formed in response to regional strike-slip movement along the Olympic–Wallowa lineament (OWL; Mann and Meyer, 1993), the overlapping sequence of Columbia River Basalt and Powder River Volcanic Field vents along the East Grande Ronde Valley fault zone suggests a more complicated tectonic history involving volcanically induced uplift, extension, and subsidence. Grande Ronde Valley's western and eastern margins are marked by active normal faults, the northern and southern margins of which are marked by inward-dipping blocks that project under valley-fill sediment (Figure 49). Valley subsidence was accompanied by uplift and deep dissection of the batholith-cored Elkhorn and Wallowa Mountains. Multiple terrace and alluvial fan levels and erosional bedrock highs in the northern end of Grande Ronde Valley formed as the basin floor tilted toward the northwest.

As the Grande Ronde Valley gradually deepened, the floor tilted toward the west. Rocks equivalent to those at the top of the Miocene Glass Hill section eventually subsided to a depth of more 650 m in the central part of the valley. As the valley floor dropped, a thick section of interbedded silt and fine sand gradually accumulated in the central part of the valley. In the southern part of the valley, the valley floor and overlying sediment tilted westward as the valley continued subsiding along the West Grande Ronde Valley fault zone. Coarse sand and gravel accumulated along the front of the West Grande Ronde fault zone as a delta plain formed where the Grande Ronde River entered the valley.

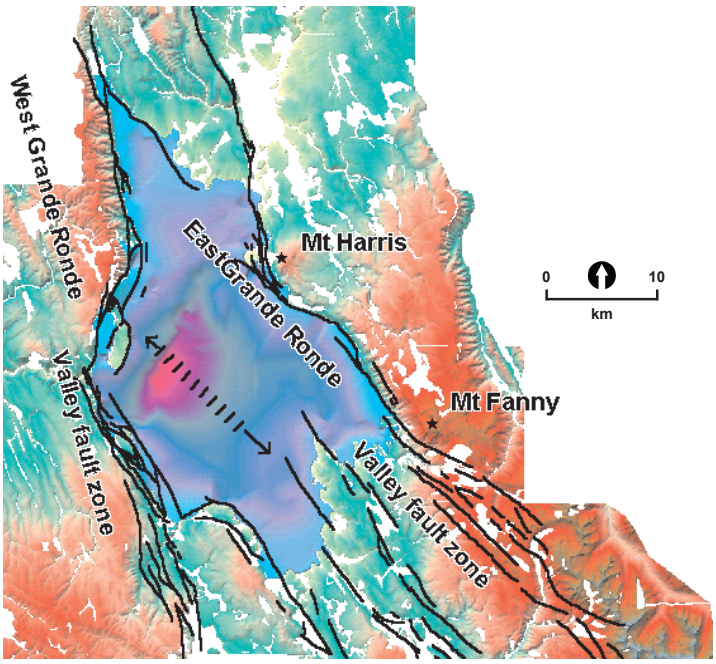

Figure 49. Shaded relief model of the top of the Cenozoic volcanics in Grande Ronde Valley, based on well logs, seismic lines, and geologic cross sections. Deepest part of the valley shows as purple. Arrows show presumed sense of extension.

Pleistocene

In the middle and late Pleistocene, alpine glaciers repeatedly formed in the Elkhorn Mountains and fed valley glaciers that extended down the Grande Ronde River to an elevation of about 1,500 m. The valley glacier on the Grande Ronde River reached its maximum extent during the Bull Lake glaciation (150,000–200,000 yr BP). Little ice reached the Grande Ronde River during the younger Pinedale glaciation (10,000–30,000 yr BP) (Geraghty, 1999). More-extensive glaciers developed in the Wallowa Mountains, where at least three stages of Pleistocene glaciation are recorded (Crandell, 1967; Bentley, 1974; Richmond and Fullerton, 1986). Bentley (1974) noted that all three branches of Catherine Creek contained glaciers, with the North Fork of Catherine Creek glacier extending down to an elevation of 1,460 m. Bentley (1974) suggested that Mount Fanny (Figure 50) was the site of a 21-km^2 body of ice that was isolated and upwind from the massive accumulations of ice in the higher-elevation Wallowa Mountains to the east. McConnell and others (2003) reported that ice may have covered the Mount Fanny plateau over an area as broad as 50 km^2 during glacial maximums. The ice sheet that accumulated on Mount Fanny plateau apparently did not flow to great extent. One valley glacier flowed a short distance down Indian Creek to the north (McConnell and others, 2004). Glacier-carved features are indicated by small cirques, nivation hollows, and glacial valleys along the eastern and western edges of the Mount Fanny plateau. McConnell and others (2004) reported cirques at elevations as low as 1,780 m near Moss Springs, lower than Bentley's (1974) suggested cutoff elevation of 1,900 m. Lower-elevation glaciation at Moss Springs apparently resulted from the uncommonly high levels of snowfall that accumulate on the Mount Fanny plateau (McConnell and others, 2003). Today, average yearly Moss

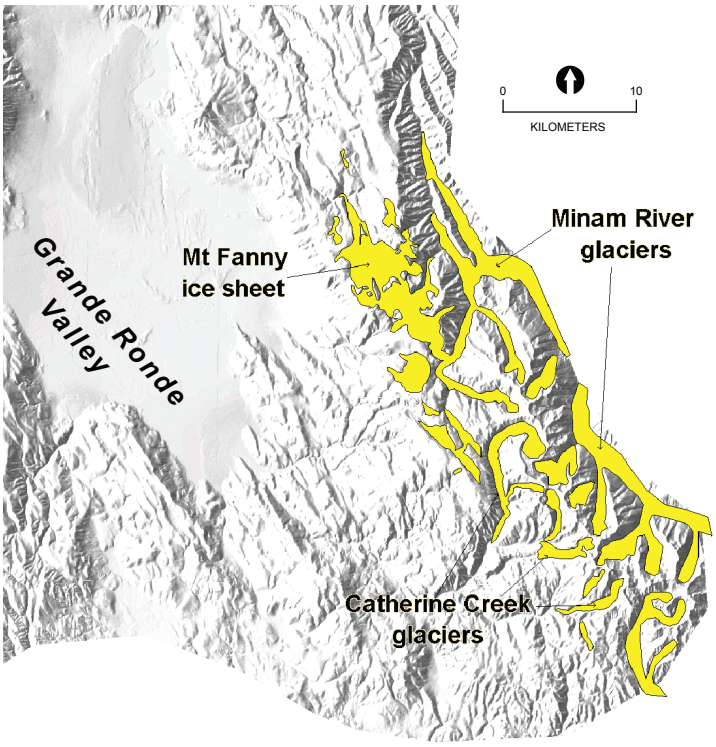

Figure 50. Shaded relief map showing extent of glaciers and ice sheets (yellow) on the eastern block. The Mount Fanny ice sheet fed small glaciers on Indian Creek and the Minam River.

Springs snow pack is equivalent to those at elevations of 2,100 m in the Elkhorn Mountains to the south (Bentley, 1974).

Throughout the Quaternary, alluvial fans at La Grande and Union expanded and contracted as sedimentation rates fluctuated during glacial advances and retreats (Van Tassell, 1997). Continued subsidence along the West Grande Ronde Valley fault zone acted to form an ever-deepening alluvial gravel trap at La Grande. Air-fall tuff from Cascade volcanic eruptions and loess from outburst glacial flood deposits near Pendleton were blown into the basin. Ephemeral lakes and marshes developed in the central part of the valley, perhaps in response to periodic blockage of the outlet of the Grande Ronde River by debris avalanches from the west ern flank of Mount Harris and landslides from the southern end of Pumpkin Ridge.

GEOLOGIC RESOURCES

Aggregate and Industrial Minerals

Locally used aggregate in the form of crushed rock and gravel has been the major mineral resource mined in the upper Grande Ronde River basin. Aphanitic lava flows of Grande Ronde Basalt Group are the main sources for the road metal used on the extensive network of U.S. Forest Service (USFS) and private industry access and haul roads. Platy, flow-banded rhyolite, dacite, and andesite have also been used as road metal sources. Sand and gravel resources suitable for aggregate are more restricted, occurring mainly as fluvial fan and terrace surfaces in Grande Ronde Valley. Coarser gravel lenses in the middle Miocene sedimentary units at Ukiah, Starkey, and Spring Creek are locally used for aggregate.

Clay used for firing brick has been mined from clay beds found where the Grande Ronde River enters Grande Ronde Valley. Clay was originally mined from lacustrine clays deposited when Grande Ronde Valley was partially filled by a shallow lake (Wagner, 1947). Clay deposits at La Grande were largely mined out between 1900 and 1966 for feedstock at the La Grande Brick yard.

Other industrial mineral resources in the basin include perlite and rhyolite facing stone from the ring-fracture domes flanking the Tower Mountain caldera. Some white to pale yellow flow-banded rhyolite has been used as facing stone on buildings in La Grande. Palagonitic breccia from hydrovolcanic deposits in the upper part of the Grande Ronde Basalt and red and pink andesite from the Jones Butte vent have been used in buildings at Elgin.

Massive dacite from the Powder River Volcanic Field is locally used as riprap for stream-bank stabilization. Some Powder River Volcanic Field dacites have zones with weathered vapor phase partings that make an attractive pink and brown flagstone. Some platy dacites are especially attractive due to large black dendrites of manganese oxides.

Intrusions in the Bald Mountain batholith hold some promise for decorative building stone. Equigranular white granodiorite exposed in the glaciated core of the Bald Mountain batholith near Anthony Lakes; pinkish-orange weathering, potassium-feldspar-megacryst-bearing granite of Anthony Buttes exposed along USFS Road 43; and hornblende- and olivine-phyric lamprophyre exposed on USFS Road 5125 (Ferns and Taubeneck, 1994) are particularly attractive.

Semi-Precious Gemstones

Semi-precious gemstones in the form of opal, chalcedony, and quartz occur locally in rhyolite domes marginal to the Tower Mountain caldera. Lithophysae cavities up to 3 cm across with terminated quartz crystals are found in silicified rhyolite domes exposed west of Sheep Creek (Ferns, 1999). Small (2 cm) thunder eggs partially filled with bands of brown jasper, blue chalcedony, and crystalline quartz have been found in silicified banded rhyolite (Ferns and others, 2001).

Metallic Mineral Resources

Only a small part of the upper Grande Ronde River basin shows evidence of precious metal mineralization (Figure 51). Potential gold resources in the quadrangle occur in three distinct geologic settings. These are, in order of importance: 1) placer deposits in modern or ancient stream channels, 2) Pre-Tertiary hydrothermal alteration zones within and marginal to the Bald Mountain and Wallowa batholiths, and 3) Tertiary hydrothermal alteration zones found mostly within and marginal to the Tower Mountain caldera. Other than a very few areas of weak clay and opaline quartz alteration along fault zones, the >1,500 km^2 expanse of middle Miocene and younger volcanic rocks shows no evidence of hydrothermal alteration.

Placer Deposits

Historical records indicate that less than 50,000 ounces of gold were produced by placer mines in the basin (Ferns and others, 2001). The large hydraulic placer mines at Camp Carson are the only workings of significant size. The workings exploited Tertiary gravel channels along the contact between the Bald Mountain batholith and the base of unit Teg. No reliable production records are available; the Camp Carson mine (Figure 52) is alleged to have produced $500,000 in gold during the peak operating years of 1892-1893 (Ferns and Taubeneck, 1994). More than 2.5 million cubic yards of Teg sediment was worked at Camp Carson as interpreted from the size of the hydraulic pits. Records show that the grade of material mined was apparently low, averaging less than about 0.01 oz/yd^3. Significantly smaller hydraulic pits worked channels in the upper blue-chert gravel part of unit Teg, but dilution due to influx of clay-rich volcanic debris likely lowered the overall grade of the upper gravel. In the 1940s, a small dragline dredge operated along the modern stream channel along Tanner Gulch and the Grande Ronde River for a distance of about 3.2 km downstream of the Camp Carson mine. Similar gold-bearing Tertiary gravel overlies granite bedrock at Wolf Creek, at French Diggings, and along Jim White Ridge, where a small amount of placer gold was apparently recovered from arkosic gravel in middle Miocene sedimentary units (Tms). Ferns and others (2001) reported old, gold-bearing placer workings on lower Beaver Creek, Sand Creek, and Five Points Creek (Figure 51).

Pre-Tertiary Mineralization Associated with the Bald Mountain Batholith

Very small amounts of silver, gold, and antimony have been produced from lode mines in and adjacent to the Bald Mountain batholith (Figure 51). Ferns and Taubeneck (1994) reported that small, discontinuous lenses of silver-bearing galena and sphalerite were mined from altered Elkhorn Pluton tonalite near the contact with the granite of Clear Creek. Here discontinuous quartz stringers with streaks and kidneys of massive galena and sphalerite occur in altered tonalite. According to Wagner (1945), lead-silver sulfide lenses at the Indianna Mine were found in a vein with a strike of N. 25° E. and a dip of 45° SE. Total production from the Indianna and adjacent mines was likely small; historic records are limited to a 1944 smelter shipment of 28 tons that assayed 0.15 oz/ton gold, 35.2 oz/ton silver, 2.4 percent lead, and 1.5 percent zinc (Wagner, 1945).

Three carloads of antimony ore were reportedly shipped from the Stibnite Mine during World War I (Richards, 1942; Wagner and Ramp, 1969). Small pods of stibnite occur there in a 0.1- to 0.3-m-thick quartz vein. The vein strikes about N. 45° E. and dips 80° NE in a host of disintegrating Elkhorn pluton granodiorite.

Pre-Tertiary Mineralization Associated with the Wallowa Batholith

A couple of small prospects explore skarns where the Wallowa batholith and satellite intrusions cut calcareous sediment of the Lower Sedimentary Series of Smith and Allen (1941). Small, discontinuous iron-stained lenses of garnet, epidote, calcite, and fine-grained quartz occur in limestone and calcareous argillite at the confluence of the South and North forks of Catherine Creek and along Catherine Creek downstream of the Catherine Creek State Park. There is no history of production at either location. Traces of gold and silver are reported from similar skarns elsewhere in the Wallowa Mountains (Weis and others, 1976).

Tertiary Mineralization Associated with the Tower Mountain Caldera

Ferns and others (2001) reported several mineralized zones in the Tower Mountain caldera. The most extreme areas of alteration occur in late-stage rhyolite domes on the eastern flank of the caldera. The quartz-phyric rhyolite exposed between Fly Creek and the Grande Ronde River appears the most intensely altered (Ferns and others, 2001). Massive opalite and chalcedonic quartz lenses are exposed in rhyolite vitrophyre along the contact between a porphyritic rhyolite and porphyritic dacite lava flows near Chicken Creek (Ferns and others, 2001). Mineralization within the caldera is associated with small silicic dikes and stocks (Ferns and others, 2001).

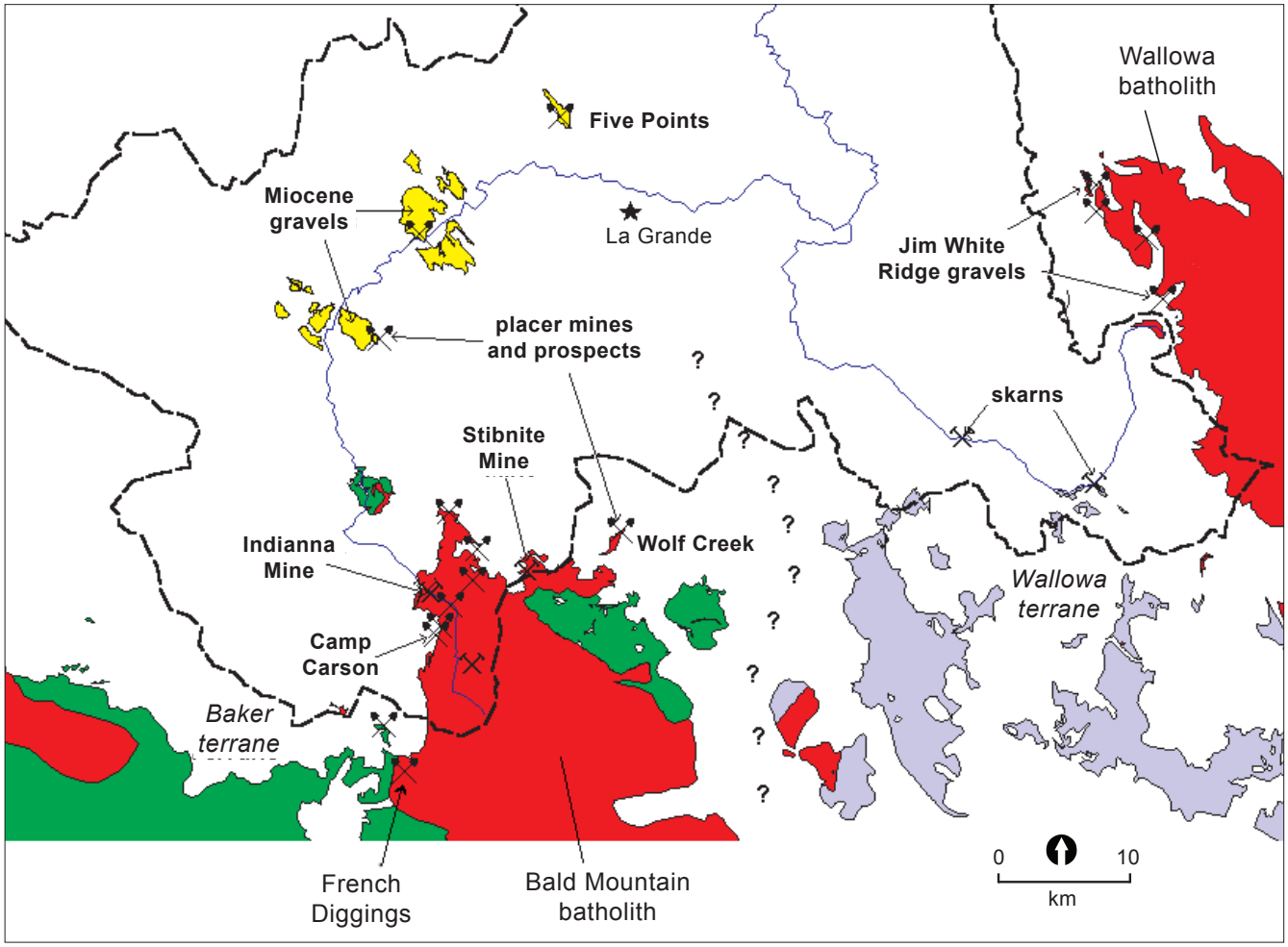

Figure 51. Distribution of gold placers and lode prospects associated with the Wallowa and Bald Mountain batholiths in the upper Grande Ronde River basin. Several small skarns are located along Catherine Creek. Diagram shows only the lode prospects and mines located within the basin. Numerous mines and prospects south of the basin are not shown.

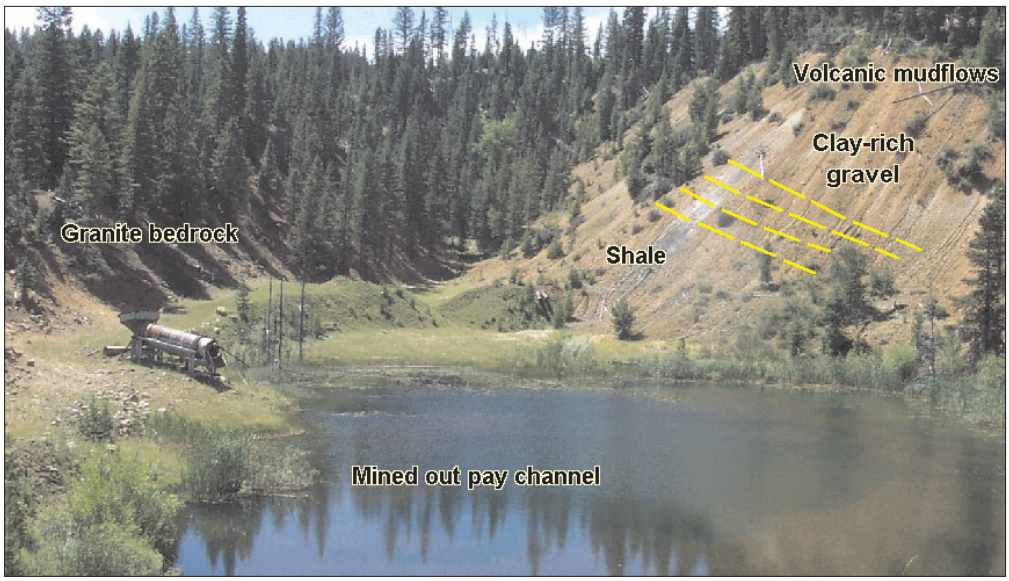

Figure 52. The largest gold mine in the basin was the Camp Carson Mine. This placer pit was part of a large hydraulic mine. The small pond shown here was originally drained by a tunnel through the granite bedrock. From available records from the 1890s, the pay streak was confined to coarse quartzite boulder channel gravel. The barren carbonaceous shales and clay-rich gravels that overlie the channel had to be removed before the gold-bearing material could be reached.

ENERGY RESOURCES

Geothermal

Grande Ronde Valley and western uplands have potential low-temperature geothermal resources. The Lehman Hot Springs resort, the Cove swimming pool, and the recreational vehicle (RV) resort near Hot Lakes are the only places in the basin where low-temperature geothermal waters are currently exploited.

The warmest surface waters in the basin are found near Hot Lake (Figure 53), where an 85°C spring produces 170 gpm (Hampton and Brown, 1964). Hot Lake spring is located close to where the N. 35° W.-trending Hot Lake fault makes a sharp left-hand bend to the west. Other springs located farther south along the foot of the Hot Lake fault, including the Duck Pond and Union Junction springs, range from 20°C to 35°C (Barrash and others, 1980; Baxter and others, 1978). The warm springs at Cove yield 226 gpm of 29°C water (Hampton and Brown, 1964). Two deep water wells in the central part of Grande Ronde Valley tap significant artesian flows of low-temperature geothermal waters at depth. The well at Alicel (Oregon Water Resources Department well UNIO-50687) intercepted a 43°C artesian flow in Grande Ronde Basalt flows at approximately 840 m depth. The Greg Bingaman well (Oregon Water Resources Department well UNIO-50684) first encountered a 32°C artesian flow in Powder River Volcanics at a depth of approximately 640 m. This well penetrated about 580 m of sediment before entering rocks of the Powder River Volcanic Field. Significant artesian flow of warmer water (approximately 42°C) was encountered after penetrating the underlying Grande Ronde Basalt at a depth of about 830 m. Nearly all of the deeper artesian wells in Grande Ronde Valley tap low-temperature (20°C to 30°C) geothermal aquifers (Brown and others, 1980; Baxter and others, 1978). Well cuttings from producing zones in the deeper warm wells in the north end of the valley invariably show evidence of weak hydrothermal alteration. Vesicles and fractures are lined with alteration minerals such as pyrite, opaline and chalcedonic quartz, zeolite, and unidentified, light blue-white to blue-green clay minerals.

Several warm springs are located along the Fly Valley and Shaw Mountain fault zones on the western uplands. Lehman Hot Springs issues from Grande Ronde Basalt flows along the projected intersection of the Fly Valley fault zone and the buried margin of the Tower Mountain caldera. Structural constraint at Lehman appears to be a set of N. 15°–20° W.-trending faults that splay off of the larger N. 65° W.-trending Fly Valley fault zone. Surface temperature at Lehman is 61°C. Several lower-temperature (25°–31°C) springs issue from northwest-trending faults south of the Shaw Mountain fault zone. These springs, which include the Starkey, Hunters, and Meadow Creek warm springs, are less likely to be underlain at shallow depths by pre-Miocene rock than is Lehman Hot Springs. The Starkey warm spring issues from a hydrothermally altered fault zone in Grande Ronde Basalt that contains thin chalcedonic quartz seams.

Figure 53. Hot Lake, the largest hot spring in the upper Grande Ronde River basin.

WATER RESOURCES

A full discussion of the geologic controls on surface and groundwater movement is beyond the scope of this report. General geologic investigations do not collect sufficient water data to allow detailed discussion of processes that influence surface and groundwater interaction. Stream flow measurements, using both long-term gauging stations and short-term seepage runs, water well measurements that include both pump tests and monitoring wells, and water use analyses are needed before the water use capacity in the upper Grande Ronde River basin can be determined.

Movement and interactions between surface and subsurface waters in the upper Grande Ronde River basin appear to be influenced mainly by stratigraphy and only secondarily by structure (Ferns and others, 2001). Much of the precipitation that falls on the older basement units feeds streams that tend to flow year round. Older basement units, including the pre-Tertiary units and older Tertiary volcanic rocks, are relatively impermeable and form poor aquifers. Wells drilled into these units can be expected to yield little if any water. Water-bearing zones are expected only where fracturing has increased permeability.

Wells drilled into Columbia River Basalt Group lavas may yield large amounts of water. The Wanapum Basalt and Grande Ronde Basalt units are a stacked series of lava flows (Figure 54). Individual lava flows are separated by rubbly interflow zones that are generally porous and may be permeable enough to transmit significant quantities of water both laterally and vertically. Central parts of individual flows are commonly dense enough to form barriers to vertical flow between the interflow zones and may act as confining layers. Although individual flows may be traced for many miles, both the permeable interflow zones and impermeable central zones tend be discontinuous. Interflow breccias do not necessarily indicate successive eruptions. Some interflow breccias may result from the overtopping of an early flow lobe by a later flow lobe from the same eruption. Hampton and Brown (1964) noted that because of these discontinuities, nearby wells drilled to the same depth may obtain water from different interflow zones and have different static water levels and different hydraulic characteristics. In the eastern block and upland areas marginal to Grande Ronde Valley the depth of the canyons cut by the Grande Ronde River and tributary streams profoundly influences the level

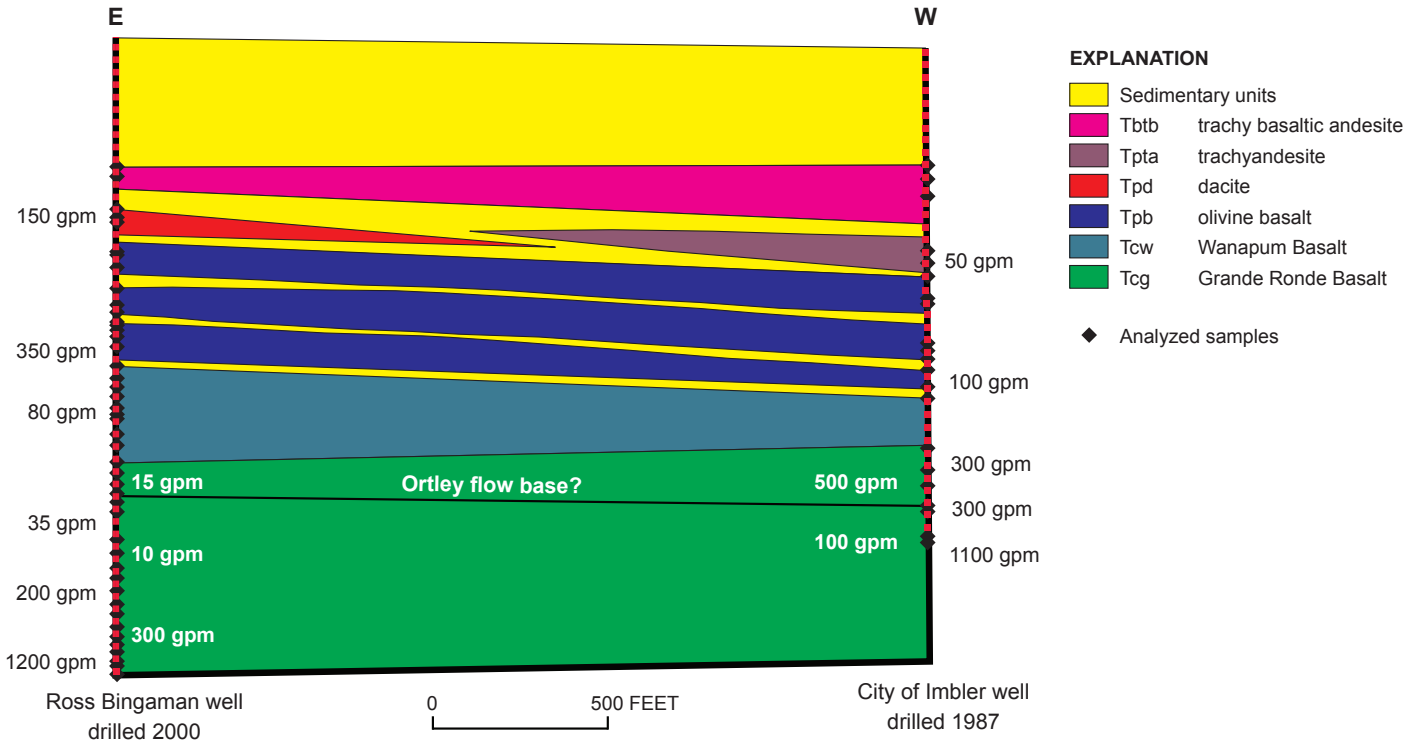

Figure 54. Stratigraphic diagram based on well logs and analyzed well cuttings from two deep wells drilled in the northern end of Grande Ronde Valley near Imbler. Zones where significant amounts of artesian water were encountered, based on drillers' logs, are marked by reported flow rates in gallons per minute (gpm). Both wells reportedly yield in excess of 1,500 gpm. Stratigraphic correlations are based on analyzed samples, locations of which are shown as black diamonds. The base of a somewhat chemically distinctive flow, the Ortley, is shown near the top of the Grande Ronde Basalt. Tptb, Tpta, Tpd, and Tpb flows are readily distinguishable from one another and from the Wanapum and Grande Ronde Basalt. Flows in the Wanapum and Grande Ronde Basalt are much less readily distinguishable.

of the regional water table. In some areas, where the deep canyons lie above the regional water table, water within interflow zones escapes from the stream and recharges the regional groundwater system. In other areas, where the canyons cut below the regional water table, water entering from the interflow zones as springs will increase the stream's base flow. Losing and gaining reaches are best determined by seepage measurements.

The Wanapum Basalt and low-MgO flows at the top of the Grande Ronde Basalt appear to be less permeable than the bulk of the Grande Ronde Basalt. Deep wells drilled in Grande Ronde Valley generally penetrate several hundred feet of Grande Ronde Basalt before reaching interflow zones permeable enough to generate sufficient artesian flow for commercial irrigation uses. North of Grande Ronde Valley, Wanapum Basalt flows appear to be more densely forested than the underlying Grande Ronde Basalt flows. The base of the Dodge flow is commonly heavily vegetated and marked by springs. Flows at the top of the Grande Ronde Basalt on the western block also appear more heavily vegetated. Perched aquifers occur in several places on the eastern block where near-vent, palagonitic breccias form barriers to groundwater flow. Similar near-vent palagonite breccias, interflow palagonitic breccias, and palagonitzed-basalt alteration zones may act to retard vertical ground water movement within the Wanapum and upper Grande Ronde Basalt flows.

Miocene sediment at the top of the Wanapum Basalt and Grande Ronde Basalt locally forms perched aquifers atop clay-rich zones. Sandy horizons are marked by springs and yield water for hand-dug wells near Elgin. In steeper regions, the same perched aquifers tend to readily form landslides.

Physical properties of the Powder River Volcanic Field lavas vary greatly. The laterally extensive thick (to 130 m) dacite and andesite flows (Tpd) have properties similar to the basement rocks and make very poor aquifers. Intervening flow breccias are generally thin and discontinuous and commonly glassy, readily weathering to clay minerals. Much of the precipitation that falls on the thick subaerial flows is retained in colluvium, soil, and disconnected bedrock fractures and is released into streams that tend to flow year round. The basal olivine basalt (Tpb) flows may have permeable interflow zones similar to those in the Grande Ronde Basalt where overlying clay-rich sediment forms perched aquifers and spring lines. The clay-rich sediment tends to inhibit vertical movement of groundwater between interflow zones. Well cuttings and drillers' logs indicate that individual olivine basalt flows are commonly bounded by thin, clay-rich sedimentary horizons and generally do not yield significant quantities of groundwater.

In places, such as the north end of Grande Ronde Valley, andesite and basaltic andesite (Tpa) lava flows in the upper part of the Powder River Volcanic Field form flow-on-flow sequences physically similar to the Grande Ronde Basalt flow-on-flow sequences. Laterally discontinuous interflow breccias between thin and discontinuous dense flow centers may yield appreciable amounts of groundwater. Storage capacity for the stacked flow sequences is small, as the sequences do not extend over more than several square kilometers.

The distribution of alluvial-plain, fan-delta, stream-channel, and alluvial-fan deposits in Grande Ronde Valley varies both laterally and vertically (Figure 55). Water well logs indicate the best sedimentary aquifers in Grande Ronde Valley are located along the distal edges of the fan deltas at La Grande and Union. The most productive wells in the fan-delta aquifer (including La Grande municipal wells) are located where lenses of coarse, well-sorted gravel overlap to form a thick, continuous sequence of permeable strata. Ferns and others (2002a) indicated that the surface of the fan delta expands laterally at shallow depths and then contracts at greater depths. Although the alluvial-plain deposits are generally fine grained and relatively impermeable, well-sorted channel-sand and fine-gravel lenses along the central axis of the valley (Ferns and others, 2002a) form shallow aquifers of limited capacity.

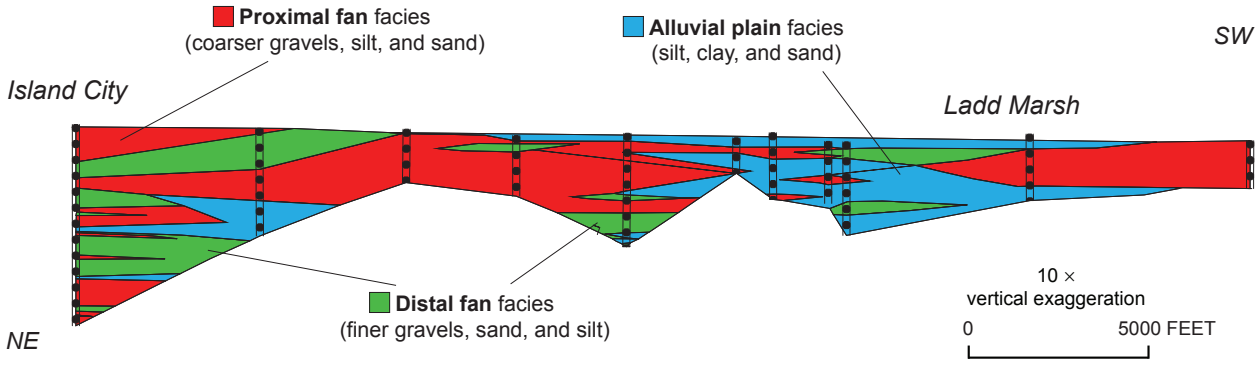

Figure 55. Diagram illustrating subsurface variability between water wells drilled into QTal sediments in Grande Ronde Valley. Facies interpretations are based on drillers' logs, which vary greatly in descriptive nomenclature and completeness.

GEOLOGIC HAZARDS

Geologic hazards are most evident along the active margins of Grande Ronde Valley. Close proximity of active or potentially active faults, high valley margins, and the unstable contact between Grande Ronde Basalt and overlying Powder River Volcanics make the margins of Grande Ronde Valley structurally unstable. Where the contact is exposed on the escarpments above the valley at Mount Emily and Gasset Bluff, debris flows and rock falls cascaded down the face of the escarpment and flowed out onto the valley in rapidly moving debris avalanches. Nonpoint source trace metals are the only other significant major geologic hazards for the rest of the upper Grande Ronde River basin.

Seismic Hazards

The West and East Grande Ronde Valley fault zones and the Little Creek fault can all be considered potentially active. All three display Quaternary offset. Individual faults along the West Grande Ronde Valley fault zone can be traced for as much as 10 km along strike. Subtle topographic features, including linear range fronts, low linear escarpments on alluvial fans and terraces, faceted spurs, and "z"-shaped benches marking faulted bedrock-alluvial fan contacts (Simpson and others, 1993; Personius, 1998; Ferns and Madin, 1999), indicate that surface ruptures along the West Grande Ronde Valley fault zone are Late Quaternary and very likely Holocene in age. The East Grande Ronde Valley fault zone can be traced for about 20 km. For most of that distance it consists of a single, 15-km-long fault line. Personius (1998) identified fault scarps below Gasset Bluff that indicate latest Pleistocene offset along the East Grande Ronde Valley fault zone.

The Little Valley fault can be traced for about 1.5 km into Grande Ronde Valley, where the fault trace forms a subdued 1- to 3-m-high scarp. The fault can be traced across the southern uplands for about another 3 km before it merges with the Catherine Creek fault. White (1981) considered the latest movement along the Little Valley fault to be late Pleistocene.

Hazard studies indicate that the West Grande Ronde Valley fault zone (Figure 56) is capable of generating a maximum credible earthquake of magnitude 7 (Simpson and others, 1993). Geomatrix Consultants (1995) defined the 1,000-year probabilistic peak acceleration for the La Grande area as 0.07 %g on the basis of slip rates of 0.03 to 0.05 mm/yr. Madin and Mabey (1996) considered the 1,000-year probabilistic peak acceleration to be 0.16 %g. Ferns and others (2001) noted that because slip rates were calculated from earlier studies (Simpson and others, 1993) that did not recognize the western Mount Emily fault, the 1,000-year probabilistic peak acceleration for the La Grande area may be greater than 0.07 %g.

Landslides

Downslope movement of rock and soil present major geologic hazards to populated areas. Although deposits formed by downslope movement are generically identified as "landslides," there are three

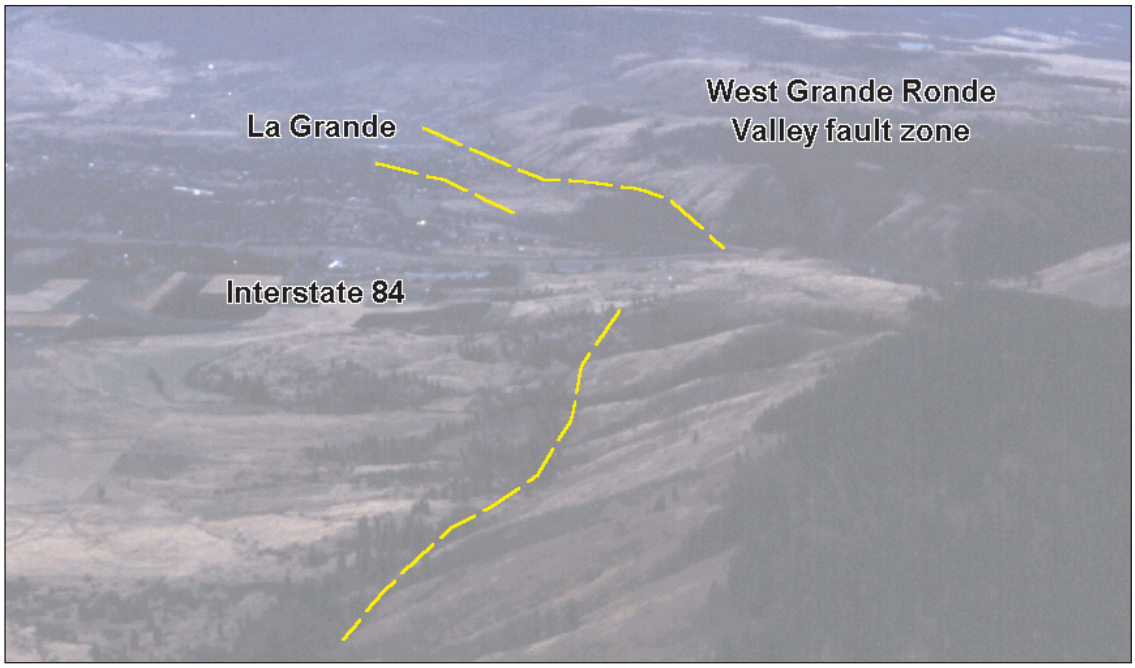

Figure 56. Aerial photograph of La Grande and the Western Grande Ronde Valley fault zone. Faceted spurs, linear features on fans and terraces, and "z" stepped scarps mark relatively young faults. Photograph was taken in 1979.

general types of "landslides" in the upper Grande Ronde River basin that should be evaluated separately. General types include 1) rock-fall and landslide-generated debris flows and mudflows, 2) complex landslides involving slow-moving unstable masses of rock and colluvium, and 3) colluvial landslides and slumps. Differentiation is based on the speed and manner in which the rock and soil move and is defined by geologic setting and triggering mechanisms.

Debris Flow Avalanches and Debris Flows

Debris-flow avalanches pose a significant geologic hazard in Grande Ronde Valley. Such avalanches may cascade down the eastern flank of Mount Emily or the western flank of Gasset Bluff at any moment. Remnants of old debris-flow avalanches and rockfalls form boulder fields composed of 2-3 m diameter dacite blocks that extend as far as 2 km into the valley. The high-standing dacite cliffs periodically collapse, sending large blocks of dacite cascading down the mountain to the valley floor, as much as 700 m below. Triggering mechanisms for these types of debris avalanches are apparently varied: heavy rainfall, earthquakes, and simple freeze-thaw cycles can all trigger cliff collapse. Debris flow hazard is most extreme where high Tpd cliffs crop out precipitously above the valley floor. Old landslide and terrace surfaces between Owsley Canyon 5 km north of La Grande and the Grande Ronde River are mantled by large dacite boulders from past debris flows. The sheer and partially undercut dacite cliff at Halfway Spring is a potential site for a debris flow avalanche. Grande Ronde Basalt shelves, such as the one south of Mount Harris near Gasset Bluff, form local catchment areas that may act to diminish collapse-generated debris flows before they reach the valley floor.

Landslide-generated debris flows and mudflows also pose a significant geologic hazard in Grande Ronde Valley. Several lobate masses (Figure 57) extend from slide headwalls down slope to the valley floor on the west side of the valley north of La Grande. It is not known whether these landslide masses initially failed as large, relatively slow moving landslides, such as the Hole-In-The-Wall slide, located 90 km southeast of La Grande (Jacobson and others, 1985), or as catastrophic mudflows (Schlicker and Deacon, 1971). One of the larger lobate masses covers about 3.7 km^2 and extends northward from an andesite high wall, down slope into the city of La Grande. Other potentially hazardous landslide complexes are located at Owsley Canyon and on the Grande Ronde River about 6 km upstream of La Grande. Slackwater deposits upstream of the Grande Ronde River slide may indicate that this landslide temporarily dammed the Grande Ronde River.

Collapse of landslide dams can result in debris flows and mudflows during flood events. Many slides in narrow, steep-walled canyons appear to have blocked streams in the past (Madin, 1998). Along the Grande Ronde River, areas that may be at risk of landslide damming include a location about 4 km south of Elgin; Andys Rapids, about 6 km north of Elgin; and at a point near Perry, about 5 km upstream from La Grande. Major tributary streams at risk of landslide damming include Beaver Creek, about 24 km southwest of La Grande and downstream of the La Grande Reservoir; Catherine Creek, in the area of Catherine Creek State Park; and along

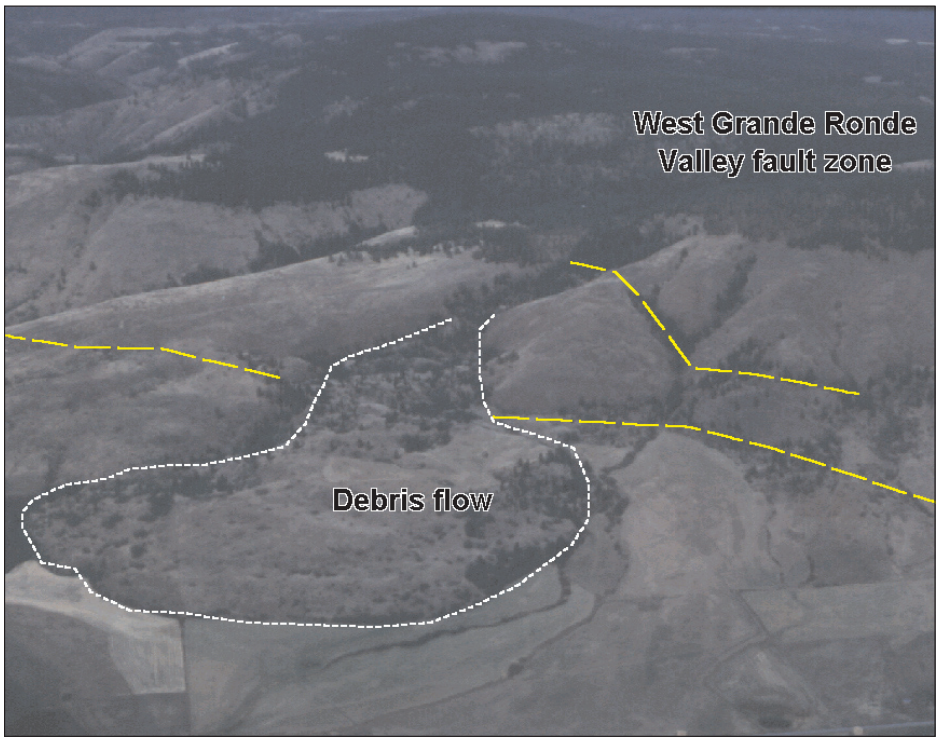

Figure 57. Aerial photograph of debris flow north of La Grande. Debris flow crosses several faults.

Lookingglass Creek, near the confluence with Little Lookingglass Creek. Storm-generated debris flows and mudflows may also flow onto alluvial fan surfaces during flash floods. Channels at the mouths of both Mill Creek and Deal Creek are cut into Holocene mudflow deposits (Personius, 1998) on the west side of the city of La Grande. Both channels contain remnants of younger mudflows.

Composite Landslides

Composite landslides are those in which different parts of the complex may be active at different times. They are typically large and may involve coherent blocks of bedrock as large as 0.5 km^2. In the upper Grande Ronde River basin, the composite landslides typically form where incompetent tuffaceous Tertiary sediment underlies competent lava flows. Very large landslide complexes are located in the headwaters of the Grande Ronde River and Catherine Creek, where tuffaceous Tertiary volcanic units rest on pre-Tertiary basement rocks.

Individual composite landslides, such as those on Beaver Creek, are as large as 16 km^2. The larger landslide complexes on the upper Grande Ronde River generally have two or more zones of weakness; a basal zone where tuffaceous, poorly consolidated tuffs overlie pre-Tertiary units and an upper zone where Columbia River Basalt or more coherent Oligocene units overlie tuffaceous sediment. Small portions of the slide complexes are periodically, and perhaps continuously, reactivated. It is presently unclear when or even whether any of the larger slide complexes underwent large-scale catastrophic failures in the past. The relative proportion of Mazama ash on landslide surfaces may provide a key for determining which slides are most active. For example, undeformed Mazama ash terraces, indicating relative stability in this area, overlie reworked debris from large slides along Fly Creek. Mazama ash along the Grande Ronde River immediately to the east is either absent or churned up with other landslide debris, indicating that the slides there are comparatively more active.

Composite landslides in the northern part of the upper Grande Ronde River basin typically form where thick Saddle Mountains Basalt or Powder River Volcanic Field lavas are underlain by tuffaceous sediment. Spectacular slides occur at the Rockwall, where blocks as long as 0.5 km are calving off of a 30-m headwall scarp. The toe of one of the Rockwall slides extends 1.5 km down slope to the Grande Ronde river, where material is being eroded to form Andys Rapids. The headwall possesses sag ponds and open linear crevices. Similar sackungen (deep-seated creep-style movements) features are found at the base of the headwall to the large slide that crosses Highway 82 south of Elgin.

Large composite landslides also occur along the western and eastern margins of Grande Ronde Valley. Some of the western margin slides, including the "jumbled block" unit of Barrash and others (1980), encompass areas of large, nearly coherent masses of internally disrupted and broken lava flows that tilt inward toward the valley.

Colluvial Landslides

Many landslides in the immediate vicinity of La Grande are slow moving, unstable wedges of soil and rock that mantle fault contacts between bedrock and alluvial fans along the West Grande Ronde Valley fault zone. Schlicker and Deacon (1971) noted that structures constructed on these unstable surfaces are susceptible to damage from continued down slope movement. Unstable colluvial wedges are also found along faulted contacts between alluvial fan gravel and bedrock units.

Geochemical Hazards

Mineralized areas with elevated levels of elements such as lead, arsenic, and mercury in the upper Grande Ronde River basin may need evaluation for possible impacts on downstream water quality. Assessment and mitigation strategies are needed to determine whether water quality problems can be attributed to point sources such as specific mine workings or to nonpoint sources of naturally weathering outcrops of mineralized rock. Ore samples from Bald Mountain batholith lead-silver veins show elevated levels of lead, zinc, and mercury (Ferns and Taubeneck, 1994). Small mine workings (dumps, tunnels, and shafts) on the lead silver veins may be potential point sources. Mineralized zones associated with the Tower Mountain caldera are also possible nonpoint sources for mercury and arsenic.

ACKNOWLEDGMENTS

Maps and geologic databases for the upper Grande Ronde River basin were compiled under the National Cooperative Geologic Mapping Program and partially funded by U.S. Geological Survey assistance award 02HQAG2037. Many thanks to Jim Evans, U.S. Geological Survey; Bob Carson, Whitman College; and Jay Van Tassell, Eastern Oregon University, for serving as peer reviewers. We thank Boise Corporation for their help, both in providing access to critical areas and for geochemical analyses and digital data.

Our appreciation is offered to the many farmers and ranchers who make a living in the upper Grande Ronde River basin, with special thanks to the extended Bingaman family. Waldo Lowe provided critical support in the form of logged water well cuttings from the deep water wells as he was drilling them. We also thank the Grande Ronde Model Watershed Board, Oregon Department of Water Resources, Confederated Tribes of the Umatilla Indian Reservation, Wallowa Whitman National Forest, and Umatilla National Forest for supporting our efforts to obtain financial support for the project.

Don A. Swanson, U.S. Geological Survey; Steve Reidel, Battel Corporation; William H. Taubeneck, Oregon State University (retired); Peter Hooper, Washington State University (retired); and Marvin H. Beeson, Portland State University (deceased) were all important sources for defining members of the Columbia River Basalt Group. Their collective works are the foundation upon which this map is built. Dr. Taubeneck also kindly provided us with his data on the Bald Mountain batholith. We are in debt to Dr. John Kauffman, Idaho Geological Survey, for providing slides and field notes from the pioneering study of Barrash and others (1980).

We thank Jay Van Tassell and students at Eastern Oregon University; Bob Carson, Kevin Pogue, and their students at Whitman College; and students and staff who participated in the 1998 Keck Foundation research project in the Elkhorn Mountains. Their work has greatly expanded our knowledge of Late Quaternary processes in the Blue Mountains Province. On the other end of the time spectrum, we owe a debt of thanks to Howard C. Brooks, Oregon Department of Geology and Mineral Industries (retired), Ellen Bishop, and Tracy L. Vallier, U.S. Geological Survey (retired) for their help with pre-Tertiary accreted terranes.

REFERENCES

AMAX Exploration, Inc., 1975, Residual magnetic intensity map and complete Bouguer and terrain corrected gravity map, Denver Colo.

Armstrong, R. L., Taubeneck, W. H., and Hales, P. O., 1977, Rb-Sr and K-Ar geochronometry of Mesozoic granitic rocks and their Sr isotopic composition,Oregon, Washington, and Idaho: Geological Society of America Bulletin, v. 88, p. 397–411.

Avé Lallemant, H. G., 1995, Pre-Cretaceous tectonic evolution of the Blue mountains province, northeastern Oregon, *in* Vallier, T. L. and Brooks, H. C., eds., Geology of the Blue Mountains region of Oregon, Idaho, and Washington; Petrology and Tectonic Evolution of Pre-Tertiary Rocks of the Blue Mountains Region: U.S. Geological Survey Professional Paper 1438, p. 271–304.

Bailey, D. E., 1990, Geochemistry and petrogenesis of Miocene volcanic rocks in the Powder River volcanic field, northeastern Oregon: Pullman, Wash., Washington State University, doctoral dissertation, 341 p.

Baksi, A. K., 1989, Reevaluation of the timing and duration of extrusion of the Imnaha, Picture Gorge, and Grande Ronde Basalts, Columbia River Basalt Group, *in* Reidel, S.P., and Hooper, P. R., Volcanism and tectonism in the Columbia River Flood-Basalt Province: Geological Society of America Special Paper 239, p. 105–111.

Barrash, W., Bond, J. G., Kauffman, J. D., and Venkatakrishnan, R., 1980, Geology of the La Grande area, Oregon: Oregon Department of Geology and Mineral Industries Special Paper 6, 67 p., 4 maps, 1:24,000 scale.

Baxter, K. W., Hull, D. A., and Ward, R. L., 1978, Geology (Chapter 2), *in* Huggins, R. M., ed., Northeast Oregon geothermal project: Eastern Oregon Community Development Council, La Grande, Oregon, p. 2-1–2-38.

Bentley, E. B., 1974, The glacial morphology of eastern Oregon uplands: Eugene, Oreg.; University of Oregon, doctoral dissertation, 250 p.

Berggren, W. A., Kent, D. V., Flynn, J. J., and Van Couvering, J. A., 1985, Cenozoic geochronology: Geological Society of America Bulletin, v. 96, no. 11, p. 1,407–1,418.

Bilderback, E., 1999, Late Quaternary glacial geology and paeloclimate interpretations of the Anthony Lakes drainages, Elkhorn Mountains, Oregon, *in* Mendelson, C. V., and Mankiewicz, C., eds., Twelfth Keck Research Symposium in Geology Proceedings: Northfield, Minn., Carleton College, p. 275–278 (available from Dept. of Geology, Beloit College, Beloit, Wisc.).

Black, G. L., 1994, Digital data and selected texts from low-temperature geothermal database for Oregon; Low-Temperature Geothermal Resources and Technology Transfer, Oregon–Phase I Final Report: Oregon Department of Geology and Mineral Industries Open-File Report O-94-09, 625 kb in 5 files; Excel and ASCII file formats.

Blome, C. D., Jones, D. L., Murchey, B. L., and Lienecki, M., 1986, Geologic implications of radiolarian-bearing Paleozoic and Mesozoic rocks from the Blue Mountains province, eastern Oregon, *in* Vallier, T.L., and Brooks, H.C., eds., Geology of the Blue Mountains Region of Oregon, Idaho, and Washington; Geologic implications of Paleozoic and Mesozoic paleontology and biostratigraphy, Blue Mountains province, Oregon and Idaho: U.S. Geological Survey Professional Paper 1435, p. 79–83.

Bostwick, D. A. and Koch, G. S., 1962, Permian and Triassic rocks of northeastern Oregon: Geological Society of America Bulletin v. 73, no. 3, p. 419–421.

Brooks, H. C., 1979, Plate tectonics and the geologic history of the Blue Mountains: Oregon Geology, v. 41, no. 5, p. 71–80.

Brooks, H. C., and Vallier, T. L., 1978, Mesozoic rocks and tectonic evolution of eastern Oregon and western Idaho, *in* Howell, D. G., and McDougall, K. A., eds., Mesozoic paleogeography of the western United States (Pacific Coast Paleogeography Symposium 2, Sacramento, Calif.): Los Angeles, Society of Economic Paleontologists and Mineralogists, Pacific Section, p. 133–146.

Brooks, H. C., Ferns, M. L., and Mullen, E. D., 1982, Geology and gold deposits map of the Granite quadrangle, Grant County, Oregon: Oregon Department of Geology and Mineral Industries Geological Map 25, scale 1:24,000.

Brooks, H. C., Ferns, M. L., and Avery, D. G., 1984, Geology and gold deposits map of the southwest corner of the Bates quadrangle, Grant County, Oregon: Oregon Department of Geology and Mineral Industries Geological Map 35, scale 1:24,000.

Brown, D. E., Black, G. L., and McLean, G. D., 1980, Preliminary Geology and Geothermal Resource Potential of the Craig Mountain–Cove area, Oregon: Oregon Department of Geology and Mineral Industries Open-File Report O-80-0468 p., 1 map

Bunker, R. C., Farooqui, S. M., and Thoms, R. E., 1982, K-Ar dates for volcanic rocks associated with Neogene sedimentary deposits in north-central and northeastern Oregon: Isochron/West, no. 33, p. 21-22.

Camp, V. E., and Ross, M. E., 2004, Mantle dynamics and genesis of mafic magmatism in the intermontane Pacific Northwest: J. Geophys. Res., 109, B08204, doi:10.1029/2003JB002838.

Carson, R. J., 2001, Where the Rockies meet the Columbia Plateau: Geologic field trip from the Walla Walla Valley to the Wallowa Mountains, Oregon: Oregon Geology, v. 63, no. 1, p. 13–35.

Carson, R. J., Spencer, P. K., Hubbard, S. E., and Thurber, B. W., 1989, Late Cenozoic volcanology, sedimentology, tectonics, and geomorphology of Elgin-Enterprise area, northeastern Oregon: 28th International Geological Congress abstracts with programs, p. I-247.

Cisneros, G., 1999, Reconstruction of Late Cretaceous–early Tertiary quartzite-bearing fluvial sediments, Elkhorn Mountains, northeastern Oregon, *in* Mendelson, C. V., and Mankiewicz, C., eds., Twelfth Keck Research Symposium in Geology Proceedings: Northfield, Minn., Carleton College, p. 291–298 (available from Dept. of Geology, Beloit College, Beloit, Wisc.).

Cochran, B. D., 1988, Significance of Holocene alluvial cycles in the Pacific Northwest Interior: Moscow, Id., University of Idaho, doctoral dissertation, 255 p.

Coward, R. I., 1983, Structural geology, stratigraphy, and petrology of the Elkhorn Ridge Argillite in the Sumpter area, northeastern Oregon: Houston, Tex, Rice University, doctoral dissertation, 144 p.

Crandell, D. R., 1967, Glaciation at Wallowa Lake, Oregon: U.S. Geological Survey Professional Paper 575C, p. 145–153.

Dickenson, W. R., 1979, Mesozoic fore-arc basin in central Oregon: Geology, v. 7, p. 166–170.

Dyksterhuis, E., and High, C. T., 1985, Soil survey of Union County area, Oregon: U.S. Department of Agriculture, Soil Conservation Service, 194 p.

EROS (Earth Resources Observation and Science), 1990, U.S. Geological Survey Side-Looking Airborne Radar (SLAR) Ritzville, WA, Walla Walla, WA, Pendleton, OR, Mariposa, CA, and Las Vegas, NV 1° × 2° quadrangles: EROS Data Center, U.S. Geological Survey.

Evans, J. G., 1989, Geologic map of the Desolation Butte quadrangle, Grant and Umatilla counties, Oregon: U.S. Geological Survey Geologic Quadrangle Map GQ-1654, scale 1:62,500.

Evans, J. G., 1992, Geologic map of the Dooley Mountain quadrangle, Baker County, Oregon: U.S. Geological Survey Geologic Quadrangle Map GQ-1694, scale 1:24,000.

Evans, J. G., 1995, Pre-Tertiary deformation in the Desolation Butte quadrangle, northeastern Oregon, *in* Vallier, T. L., and Brooks, H. C., eds., Geology of the Blue Mountains region of Oregon, Idaho, and Washington; Petrology and tectonic evolution of Pre-Tertiary rocks of the Blue Mountains region: U.S. Geological Survey Professional Paper 1438, p. 305–330.

Farooqui, S. M., Bunker, R. C., Thoms, R. E., Claygon, D. C., and Bela, J.L., 1981, Post-Columbia River Basalt Group stratigraphy and map compilation of the Columbia Plateau: Oregon Department of Geology and Mineral Industries Open-File Report O-81-10, 79 p., 6 pls.

Ferns, M. L., 1999, Geologic Map of the Fly Valley quadrangle, Union County, Oregon: Oregon Department of Geology and Mineral Industries Geological Map 113; scale 1:24,000.

Ferns, M. L., 2002, Tower Mountain; a Northeast Oregon late Oligocene caldera: Geological Society of America, Cordilleran Section, 98th annual meeting, Abstracts with programs, v. 34, p. 83.

Ferns, M. L., and Brooks, H. C., 1995, The Bourne and Greenhorn subterranes of the Baker terrane, northeastern Oregon: Implications for the evolution of the Blue Mountains island-arc system, *in* Vallier, T. L. and Brooks, H. C., eds., Geology of the Blue Mountains Region of Oregon, Idaho, and Washington; Petrology and Tectonic Evolution of Pre-Tertiary Rocks of the Blue Mountains Region: U.S. Geological Survey Professional Paper 1438, p. 331–358.

Ferns, M. L., and Madin, I. P., 1999, Geologic Map of the Summerville quadrangle, Union County, Oregon: Oregon Department of Geology and Mineral Industries Geologic Map Series GMS-111. scale 1:24,000.

Ferns, M. L., and Taubeneck, W. H., 1994, Geology and Mineral Resources Map of the Limber Jim Creek Quadrangle, Union County, Oregon: Oregon Department of Geology and Mineral Industries Geological Map 82, scale 1:24,000.

Ferns, M. L., Brooks, H. C., and Ducette, J., 1982, Geology and gold deposits map of the Mount Ireland quadrangle, Baker and Grant counties, Oregon: Oregon Department of Geology and Mineral Industries Geological Map 22, scale 1:24,000.

Ferns, M. L., Brooks, H. C., Avery, D. G., and Blome, C. D., 1987, Geology and gold deposits map of the Elkhorn Peak quadrangle, Baker County, Oregon: Oregon Department of Geology and Mineral Industries Geologic Map 41, scale 1:24,000.

Ferns, M. L., Madin, I. P., and Taubeneck, W. H., 2001, Reconnaissance geologic map of the La Grande 30′ × 60′ quadrangle, Baker, Grant, Umatilla, and Union counties, Oregon: Oregon Department of Geology and Mineral Industries Reconnaissance Map 1, map scale 1:24,000, 52 p.

Ferns, M. L., Madin, I. P., McConnell, V. S., and Johnson, J. J., 2002a, Geology of the surface and subsurface of the southern Grande Ronde Valley and Lower Catherine Creek drainage: Oregon Department of Geology and Mineral Industries Open-File Report O-0-02, 58 p.

Ferns, M. L., McConnell, V. S., Madin, I. P., and Van Tassell, J., 2002b, Geology of the Imbler quadrangle, Union County, Oregon: Oregon Department of Geology and Mineral Industries Geological Map 114, scale 1:24,000.

Fiebelkorn, R. B., Walker, G. W., MacLeod, N. S., McKee, E. H., and Smith, J. G., 1983, Index to K-Ar determinations for the State of Oregon: Isochron/West, no. 37, p. 3–60.

Fisk, L. H., 1986, Stratigraphy, age and petroleum potential of Cretaceous and Paleogene rocks in north-central Oregon: Lansing, Mich., Michigan State University, unpublished Ph.D. dissertation.

Gehrels, G. E., 1981, The geology of the western half of the La Grande Basin, northeastern Oregon: Los Angeles Calif, M.S. thesis, 97 p.

Geomatrix Consultants, 1995, Seismic design mapping, State of Oregon: Final report to Oregon department of Transportation, Project no. 2442, var. pages.

Geraghty, 1999, Glaciation of the Elkhorn Mountains, northeastern Oregon, *in* Mendelson, C. V., and Mankiewicz, C., eds., Twelfth Keck Research Symposium in Geology Proceedings: Northfield, Minn., Carlton College, p. 283–286 (available from Dept. of Geology, Beloit College, Beloit, Wisc.).

Gillespie, M. R., and Styles, M. T., 1999, BGS rock classification scheme, V. 1: Classification of igneous rocks: British Geological Survey Research Report RR 99-06, 2nd ed., 52 p.

Gilluly, J., 1937, Geology and mineral resources of the Baker quadrangle, Oregon: U.S. Geological Survey Bulletin 879, 119 p.

Godwin, E. H., 1999, Metamorphism of argillaceous and schistose rocks of the Bellevue Wedge, Elkhorn Mountains, northeastern Oregon, *in* Mendelson, C. V., and Mankiewicz, C., eds., Twelfth Keck Research Symposium in Geology Proceedings: Northfield, Minn., Carlton College, p. 307–309 (available from Dept. of Geology, Beloit College, Beloit, Wisc.).

Gray, J. J., 1993, Mineral information layer for Oregon by County, 1993 update: Oregon Department of Geology and Mineral Industries Open-File Report O-94-09 (1.8 MB in 8 files; data set in compressed lzh file format; extracted data in dbf file format).

Hallsworth, C. R., and Knox, R. W. O'B. 1999, BGS Rock classification scheme, V. 3, Classification of sediments and sedimentary rocks: British Geological Survey Research Report RR 99-03, 44 p.

Hampton, E. R., and Brown, S. G., 1964, Geology and groundwater resources of the upper Grande Ronde River Basin, Union County, Oregon: U.S. Geological Survey Water-Supply Paper 1597, 99 p.

Heller, P. L., Peterman, Z. E., O'Neil, J. R., and Shafiqullah, M., 1985, Isotopic provenance of sandstones from the Eocene Tyee Formation, Oregon coast Range: Geological Society of America Bulletin, v. 96, no. 6, p. 770–780.

Hillhouse, J. W., Gromme, C. S., and Vallier, T. L., 1982, Paleomagnetism and Mesozoic tectonics of the Seven Devils volcanic arc in northeastern Oregon: Journal of Geophysical Research, v. 87, p. 3,777–3,794.

Hooper, P. R., and Conrey, R. M., 1989, A model for the tectonic setting of the Columbia River basalt eruptions, *in* Reidel, S.P., and Hooper, P. R., eds., Volcanism and tectonism in the Columbia River Flood-Basalt Province: Geological Society of America Special Paper 239, p. 293–306.

Hooper, P. R., and Swanson, D. A., 1990, The Columbia River Basalt Group of the Blue Mountains Province, *in* Walker, G.W., ed., Geology of the Blue Mountains region of Oregon, Idaho, and Washington: Cenozoic Geology: U.S. Geological Survey Professional Paper 1437, p. 63–99.

Hooper, P. R., Kleck, W. D., Knowles, C. R., Reidel, S. P., and Thiessen, R. L., 1984, Imnaha Basalt, Columbia River Basalt Group: Jounal of Petrology, v. 25, no. 2, p. 323–328.

Hooper, P. R., Johnson, D. M., and Conrey, R. M., 1993, Major- and trace-element analyses of rocks and minerals by automated X-ray spectrometry: Washington State University Geology Department Open-File Report, 36 p.

Hooper, P. R., Binger, G. B., and Lees, K. R., 2002, Ages of the Steens and Columbia River flood basalts and their relationship to extension-related calc-alkalic volcanism in eastern Oregon: Geological Society of America Bulletin v. 114, no. 1, p. 43-50.

Jacobson, R., Milne, W., Brooks, H. C., Zollweg, J., and Brandsdottir, B., 1985, The 1984 landslide and earthquake activity on the Baker-Homestead highway near Halfway, Oregon: Oregon Department of Geology and Mineral Industries, Oregon Geology, v. 47, no. 5, p. 51-57.

Johnson, K. S., 1995, Petrogenesis of high-alumina tonalite and trondhjemites of the Cornucopia stock, Blue Mountains, northeastern Oregon: Lubbock, Tex, Texas Tech University doctoral dissertation, 206 p.

Johnson, K. S., Walton, C., Barnes, C. G., and Kistler, R. W., 1995, Time-dependent geochemical variations of Jurassic and Cretaceous plutons in the Blue Mountains, northeastern Oregon: Geological Society of America, annual meeting, Abstracts with Programs, v. 27, p. 435.

Kays, M. A., Ferns, M. L., and Brooks, H. C., 1987, Metamorphism of Triassic-Paleozoic belt rocks--A guide to field and petrologic relations in the oceanic melange, Klamath and Blue Mountains, California and Oregon, *in* Ernst, W. G., ed., Metamorphism and crustal evolution of the Western United States (Rubey Volume VII): Englewood, Cliffs, N.J., Prentice-Hall, p. 1,098-1,120.

Kienle, C. F., Jr., Hamill, M. L., and Clayton, D. N., 1979, Geological reconnaissance of the Wallula Gap, Washington - Blue Mountains - LaGrande, Oregon region: Technical report to Shannon & Wilson, Inc., Portland, Oregon, under Contract 44013, December 1979, 58 p., 1 pl., scale 1:125,000.

Kuehn, S. C., 1995, The Olympic-Wallowa Lineament, Hite Fault System, and Columbia River Basalt Group Stratigraphy in Northeast Umatilla County, Oregon: Pullman, Wash., Washington State University, M.S. thesis, 170 p.

Le Maitre, R. W., Bateman, P. L., Dudek, A., Keller, J., Lameyre, P. A., Le Bas, M. J., Sabine, P. A., Schmid, R., Sorensen, H., Streckeisen, A., Wooley, A. R., and Zanettine, B., 1989, A classification of igneous rocks and glossary of terms: Oxford, Blackwell, 193 p.

Liberty, L. M., and Barrash, W., 1998, Southern Grande Ronde Valley Seismic Project–Phase II: Reflection seismic results (Center for Geophysical Investigation of the Shallow Subsurface (CGISS): Boise State University, Technical Report BSU CGISS 98-05: Unpublished report prepared for the Oregon Department of Geology and Mineral Industries, 10 p.

Lilligren, S. P., 1992, Geology and Geochemistry of a portion of the eastern Clarno Formation, Grant County, Oregon: Pullman, Wash., Washington State University, M.S. thesis, 155 p.

Lindgren, W., 1901, Gold belt of the Blue Mountains of Oregon: U.S. Geological Survey Annual Reports, no. 22, p. 551–776.

Livingston, V. E., 1958, Oil and gas exploration in Washington: Washington Division of Mines and Geology Information Circular 29, 61 p.

McConnell, V. S., 1995, Hydrothermal history of the Long Valley caldera, California: Life after collapse: Fairbanks, Alaska, University of Alaska, Ph.D. dissertation, 238 p.

McConnell, V. S., Ferns, M. L., Procsal, M. A., Wacaster, S. G., Madin, I. P., and Betteridge, I. P., 2002, New mapping of a mid to late Miocene calc-alkaline volcanic field in NE Oregon: Geological Society of America, Cordilleran Section, 98th annual meeting, Abstracts with Programs v. 34, no. 5, p. 82–83.

McConnell, V. S., Betteridge, I. P, and Ferns, M. L., 2003, Geologic map of the Mount Fanny and Little Catherine Creek quadrangles, Union and Wallowa counties, Oregon: Oregon Department of Geology and Mineral Industries Geological Map Series GMS-115, scale 1:24,000.

Madin, I. P., 1998, Geologic map of the Tucker Flat quadrangle, Union and Baker counties, Oregon: Oregon Department of Geology and Mineral Industries Geological Map 110, scale 1:24,000.

Madin, I. P., and Mabey, M. A., 1996, Earthquake hazard maps for Oregon: Oregon Department of Geology and Mineral Industries Geologic Map 100.

Madin, I. P., and Taubeneck, W. H., 2003, Geologic map of the Anthony Buttes quadrangle, Union and Baker counties, Oregon: Oregon Department of Geology and Mineral Industries Geological Map 107, scale 1:24,000.

Mann, G. M., 1989, Seismicity and late Cenozoic faulting in the Brownlee Dam area—Oregon-Idaho: A preliminary report: U.S. Geological Survey Open-File Report 89-429, 46 p.

Mann, G. M., and Meyer, C. E., 1993, Late Cenozoic structure and correlations to seismicity along the Olympic-Wallowa Lineament, northwest United States: Geological Society of America Bulletin, v. 105, p. 853–871.

Miyashiro, A., 1974, Volcanic rock series in island arcs and active continental margins: American Journal of Science, v. 274, p. 321–355.

Morris, E. M., and Wardlaw, B. R., 1986, Conodont ages for limestone of eastern Oregon and their implication for pre-Tertiary melange terranes, and Wardlaw, *in* Vallier, T. L., and Brooks, H. C., eds., Geology of the Blue Mountains Region of Oregon, Idaho, and Washington; Geologic implications of Paleozoic and Mesozoic paleontology and biostratigraphy, Blue Mountains province, Oregon and Idaho: U.S. Geological Survey Professional Paper 1435, p. 59–63.

Personius, S. F., 1998, Surficial geology and neotectonics of selected areas of western Idaho and northeastern Oregon: U.S Geological Survey Open-File Report 98–771, 26 p.

Pogue, K. R., Carson., R. J., Crowley, P. D., and Hazlett, R. W., 1999, Geology of the Elkhorn Mountains, northeastern Oregon: Twelfth Keck Research Symposium on Geology: Northfield, Minn., Carleton College, p. 256–258 (available from Dept. of Geology, Beloit College, Beloit, Wisc.).

Raisz, E., 1945, The Olympic-Wallowa Lineament: American Journal of Science, v. 243A, p. 479–485.

Reidel, S. P., Tolan, T. L, Hooper, P.R., Beeson, M. H., Fecht, K. R., Bentley, R. D., and Anderson, J. L., 1989, The Grande Ronde Basalt, Columbia River Basalt Group; Stratigraphic descriptions and correlations in Washington, Oregon, and Idaho, *in* Reidel, S. P., and Hooper, P. R., eds., Volcanism and tectonism in the Columbia River Flood-Basalt Province: Geological Society of America Special Paper 239, p. 21–53.

Reidel, S. P., Beeson, M. H., Tolan, T. L., and Lindsey, K. A., 1996, The age of La Grande basin (LGB), northeast Oregon: New evidence for middle Miocene deformation and basin formation [abs.]: Geological Society of America Abstracts with Programs, v. 28, no. 5, p. 104.

Reinthal, W. A., 1986, Geochemical evolution of precious metal mineralization in the Cracker District of the blue Mountains, northeastern Oregon: Madison, Wisc., University of Wisconsin, Ph.D. dissertation, 152 p.

Richards, L. C., 1942, Stibnite Mine (Antimony), Union County, Oregon: Oregon Department of Geology and Mineral Industries unpublished mine file report, 3 p.

Richmond, G. M., 1986, Stratigraphy correlation of glacial deposits of the Rocky Mountains, the Colorado Plateau, and the ranges of the Great Basin, *in* Sibrava, V., Bowen, D. Q., and Richmond, G. M., eds., Quaternary glaciations in the northern hemisphere: Oxford, Pergamon Press, p. 183–196.

Richmond, G. M., and Fullerton, D. S., 1986, Summation of Quaternary glaciations in the United States of America, *in* Sibrava, V., Bowen, D. Q., and Richmond, G. M., eds., Quaternary glaciations in the northern hemisphere, Oxford, Pergamon Press, p. 183–195.

Robertson, S., 1999, BGS Rock Classification Scheme, Volume 2: Classification of metamorphic rocks: British Geological Survey Research Report, RR 99-02, 24 p.

Robinson, P. T., Walker, G. W., and McKee, E. H., 1990, Eocene(?), Oligocene, and lower Miocene rocks of the Blue Mountains region, *in* Walker, G. W., ed., Geology of the Blue Mountains region of Oregon, Idaho, and Washington: Cenozoic Geology: U.S. Geological Survey Professional Paper 1437, p. 29–62.

Ross, M. E., 1978, Stratigraphy, structure, and petrology of the Columbia River basalt in a portion of the Grande Ronde River-Blue Mountains area of Oregon and Washington: Moscow, Id., University of Idaho, doctoral dissertation, 407 p.

Schlicker, H. J., and Deacon, R. J., 1971, Engineering geology of the La Grande area, Union County, 16 p, 1 map, scale 1:24,000.

Schweickert, R. A., and Cowan, D. S., 1975, Early Mesozoic tectonic evolution of the western Sierra Nevada, California: Geological Society of America Bulletin, v. 86, p. 1,329–1,336.

Shorey, D. F., 1976, Geology of part of southern Morrow County, northeast Oregon, Covallis, Oreg., Oregon State University M.S. thesis, 131 p.,

Shubat, M. A., 1979, Stratigraphy, petrochemistry, petrography, and structural geology of the Columbia River Basalt in the Minam-Wallowa River area, northeast Oregon: Pullman, Wash.; Washington State University, M.S. thesis, 156 p.

Silberling, N.J., Jones, D.L., Blake, M. C., Jr., and Howell, D. G., 1984, Lithotectonic terrane map of the western conterminous United States, *in* Silberling, N.J., and Jones, D. L., eds., Lithotectonic terrane maps of the North American Cordillera: U.S. Geological Survey Open-File Report 84-523, 43 p.

Simpson, G. D., Hemphill-Haley, M.A., Wong, I. G., Bott, J. D. J., Silva, W. J., and Lettis, W. R., 1993, Seismotectonic evaluation, Unity Dam, Burnt River Project—Thief Valley Dam, Baker Project, Northeastern Oregon: Final report prepared for U.S. Bureau of Reclamation by William Lettis & Associates and Woodward-Clyde Federal Services, 167 p.

Smith, G. O., 1901, Geology and water resources of a portion of Yakima County, Washington: U.S. Geological Survey Water Supply Paper 55, 68 p.

Smith, W. D., and Allen, J. E., 1941, Geology and physiography of the northern Wallowa Mountains, Oregon: Oregon Department of Geology and Mineral Industries Bulletin 12, 64 p.

Stoffel, K. L., 1984, Geology of the Grande Ronde lignite field, Asotin County, Washington: Washington Department of Natural Resources Report of Investigations 27, 79 p.

Swanson, D. A., and Wright, T. L., 1981, Guide to geologic field trip between Lewiston, Idaho, and Kimberly, Oregon, emphasizing the Columbia River Basalt Group, *in* Johnston, D. A., and Donnelly-Nolan, J., eds., Guides to some volcanic terranes in Washington, Idaho, Oregon, and northern California: U.S. Geological Survey Circular 838, p. 1–28.

Swanson, D. A., Wright, T. L., Hooper, P. R., and Bentley, R. D., 1979, Revisions in stratigraphic nomenclature of the Columbia River Basalt Group: U.S. Geological Survey Bulletin 1457-G, 59 p.

Swanson, D. A., Anderson, J. L., Camp, V. E., Hooper, P. R., Taubeneck, W. H., and Wright, T. L., 1981, Reconnaissance geologic map of the Columbia River Basalt Group, northern Oregon and western Idaho: U.S. Geological Survey Open-File Report 81-797, 33 p, 5 map sheets, scale 1:250,000.

Taubeneck, W. H., 1957, Geology of the Elkhorn Mountains, northeastern Oregon: Bald Mountain batholith: Geological Society of America Bulletin v. 68, p. 181–238.

Taubeneck, W. H., 1964, Wallowa Mountains, northeastern Oregon; Field relationships: Geological Society of America Bulletin, v. 97, p. 1,093–1,116.

Taubeneck, W. H., 1980, Diatremes in Columbia River Basalt near the crest of the west escarpment of the Grande Ronde Graben, northeast Oregon: Geological Society of America Abstracts with Programs (Cordilleran Section meeting), Corvallis, Oreg., p. 135.

Taubeneck, W. H., 1987, The Wallowa Mountains, northeast Oregon: Geological Society of America Centennial Field Guide-Cordilleran Section, p. 321–332.

Taubeneck, W. H., 1995, A closer look at the Bald Mountain batholith, Elkhorn Mountains, and some comparisons with the Wallowa batholith, Wallowa Mountains, northeastern Oregon, *in* Vallier, T. L., and Brooks, H. C., eds., Geology of the Blue Mountains region of Oregon, Idaho, and Washington; Petrology and tectonic evolution of pre-Tertiary rocks of the Blue Mountains region: U.S. Geological Survey Professional Paper 1438, p. 45–123.

Tolan, T. L., Reidel, S. P., Beeson, M. H., Anderson, J. L., Fecht, K. R., and Swanson. D. A., 1989, Revisions to the estimates of the areal extent and volume of the Columbia River Basalt Group, *in* Reidel, S. P., and Hooper, P. R., eds., Volcanism and tectonism in the Columbia River Flood-Basalt Province: Geological Society of America Special Paper 239, p. 1–20.

Trafton, K. S., 1999, Paleogeographic implications of Late Cretaceous–early Tertiary quartzite-bearing fluvial sediments, Elkhorn Mountains, northeastern Oregon, *in* Mendelson, C. V., and Mankiewicz, C., eds., Twelfth Keck Research Symposium in Geology Proceedings: Northfield, Minn., Carleton College, p. 291–298 (available from Dept. of Geology, Beloit College, Beloit, Wisc.).

Vallier, T. L., 1995, Petrology of pre-Tertiary igneous rocks in the Blue Mountains Region of Oregon, Idaho, and Washington: Implications the geologic evolution of a complex island arc, *in* Vallier, T. L., and Brooks, H. C., eds., Geology of the Blue Mountains region of Oregon, Idaho, and Washington; Petrology and tectonic evolution of pre-Tertiary rocks of the Blue Mountains region: U.S. Geological Survey Professional Paper 1438, p. 125–209.

Van Tassell, J., 1993, Geology of Grande Ronde Valley, Field Trip Guide for the Northwest Scientific Association 66th Annual Meeting, 18 p.

Van Tassell, J., 1997, Cyclostratigraphy of the Grande Ronde graben, NE Oregon (abstract): GSA Abstracts with Programs, Cordilleran section, p. 71.

Van Tassell, J., Ferns, M. L., and McConnell, V. S., 2000, Neogene sediment accumulation and subsidence rates, La Grande Basin, northeast Oregon: Geological Society of America, Cordilleran Section, 96th annual meeting, Abstracts with Programs, v. 32, no. 6, p. 73–74.

Van Tassell, J., Ferns, M. L., McConnell, V. S., and Smith, G. R., 2001, the mid-Pliocene Imbler fish fossils, Grande Ronde Valley, Union County, Oregon, and the connection between Lake Idaho and the Columbia River: Oregon Geology, v. 63, no. 3, p. 77–96.

Wagner, N. S., 1945, Indianna Mine: Oregon Department of Geology and Mineral Industries unpublished mine file report, 6 p.

Wagner, N. S., 1947, La Grande Brick Yard: Oregon Department of Geology and Mineral Industries unpublished mine file report.

Wagner, N. S., 1954, Preliminary report on the geology of the southern half of Umatilla County: Ore Bin, v. 16, no. 3, p. 13–17.

Wagner, N. S., and Ramp, L., 1969, Metallic mineral resources–antimony, *in* Weissenborn, A. E., ed., Mineral and water resources of Oregon: Oregon Department of geology and Mineral Industries Bulletin 64, p. 93–98.

Walker, G. W., 1973, Reconnaissance geologic map of the Pendleton quadrangle, Oregon and Washington: U.S. Geological Survey Miscellaneous Geologic Investigations Map I-727, scale 1:250,000.

Walker, G. W., 1979, Reconnaissance geologic map of the Oregon part of the Grangeville quadrangle, Baker, Union, Umatilla, and Wallowa counties, Oregon: U.S. Geological Survey Miscellaneous Geological Investigations Map I-1116, scale 1:250,000.

Walker, G. W., 1990, Miocene and younger rocks of the Blue Mountains Region, exclusive of the Columbia River Basalt Group and associated mafic lava flows, *in* Walker, G.W., ed., Geology of the Blue Mountains region of Oregon, Idaho, and Washington: Cenozoic Geology: U.S. Geological Survey Professional Paper 1437, p. 101–118.

Walker, N. W., 1986, U/Pb geochronologic and petrologic studies in the Blue Mountains terrane, northeastern Oregon and westernmost-central Idaho – implication for pre-Tertiary tectonic evolution: Santa Barbara, Calif.; University of California Santa Barbara, doctoral dissertation, 224 p.

Walker, N. W., 1989, Early Cretaceous initiation of post-tectonic plutonism and the age of the Connor Creek fault, northeastern Oregon: Geological Society of America Abstracts with Programs, v. 21, p. 155.

Weis, P. L., Gualtieri, J. L. Cannon, W. F., Tucher, E. T., McMahan, A. B., and Federspiel, F. E., 1976, Mineral resources of the Eagle Cap Wilderness and adjacent areas, Oregon: U.S. Geological Survey Bulletin 1385-E, 100 p.

White, R. R., 1981, Structural geology of the eastern half of the La Grande basin, northeastern Oregon: Los Angles, Calif., University of Southern California, M.S. thesis, 133 p.

Wilkinson, W. D., and Oles, K. E., 1968, Stratigraphy and paleoenvironments of Cretaceous rocks, Mitchell quadrangle, Oregon: American association of Petroleum Geologists Bulletin v. 52, p. 129–161.

Wilson, D., and Cox, A., 1980, Paleomagnetic evidence for tectonic rotation of Jurassic plutons in Blue Mountains, eastern Oregon: Journal of Geophysical Research, v., 85, p. 3,681–3,689.

Wright, T. L., Swanson, D. A., Helz, R. T., and Byerly, G. R., 1979, Major oxide, trace element, and glass chemistry of Columbia River Basalt samples collected between 1971 and 1979: U.S. Geological Survey Open-File Report 79-711, 144 p.

Wright, T. L., Black, K. B, Swanson, D.A., and O'Hearn, T., 1980, Columbia River Basalt: 1978-1979 sample data and chemical analyses: U.S. Geological Survey Open-File Report 80-921, 99 p.

Wright, T. L., Black, K. B, Swanson, D. A., and O'Hearn, T., 1982, Columbia River Basalt: 1980-1981 sample data and chemical analyses: U.S. Geological Survey Open-File Report 82-532, 51 p.

APPENDIX — DATA

Shape files with metadata as well as a basic map view for these data in Ersi ArcMap 9.3 format are located on this CD at:

Appendix-data/shp/mapview_UGRB.mxd
Appendix-data/shp/Geology_UGRB.shp
Appendix-data/shp/Faults_UGRB.shp
Appendix-data/shp/Structure_UGRB.shp
Appendix-data/shp/XRF_UGRB.shp
Appendix-data/shp/Waterwells-UGRB.shp

Geologic Data

Separate geology (region), fault (line), and structural (point) databases were used to construct the geologic map.

Geology

The geology database and spreadsheet files are located at:
Appendix-data/dbf/Geology_UGRB.dbf and
Appendix-data/xls/Geology_UGRB.xls

Fields for the **geology** database include:

POLYGON_ID – a unique number that identifies each polygon
LABEL_100K – the unit designator keyed to the map explanation at 1:100,000 scale
LABEL_24K – a unit designator keyed to more detailed source maps publishable at 1:24,000 scale
FORMATION – Formation
MMBR_NAME – member
DESCRIPTIO – description
ERA – era
EPOCH – epoch
PERIOD – period
TERRANE – terrane
NOTES – notes

Faults

The faults database and spreadsheet files are located at:
Appendix-data/DATA/dbf/Faults_UGRB.dbf and
Appendix-data/DATA/xls/Faults_UGRB.xls

Fields for the **faults** database include:

FAULT_ID – a unique number that identifies each fault segment
LABEL – label for fault on map plate
TRACE_TYPE – approximate, inferred, or concealed
STYLE – normal, reverse, thrust, etc.
FAULT_NAME – where appropriate
SIDE_DOWN – where determined
OFFSET – whether the fault was drawn based on displacement of units in the field
PHOTO – whether the fault was drawn based on aerial photographs
LINEAE – whether the fault is was drawn on the basis of a topographic lineament
ATTITUDES – fault plane measurements
NOTES – notes
DIP_AZIMUT – dip azimuth
REFERENCE – previously published or unpublished source

Structure

The structure database and spreadsheet files are located at:
Appendix-data/dbf/Structure_UGRB.dbf and
Appendix-data/xls/Structure_UGRB.xls

Fields for the **structure** database include:

TYPE – foliation, bedding plane, lava flow top, etc.
STRIKE_AZI – strike azimuth
DIP_ANGLE – dip angle
DIP_AZIMUT – dip azimuth
MEASUREMEN – measurement
PLUNGE – plunge
TREND – trend
REFERENCE – publication reference, keyed to the Reference list in this report

Digitizing methods

Hand-plotted field data were converted to digital data using the MapInfo™ GIS platform. Point, line, and region vector data were derived by heads-up digitizing over the top of digitally georegistered raster images of 7.5′ topographic quadrangles. The digital raster images, publicly available through the U.S. Geological Survey, were digitally georegistered in the Oregon Plane coordinate system UTM Zone 11.

The base map was derived using contours digitally derived from U.S. Geological Survey 30-m digital elevation model (DEM) data. Computer-drawn contours were generated using the Vertical Mapper program. Stream and road layers are derived from 1995 Census Bureau TIGER (Topologically Integrated Geographic Encoding and Referencing system) files downloaded from Oregon Geospatial Enterprise Office (http://gis.oregon.gov/).

The map projection of the map plate PDF is Universal Transverse Mercator, North American Datum 1927, Zone 11. The base map source data for the map plate are derived from USGS 10-m DEM and 100,000-scale DRG data.

Geochemical Data

A spreadsheet with over 1,100 XRF analyses for middle Cenozoic volcanic rocks of the Powder River Volcanic Field, the Columbia River Basalt Group, and the Tower Mountain caldera, grouped by unit, is located at: `Appendix-data/xls/XRF_UGRB_Cenozoic.xls`.

Complete geochemical sample data database and spreadsheet files, organized by source reference, are located at:
`Appendix-data/dbf/XRF_UGRB.dbf` and
`Appendix-data/xls/XRF_UGRB.xls`

Fields for the geochemical sample database include:

SAMPLE_ID	–	a unique number
QUADRANGLE_24K	–	the 1:24,000-scale quadrangle in which the sample is located
FIELD_ID	–	the field sample number
DESCRIPTIO	–	simple rock description
MAGMATIC_SUITE	–	(if applicable)
LITHOLOGY	–	based on formally accepted criteria
LONGITUDE LATITUDE FT [elevation] M [elevation]	–	combined to give the sample site location
ANALYTICAL	–	the laboratory that analyzed the sample
GROUP_TERRANE FORMATION MEMBER UNIT_100K UNIT_OTHER ERA PERIOD EPOCH	–	all keyed to the geology database
SOURCE_REF	–	publication reference, keyed to the Reference list in this report
REF_NUMBER	–	for samples from published sources
SIO2 through TH	–	26 elements total
LOI	–	Loss on ignition
ACOL50	–	Total
ROCK_TYPE	–	Basic rock type

The 10 major elements (SiO_2 through P_2O_5) have been normalized so that they total 100 percent. Major elements are recorded in weight percent. Minor element analyses are recorded as parts per million (ppm). Projection is NAD_1927_UTM_Zone_11N. The geochemical database includes samples from previously published sources in addition to samples collected during the mapping project.

Analytical methods

Samples collected by Oregon Department of Geology and Mineral Industries staff were trimmed and submitted to either the Washington State University (WSU) GeoAnalytical Laboratory at Pullman, Washington, or the X-Ray Analytical Laboratories (XRAL) at Toronto, Canada. Both laboratories use glass beads fused with lithium tetraborate. The Washington State University GeoAnalytical Laboratory uses an automatic Rigaku 3370 spectrometer. Each element analysis is fully corrected for line interference and matrix effects. See Hooper and others (1993) for a more complete description of Washington State University GeoAnalytical Laboratory analytical methods. XRAL uses a Siemens SRS 3000 sequential X-ray fluorescence spectrometer, which reportedly gives instrumental precision on most elements of about 0.5 percent. Results from both labs have been normalized on a volatile-free basis and recalculated with total iron expressed as FeO.

Trace metal analyses of 26 altered rock samples were performed by two different laboratories; Chemex Labs Inc., Sparks, Nevada, and SVL Analyatical Inc., Kellogg, Idaho. SVL analyzed for gold and silver by atomic absorption with a fire assay preconcentration. Mercury was determined by cold vapor-atomic absorption. Arsenic, selenium, and antimony were determined by graphite furnace-atomic absorption. Molybdenum, copper, lead, zinc, and tin were determined using induction-coupled plasma (ICP).

Chemex analyzed gold by atomic absorption with a fire assay concentration from a 30-g sample. Mercury was determined by cold vapor-atomic absorption. All other elements were determined using induction-coupled plasma techniques.

Radiometric ages were determined by two different research laboratories. Whole-rock $^{40}Ar/^{39}Ar$ analyses were performed by Dr. R. A. Duncan, College of Atmospheric and Oceanographic Sciences, Oregon State University, Corvallis. Ages were derived by stepwise analyses of powdered whole-rock samples.

Washed glass shards from ashes were analyzed by the Geochronology Laboratory, Geophysical Institute, University of Alaska Fairbanks. Radiometric age was derived by laser ablation stepwise $^{40}Ar/^{39}Ar$ age determinations on hand-picked, washed glass shards. Samples were irradiated for 2 MW hours at the McMaster University Nuclear Reactor, Ontario, Canada. Irradiated samples were subsequently fused with a coherent 6W Ar-ion laser and argon isotopic rations measured on a VG3600 mass spectrometer at the University of Alaska Geochronology Laboratory.

Water Well Data

The well log database is derived from written drillers' logs, which vary greatly in completeness and accuracy. Interpretations are based on adjacent logs and general geographic setting.

The water well database and spreadsheet files are located at:
`Appendix-data/dbf/WaterWellLg.dbf` and
`Appendix-data/xls/WaterWellLg.xls`

Fields for the water well database include:

`Hole_id` – keyed to the Oregon Department of Water Resources database
`Top` – distance to the top of the interval
`Base` – distance to the base of the interval
`Material` – dominant material within the interval
`Color` – dominant color within the interval
`Size` – dominant size within the interval
`Comments`
`Unit` – keyed to the geologic map and geology database
`Facies` – as interpreted in this study
`Map_unit` geologic unit designator keyed to this report
`Utm_n and Utm_e` – which gives the coordinates for the well, based on the well log
`Surface_el` – elevation of the surface of the well, based on assumed location
`Top_el` – elevation of the top of the interval
`Base_el` – elevation of the base of the interval

Projection is NAD_1927_UTM_Zone_11N.
Water well locations were first plotted using the Oregon Department of Water Resources GRID (Groundwater Resource Information Database), which plotted all wells as section centroids. A plot of all wells deeper than 100 ft was next superimposed on georeferenced raster images of USGS 7.5′ topographic maps (USGS DRGs). Well locations were adjusted to match more detailed locations described on actual water well logs. Wells with street addresses were located within appropriate city blocks atop an overlay of MapInfo StreetInfo files (proprietary enhanced TIGER files with address coding). Wells with bearing and distance data were plotted from raster image section corners.

Important deep wells were field located by direct contact with well owners or in some cases direct visual confirmation. Locations of important new wells were plotted on appropriate topographic maps during field visits as samples were collected.

Photographs

Nineteen photographs of the Upper Grande Ronde Valley in jpg format along with a spreadsheet providing GPS coordinates are located at:
`Appendix-data/photos/`

Page-size geologic map of the upper Grande Ronde River basin. The full-scale geologic map with cross sections and a stratigraphic column can be found on this CD in the folder “Map-plate.”

Return to Figure 2 on page 2

Return to “Explanation of Map Units” on page 6